Inaugural dissertation

for

obtaining the doctoral degree

of the

Combined Faculty of Mathematics, Engineering and Natural Sciences

of the

Ruprecht - Karls - University

Heidelberg

Presented by

M.Sc. Josina Großmann

born in Hamburg, Germany

Oral examination: 13th June 2024

The regulation of polo-like kinase 4 in centrosome duplication

Referees: Prof. Dr. Ingrid Hoffmann

Prof. Dr. Martin Müller

Table of contents

Summary

Centrosomes are important cell organelles that serve as main microtubule-organizing centers and are involved in diverse cellular processes, most importantly cell division by facilitating formation of the bipolar spindle in mitosis. Each centrosome consists of a pair of centrioles, which is duplicated exactly once per cell cycle. The serine/threonine protein kinase polo-like kinase 4, PLK4, is known as the master regulator of centriole duplication. Overexpression of PLK4 is sufficient to induce tumor formation in mice, by causing centrosome amplification and chromosome missegregation in mitosis as a source for genomic instability. In order to prevent centriole overduplication, PLK4 protein levels are tightly regulated by ubiquitylation and proteasomal degradation. Protein ubiquitylation is a post-translational modification, carried out by an enzymatic cascade consisting of three enzymes: E1, E2 and E3. The SKP1-CUL1-β-TrCP E3 ubiquitin ligase complex has been shown to recognize the substrate PLK4 upon trans-autophosphorylation of a degron motif and regulate its protein levels by ubiquitylation and proteasomal degradation. However, a β-TrCP binding mutant of PLK4 has been found to be still ubiquitylated and partly degraded, indicating that the exact regulation of PLK4 protein levels has not been unraveled entirely yet.

In the presented thesis, I identified PLK4 as a novel substrate of the E3 ubiquitin ligase CUL4-DDB1-DCAF1, $CRL4^{DCAF1}$, which ubiquitylates and thereby targets PLK4 for degradation in G2 phase of the cell cycle to prevent premature centriole duplication in mitosis. DCAF1 serves as a substrate binding domain of the complex, which I showed to bind PLK4 in a phosphorylation-independent manner. Overexpression of DCAF1 enhanced the ubiquitylation of PLK4, while knockdown of DCAF1 increased PLK4 protein levels and caused the formation of multipolar spindles in mitosis. I found that the regulation of PLK4 by $CRL4^{DCAF1}$ also affects the interaction between PLK4 and its substrate STIL, as well as the process of centriole disengagement at the onset of centriole biogenesis. Taken together, I identified a new mechanism for regulating PLK4 protein levels in centriole duplication that is dependent on the $CRL4^{DCAF1}$ ubiquitin ligase complex. My results contribute to a better understanding of the complex regulation and might open up new possibilities to target deregulated or overexpressed PLK4 as a novel approach for cancer therapy.

Zusammenfassung

Zentrosomen sind Zellorganellen, die als Mikrotubuli-organisierendes Zentrum dienen und an einer Vielzahl zellulärer Prozesse beteiligt sind. Das wichtigste Beispiel ist die Zellteilung, wo sie für die Ausbildung des bipolaren mitotischen Spindelapparats verantwortlich sind. Ein Zentrosom besteht aus zwei Zentriolen, welche genau einmal pro Zellzyklus verdoppelt werden. Die Serin/ Threonin Proteinkinase PLK4 ist der wichtigste Regulator der Zentriolenverdopplung. Überexpression von PLK4 ist ausreichend, um als Folge von einer vermehrten Zentriolenverdopplung, einer Fehlteilung der Chromosomen in der Mitose und der daraus entstehenden genomischen Instabilität, die Entstehung von Tumoren zu verursachen. Um dies zu vermeiden, sind die Proteinmengen von PLK4 durch Ubiquitylierung und proteasomale Degradation reguliert. Ubiquitylierung ist eine posttranslationale Proteinmodifikation, die das Anheften des Proteins Ubiquitin an Substrate beschreibt und von einer enzymatischen Kaskade bestehend aus E1, E2 und E3 Enzymen ausgeführt wird. Die E3 Ubiquitin-Ligase SKP1-CUL1-β-TrCP ist bereits als Regulator von PLK4 bekannt und erkennt und bindet sein Substrat nach Autophosphorylierung einer bestimmten Sequenz innerhalb von PLK4. Allerdings wurde festgestellt, dass eine Variante von PLK4, die nicht von β-TrCP erkannt und gebunden werden kann, noch immer ubiquityliert und teilweise degradiert wird. Dies deutet darauf hin, dass die genaue Regulierung der PLK4 Proteinmengen in der Zelle noch nicht vollständig aufgeklärt und verstanden wurde.

Im Rahmen meiner Doktorarbeit konnte ich das Protein PLK4 als ein neues Substrat der E3 Ubiquitin-Ligase CUL4-DDB1-DCAF1, $CRL4^{DCAF1}$, identifizieren. Meine Ergebnisse zeigen, dass $CRL4^{DCAF1}$ an der Regulation von PLK4 durch Ubiquitylierung und proteasomale Degradation in der G2-Phase des Zellzyklus in menschlichen Zellen beteiligt ist. In diesem Ubiquitin-Ligase-Komplex dient das Protein DCAF1 als Substratrezeptor und bindet unabhängig vom bekannten Mechanismus der Autophosphorylierung an PLK4. Ich konnte zeigen, dass die Überexpression von DCAF1 eine verstärkte Ubiquitylierung von PLK4 in der G2-Phase verursacht. Umgekehrt führt die Herunterregulation von DCAF1 zu einer Erhöhung der PLK4 Proteinmengen und zur Ausbildung von multipolaren Spindeln in der Mitose. Zudem trägt die Regulation von PLK4 durch die $CRL4^{DCAF1}$ Ubiquitin-Ligase auch zur Regulation der Interaktion zwischen PLK4 und seinem Substrat STIL bei und

beeinflusst den Prozess der Trennung des Zentriolenpaars zu Beginn der Zentriolenverdopplung.

Zusammengefasst konnte ich in der vorliegenden Arbeit den $CRL4^{DCAF1}$ E3 Ligase-Komplex als eine weitere Ubiquitin-Ligase identifizieren, welche für die strenge Regulation der PLK4 Proteinmengen während der Zentriolenverdopplung notwendig ist. Meine Ergebnisse tragen zu einem besseren Verständnis dieser komplexen Regulation bei und können neue Möglichkeiten eröffnen, fehlreguliertes oder überexprimiertes PLK4 zu einem Ziel von neuen Krebstherapien zu machen.

1. Introduction

1.1 The centrosome

1.1.1 Structural organization and functions of the centrosome

The centrosome is the major microtubule-organizing center (MTOC) in eukaryotic cells. More than hundred years ago, it has been discovered that centrosomes form the poles of the bipolar spindle in mitosis, which separates the chromosomes to the two daughter cells during cell division. The centrosome is comprised of a pair of orthogonally arranged, microtubule-based centrioles, which are surrounded by the pericentriolar material (PCM) (Bettencourt-Dias and Glover, 2007). A mature centriole is a cylindric structure of around 450 nm in length and 250 nm in diameter. At the base, referred to as the proximal end, the centriole pair is connected through a flexible linker. The tip of the centriole is referred to as the distal end (Gönczy, 2012). The structure of the centriole is determined by the ninefold radially symmetric arrangement of microtubule triplets. The older, mature centriole of the centriole pair is termed mother centriole and has subdistal and distal appendages, which are important for microtubule anchoring or anchoring centrioles to the plasma membrane, where they can act as basal bodies during ciliogenesis. The younger of the two centrioles, which assembled in the previous cell cycle, is termed daughter centriole (Piel et al., 2000) (Figure 1).

The PCM surrounding the centriole pair functions to anchor and nucleate microtubules during interphase and mitosis. The dynamic assembly and disassembly of the PCM is coupled to the centriole duplication cycle. During mitosis, the mother centriole accumulates and expands its PCM, while upon mitotic exit the expanded PCM is disassembled (Bettencourt-Dias and Glover, 2007). The PCM is composed of a large number of proteins, including many microtubule-organizing proteins, cell cycle regulators and cell cycle checkpoint proteins (Andersen et al., 2003). PCM proteins mostly contain coiled-coil domains and form a lattice-like structure, which allows for the docking of molecules that mediate the nucleation of microtubules, such as the γ-tubulin ring complex (γ-TuRC) (Zheng et al., 1995).

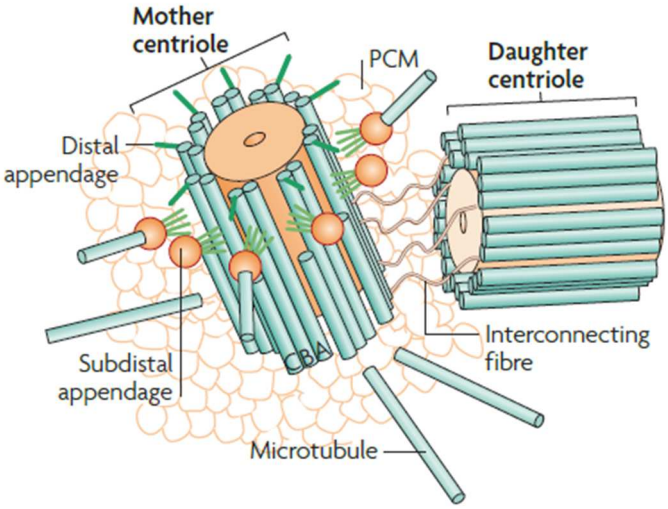

Figure 1: Schematic view of the centrosome structure.

The centrosome is comprised of a pair of centrioles, which is surrounded by the pericentriolar material (PCM). One mammalian centriole has nine microtubule triplets, which become doublets at the distal end. In contrast to the younger daughter centriole, the older and mature mother centriole is characterized by distal and subdistal appendages. In G1 phase of the cell cycle, mother and daughter centriole are connected by a flexible linker at their proximal ends. Adapted from Bettencourt-Dias and Glover, 2007.

In interphase, centrosomes function to nucleate and anchor microtubules and thereby regulate tissue architecture, cell motility and positioning of cell organelles. Additionally, centrosomes have been suggested to participate in cellular signaling by acting as platforms for signaling components such as kinases and phosphatases (Arquint et al., 2014). The mitotic function of centrosomes is well established. Centrosomes duplicate exactly once per cell cycle, beginning at the G1 to S phase transition, and by the time the cell enters mitosis, the two centrosomes form the poles of the bipolar mitotic spindle, ensuring a correct cell division. Furthermore, correct spindle positioning is mediated by centrosomes, as they are needed for the formation of astral microtubules. Although centrosomes play a critical role in organizing bipolar spindles in mitosis, cell division can occur in the absence of centrosomes. Higher plant cells as well as oocytes of many animals form mitotic or meiotic spindles without centrosomes, by self-organizing acentriolar MTOCs for nucleation and stabilization of microtubules (Schuh and Ellenberg, 2007). Several other pathways exist, that can nucleate and stabilize microtubules and organize them into a bipolar spindle in the absence of centrosomes. Interestingly, these pathways also contribute to spindle assembly in presence of centrosomes. However, despite these alternative pathways, it has been clearly shown that the presence of centrosomes contributes to the efficiency of spindle assembly,

orientation and efficient cell cycle progression (Khodjakov et al., 2000; Sir et al., 2013; Conduit et al., 2015).

Centrioles are essential for cilia formation and accordingly, centrioles can be found in all eukaryotic species that form cilia or flagella but are absent from higher plants and yeasts (Marshall, 2009). In quiescent cells, the mother centriole can convert into a basal body close to the cell membrane and assemble a primary or motile cilium. While primary cilia transmit signals between the cell environment and cell interior, motile cilia are involved in dynamic processes such as moving sperm, transporting fluids for mucus clearance or transporting the egg cell (Vasquez-Limeta and Loncarek, 2021).

Centrosomes are involved in diverse cellular and developmental processes; thus, many human diseases and disorders are linked to centrosome defects. Structural or numerical centrosome abnormalities can cause chromosome segregation errors and aneuploidy, contributing to genomic instability and cancer. Mutations in centriolar genes can be the cause of microcephaly or ciliopathies, hereditary diseases associated with defects in cilia formation and function (Vasquez-Limeta and Loncarek, 2021).

1.1.2 Centrosome duplication

Similar to the DNA, centrosomes are duplicated exactly once per cell cycle. The centrosome duplication cycle is coupled to the cell cycle, as core components of the cell cycle machinery such as cyclin-dependent kinase 1 and 2 (CDK1 and CDK2) are also involved in the regulation of centrosome duplication (Hinchcliffe and Sluder, 2001). In G1 phase of the cell cycle, mother and daughter centriole are close to one another and connected by a proteinaceous linker at their proximal ends. Around the G1/S phase transition, a procentriole starts to assemble orthogonal to the proximal end of each parental centriole and elongates throughout the remaining cell cycle. At the end of G2 phase, the linker is removed and the two centrosomes separate to assemble the bipolar spindle in mitosis, which segregates both the duplicated chromosomes and centrosomes equally between the two daughter cells (Gönczy, 2015) (Figure 2).

Formation of the procentriole adjacent to the mother centriole is the first step of the centrosome duplication cycle, which is initiated by the recruitment of polo-like kinase 4 (PLK4) to the site of procentriole assembly. In mammalian cells, CEP152 and CEP192 were shown to interact via their acidic regions with the positively charged

polo-box domain of PLK4 and thereby cooperate in the recruitment of PLK4 to the centriole (Cizmecioglu et al., 2010; Hatch et al., 2010; Kim et al., 2013b; Sonnen et al., 2013). Once the site of origin for centriole duplication is defined by PLK4, the ninefold symmetric cartwheel structure is formed by spindle assembly abnormal protein 6 (SAS-6) homodimers, which act as a scaffold for procentriole formation. PLK4 interacts with and phosphorylates SCL-interrupting locus (STIL) (Kratz et al., 2015), which allows for recruitment of SAS-6 and formation of the procentriolar cartwheel (Ohta et al., 2014). PLK4, SAS-6 and STIL were shown to be centriolar proteins with critical function, as their depletion prevents procentriole formation and their overexpression causes supernumerary procentrioles (Brito et al., 2012). STIL also interacts with CPAP which is recruited to the outer cartwheel region and bridges the cartwheel with peripheral centriolar microtubules (Hatzopoulos et al., 2013).

The phase of procentriole elongation starts almost simultaneously with cartwheel assembly and is active between S and G2 phase. γ-tubulin is recruited to the proximal region of the procentriole and nucleates centriolar microtubules around the cartwheel scaffold. CPAP and centrobin were shown to be required for this process, as they interact with tubulin and facilitate the incorporation of tubulin dimers at centriolar microtubule plus ends. Centriole elongation is regulated by the counteracting activities of CPAP and CP110, a protein localizing to the distal end of the centriole and suggested to act as a cap-like structure for the growing centriole (Schmidt et al., 2009).

Centrosome maturation in G2 phase and mitosis involves the recruitment of PCM proteins and a general expansion of the PCM around centrioles. PLK1 has been shown to be critical for the initiation of centrosome maturation, as it phosphorylates the PCM protein pericentrin, among other substrates, and thereby promotes the recruitment of several PCM components (Lee and Rhee, 2011). During centrosome maturation, daughter centrioles convert into mother centrioles by acquiring distal and subdistal appendages and thereby reach full maturation. The newly formed procentrioles have to pass through one mitotic phase in order to become parental centrioles in the next S phase and reach full maturation during G2/M phase of the following cell cycle (Brito et al., 2012).

For centrosome separation at the G2/M transition, the proteinaceous linker connecting the two centrosomes is removed. The protein kinase NEK2 is activated and

phosphorylates its substrates and centrosome cohesion components C-NAP1 and rootletin, initiating their displacement from the centrosomes (Bahe et al., 2005). Subsequently, the two centrosomes separate along the nuclear envelope and organize the formation of the bipolar spindle (Gönczy, 2015).

Centriole disengagement in late mitosis/ early G1 phase is considered as the licensing step for the next round of centrosome duplication. Tight centriole-procentriole engagement in an orthogonal configuration from procentriole assembly until late mitosis normally prevents unscheduled or additional procentriole assembly. PLK1 and separase were shown to cooperate in centriole disengagement during early and late M phase, thereby licensing centrioles for the next duplication cycle (Tsou et al., 2009).

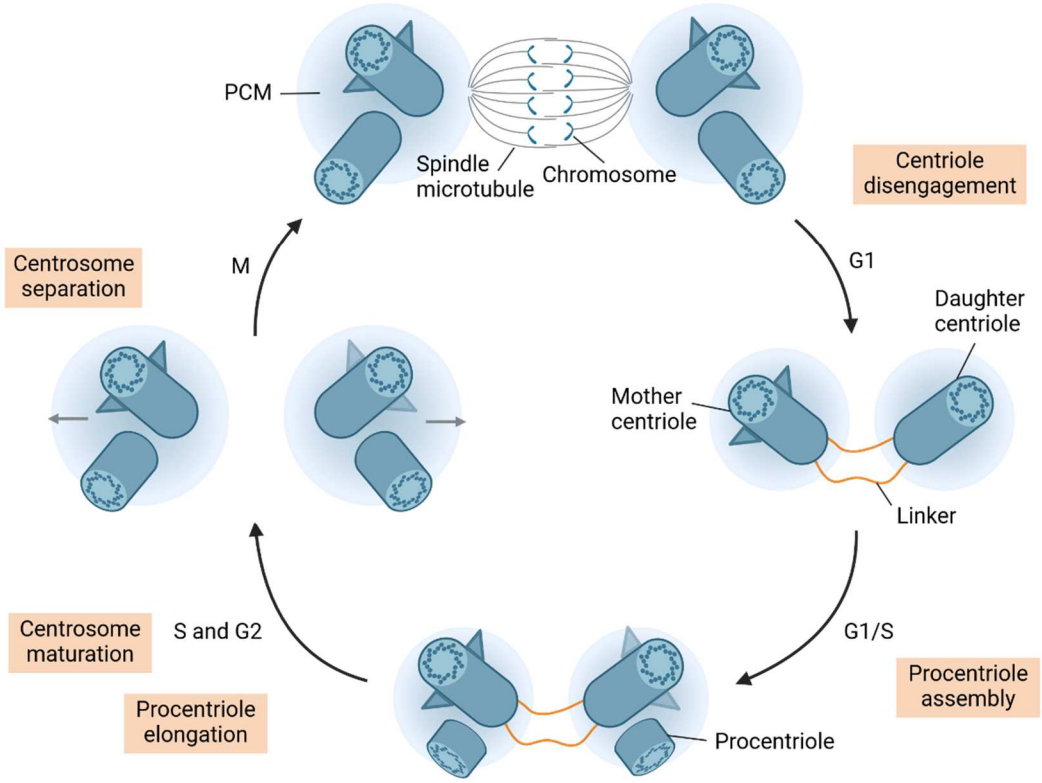

Figure 2: Schematic view of the centrosome duplication cycle.

In G1 phase of the cell cycle, two centrioles are present, which are connected through their proximal ends by a flexible linker. The mature mother centriole harbors distal and subdistal appendages. At the G1/S phase transition, procentriole assembly starts with formation of the cartwheel structure orthogonal to the proximal end of the parental centrioles. The procentrioles elongate throughout S and G2 phase. Centrosome maturation occurs simultaneously and involves the acquisition of appendages at the daughter centriole, as well as expansion of the PCM. At the G2/M phase transition the connecting linker is removed and the two centrosomes separate to form the poles of the bipolar spindle in mitosis. The centriole-procentriole disengagement during mitosis licenses a new round of centrosome duplication.

After completion of mitosis, each daughter cell inherits two loosely connected centrioles, thereby completing the duplication cycle. Adapted from Gönczy, 2015. Created with BioRender.com.

1.1.3 Centrosome abnormalities and cancer

A causal relationship between aberrations in centriole numbers and cancer has been proposed by Theodor Boveri already more than 100 years ago (Boveri, 2008). Today, numerical as well as structural centrosome abnormalities are found in many cancer types and are linked to aberrant spindle formation during cell division, which leads to chromosomal instability and aneuploidy (Nigg and Holland, 2018). However, the question whether centrosome amplification is a cause or a consequence of cancer has not been answered thoroughly yet.

Studies in flies revealed that supernumerary centrosomes generated due to constitutive overexpression of PLK4 caused overduplication of cells and tumorigenesis (Basto et al., 2008). Interestingly, *Drosophila* cells initially form multipolar spindles due to the presence of extra centrosomes but ultimately cluster their centrosomes at two spindle poles to form a pseudo-bipolar spindle and divide in a bipolar fashion. Although this does not generate large-scale chromosomal instability, it might cause syntelic or merotelic chromosomal attachments, where both sister kinetochores attach to microtubules from the same spindle pole or a single kinetochore attaches to microtubules from two spindle poles, respectively. This leads to chromosome missegregation and can generate low-level chromosomal instability, facilitating the development of malignant phenotypes (Nigg and Raff, 2009). Studies in mice supported the hypothesis that extra centrosomes are not only bystanders but rather initiators of tumor development, by demonstrating that centrosome amplification due to modest overexpression of PLK4 triggers spontaneous tumor development (Levine et al., 2017). However, in other mouse studies amplified centrosomes due to high overexpression of PLK4 were not sufficient to promote tumorigenesis, suggesting that centrosome amplification might not be a tumor-initiating event (Vitre et al., 2015; Serçin et al., 2016). Additionally, centrosome amplification has been shown to promote the process of cell invasion during tumorigenesis through changes in microtubule organization and nucleation (Godinho et al., 2014).

Considering that centrosome abnormalities are present in many tumors, independent of whether they are a cause or a consequence of tumorigenesis, these abnormalities

could be an attractive target for cancer therapy. Cells with extra centrosomes are highly dependent on certain proteins or pathways that are less crucial in normal cells. Studies in *Drosophila* demonstrated that cells with extra centrosomes are more dependent on a functional spindle assembly checkpoint (SAC) than normal cells, since centrosome clustering and formation of the pseudo-bipolar spindle requires more time than a normal cell division (Basto et al., 2008). Inhibiting such pathways could selectively target cancer cells.

1.2 PLK4 – Master regulator of centriole duplication

1.2.1 Structure of PLK4

PLK4 belongs to the family of polo-like kinases (PLKs), a family of serine/threonine protein kinases that are characterized by the presence of an N-terminal kinase domain and polo-box (PB) domains in their C-terminal region (Zitouni et al., 2014). Among the PLKs, PLK4 is structurally unique and contains three instead of two polo-boxes (PB1 – PB3) (Slevin et al., 2012) (Figure 3). The first two polo-boxes PB1 and PB2, also referred to as cryptic polo-box (CPB), were shown to be involved in intermolecular homodimer formation and are sufficient for centriolar localization of PLK4 (Leung et al., 2002; Slevin et al., 2012). The PLK4 PB1-PB2 domain also mediates binding to the acidic regions of the centriolar proteins CEP152 and CEP192, which are involved in centrosomal recruitment of PLK4 (Cizmecioglu et al., 2010; Hatch et al., 2010; Kim et al., 2013b; Sonnen et al., 2013). Further, PB1-PB2 homodimerization initiates trans-autophosphorylation to induce PLK4 degradation for a tight regulation of PLK4 protein levels. Although PLK4 homodimerization is primarily mediated through the PB1-PB2 domain and PB3 is not required, also PB3 has been shown to contribute to homodimerization (Slevin et al., 2012). An additional function of PB3 has been revealed in the regulation of PLK4 kinase activity by relieving autoinhibition of the PLK4 dimer (Klebba et al., 2015). The PLK4 sequence comprises three PEST motifs, which are domains rich in proline (P), aspartate (D), glutamate (E), serine (S) and threonine (T) residues and regulate protein stability (Fode et al., 1994; Rechsteiner and Rogers, 1996). The first PEST motif located near the N-terminus contains a degron motif, which is highly conserved between species. Upon trans-autophosphorylation of the serine and threonine residues, it is recognized by the F-box protein β-TrCP/ Slimb, leading to ubiquitylation and proteasomal degradation of PLK4 mediated by the SKP1-CUL1-F-

box $(SCF)^{\beta\text{-TrCP/Slimb}}$ ubiquitin ligase complex (Cunha-Ferreira et al., 2009; Rogers et al., 2009).

Figure 3: Domain organization of human PLK4.
PLK4 contains a kinase domain in the N-terminal region and three polo-box domains in the C-terminal region, two tandem homodimerized polo-boxes (PB1-PB2), also referred to as cryptic polo-box (CPB), and a third single polo-box (PB3). The PB domains mainly function to mediate PLK4 homodimerization, centriolar localization and protein-protein interactions. The N-terminal PEST motif is involved in the regulation of PLK4 protein stability, as it contains the conserved phosphodegron motif recognized by β-TrCP for subsequent ubiquitylation and proteasomal degradation of PLK4. Created with BioRender.com.

1.2.2 Functions of PLK4

PLK4 has been originally identified in mice as a serine/ threonine protein kinase related to the *Drosophila* polo kinase and named SAK, due to its homology with murine Snk and Plk kinases (Fode et al., 1994). Mouse studies have demonstrated a crucial role of PLK4 in embryonic development and mitotic progression, as PLK4 knockout mouse embryos ($PLK4^{-/-}$) arrest at embryonic stage E7.5 (Hudson et al., 2001). $PLK4^{+/-}$ embryos were shown to develop normally but demonstrate defects in mitotic spindle formation in hepatocytes, higher levels of aneuploidy and an increased incidence of spontaneous tumor development (Ko et al., 2005).

PLK4 localizes to the centrosome and is an essential regulator of centriole duplication. Depletion of PLK4 prevents centriole duplication and causes mitotic defects (Bettencourt-Dias et al., 2005; Habedanck et al., 2005). Conversely, overexpression of PLK4 results in an excessive formation of centrioles and amplification of centrosomes in somatic cells or *de novo* formation of centrioles in Drosophila oocytes (Habedanck et al., 2005; Rodrigues-Martins et al., 2007). A few substrates of PLK4 at the centrosome have been reported and how their phosphorylation by PLK4 triggers centriole assembly is understood partially. In *C. elegans*, the PLK4 analogue ZYG-1 binds to, recruits and phosphorylates SAS-6 for cartwheel assembly, however this phosphorylation was shown to be potentially dispensable (Kitagawa et al., 2009;

Lettman et al., 2013). Furthermore, PLK4 has been shown to physically interact with and phosphorylate STIL/Ana2 within the STAN motif in mammalian cells and in *Drosophila*, which is of functional relevance for centriole duplication (Stevens et al., 2010; Dzhindzhev et al., 2014; Ohta et al., 2014; Kratz et al., 2015). STIL phosphorylation by PLK4 at a conserved site outside the STAN motif, S428, has been shown to promote STIL binding to centrosomal P4.1-associated protein (CPAP), a protein that positively regulates centriolar microtubule growth (Moyer and Holland, 2019). Centriolar coiled-coil protein 110 (CP110) is a protein that is also involved in centriolar length control and has been shown to be phosphorylated by PLK4 at S98 as an essential step for centriole assembly (Lee et al., 2017). The centriolar proteins CEP152 and CEP135 are additional substrates of PLK4 and have been shown to be phosphorylated by PLK4 *in vitro* (Hatch et al., 2010; Galletta et al., 2016). γ-tubulin complex protein 6 (GCP6) is a core component of the γ-tubulin ring complex (γ-TuRC) and another target protein of PLK4 in centriole biogenesis. Phosphorylation of GCP6 by PLK4 was shown to be required for centriole duplication (Bahtz et al., 2012).

Several studies report functions of PLK4 outside of centriole duplication. PLK4 binds and phosphorylates S372 of pericentriolar material 1 (PCM1), which is required for maintaining centriolar satellite organization by allowing PCM1 to interact with other satellite components (Hori et al., 2016). In the context of cancer, a role of PLK4 in tumor invasion and metastasis has been well described. PLK4 was shown to activate the ARP2/3 complex by interacting with Arp2 and phosphorylating it on Thr237/238, which promotes cell motility and facilitates the invasiveness of cancer cells. Additionally, several studies established a role of PLK4 in cancer cell proliferation, as increased PLK4 levels enhanced cell proliferation in various cancer cell lines and mice, which was suppressed by PLK4 inhibition using small molecule inhibitors (Serçin et al., 2016; Lei et al., 2018).

1.2.3 Regulation of PLK4

Tight regulation of PLK4 levels is essential for accurate centriole duplication, which is limited to exactly once per cell cycle and necessary for a correct chromosome segregation in mitosis. The kinase PLK4 is a low abundance, cell cycle regulated protein with a short half-life. At the transcription level, human PLK4 is undetectable in G0 phase, levels increase in G1/S phase, remain until M phase and finally decrease in early G1 phase (Uchiumi et al., 1997). A number of transcription factors act at the

PLK4 promoter and are involved in the activation or repression of PLK4 transcription (Zhang et al., 2021). Studies on the transcription factor E2F suggested that it directly binds to the PLK4 promoter and increases the transcriptional activity (Lee et al., 2014). In addition, nuclear factor kappa B (NFκB) has been identified as a transcriptional activator of PLK4 (Ledoux et al., 2013). Conversely, Krüppel-like factor 14 (KLF14) acts as a transcriptional repressor of PLK4 and its absence upregulates PLK4 at the mRNA and protein level (Fan et al., 2015). The tumor suppressor p53 is involved in the transcriptional repression of PLK4 via several pathways (Li et al., 2005; Ward and Hudson, 2014).

At the protein level, PLK4 autoregulates itself by dimerization. After protein synthesis, PLK4 is present in an autoinhibited, monomolecular state, in which linker 1 (L1) prevents phosphorylation of the activation loop (AL) of the kinase domain. Upon homodimerization, mediated by PB1 and PB2, PB3 separates L1 from AL thereby relieving the autoinhibition and stimulating PLK4 kinase activity. Autophosphorylation of AL fully activates PLK4 enzymatic activity (Klebba et al., 2015). Not only PLK4 kinase activity, but also PLK4 protein degradation is linked to the autophosphorylation mechanism. In 1996, Fode et al. showed that PLK4 is posttranslationally modified by ubiquitylation and thereby targeted for proteasomal degradation (Fode et al., 1996). Inhibition of proteasome function causes centriole overduplication, similarly to overexpression of PLK4 (Duensing et al., 2007). Additional studies identified the E3 ubiquitin ligase SKP1-CUL1-F-box $(SCF)^{\beta\text{-TrCP/Slimb}}$ as the mediator of PLK4 (SAK) ubiquitylation and proteasomal degradation (Cunha-Ferreira et al., 2009; Rogers et al., 2009; Holland et al., 2010). The phosphodegron within PLK4 (SAK), which is recognized and bound by the F-box protein β-TrCP (Slimb), is conserved in vertebrates and its mutation or depletion of β-TrCP (Slimb) was shown to cause an increase in centrosome numbers (Guardavaccaro et al., 2003; Cunha-Ferreira et al., 2009). Further, it has been shown that PLK4 protein stability is directly correlated with its enzymatic activity. The PLK4 homodimer trans-autophosphorylates two amino acid residues within the β-TrCP recognition motif, which recruits the $SCF^{\beta\text{-TrCP}}$ ubiquitin ligase complex and initiates ubiquitylation and subsequent proteasomal degradation of PLK4 (Guderian et al., 2010; Holland et al., 2010; Cunha-Ferreira et al., 2013). Protein phosphatase 2A (PP2A) counteracts PLK4 autophosphorylation and thereby stabilizes PLK4 in mitosis (Brownlee et al., 2011). Activation-dependent degradation is

a common regulatory mechanism of several protein kinases that catalyze their own degradation (Kang et al., 2000; Lu and Hunter, 2009). The autophosphorylation mechanism has also been harnessed to monitor PLK4 activity throughout the cell cycle, by using a phospho-specific antibody against the autophosphorylation site S305 (Sillibourne et al., 2010). PLK4 is present at the centrioles in G1 phase but the kinase is inactive at this point of the cell cycle. It first becomes active in S phase and the amount of active kinase increases to reach a maximum in mitosis. Active PLK4 is first detectable at the mother centriole in S phase and slightly delayed at the daughter centriole in G2 phase. Additionally, active PLK4 has been shown to be restricted to the centrosome, potentially preventing aberrant centriole formation elsewhere in the cell (Sillibourne et al., 2010; Sillibourne and Bornens, 2010).

1.2.4 PLK4 in cancer

PLK4 overexpression causes centrosome amplification, which is commonly observed in human tumors. However, whether centrosome amplification is a cause or a consequence of tumor development remained a complex question. Levine et al. demonstrated that PLK4 overexpression in mice induces centrosome amplification, which causes aneuploidy and triggers spontaneous tumorigenesis in multiple tissues independently of the p53 status, suggesting that elevated centrosome numbers are not only bystanders but rather active promotors of tumor development (Levine et al., 2017). However, in other studies PLK4 overexpression was only sufficient to induce centrosome amplification in liver and skin but did not promote spontaneous tumor development (Vitre et al., 2015) or it generated aneuploidy and triggered development of spontaneous skin tumors, but only upon knockout of p53 (Serçin et al., 2016). Potentially, the outcome highly depends on the level of PLK4 overexpression and thus the mouse model. Small increases in centrosome numbers might be tolerated for continued cell divisions and allow for tumor development, while large numbers of extra centrosomes might cause lethal multipolar cell divisions and are detrimental to cell survival (Levine et al., 2017).

Generally, PLK4 expression levels in mammalian somatic cells are closely related to the level of proliferation of these cells (Fode et al., 1994). Vigorously dividing germ cells in the testes express higher levels of PLK4 compared to cells in epithelial tissues that are barely renewing. Accordingly, PLK4 levels are high in strongly proliferating cancer cells, but vary between different cancer types (Zhang et al., 2021). In pancreatic

cancer, PLK4-mediated centriole overduplication has been identified as a biomarker and linked with a poor prognosis. The PLK4 inhibitor CFI-400945 was suggested as a potential drug, as it reduced the tumor size in patient-derived xenografts (Lohse et al., 2017). Also in glioblastoma, PLK4 knockdown or PLK4 inhibition by the small molecule inhibitor CFI-400945 demonstrated anti-tumor effects (Zhang et al., 2019b; Wang et al., 2020). In breast cancer tissues, PLK4 is found to be overexpressed frequently and high expression levels are correlated with a poor prognosis (Denu et al., 2016) (Li et al., 2016), suggesting PLK4 as a promising target for cancer therapy. Additionally, in lung cancer, the most common type of cancer, and melanoma, the most aggressive form of skin cancer, PLK4 was found to be upregulated and high expression levels were correlated with a poor prognosis (Zhou et al., 2020a) (Denu et al., 2018). PLK4 inhibition either by CF-400945 treatment of murine or human lung cancer cells or by treatment of melanoma cells with the selective PLK4 inhibitor centrinone B induced apoptosis, further suggesting PLK4 as a drug target (Denu et al., 2018; Kawakami et al., 2018).

1.3 Ubiquitylation and protein degradation

1.3.1 Protein ubiquitylation

Ubiquitylation was first identified as a post-translational modification that targets proteins for degradation by the 26S proteasome and has been later shown to control almost every process in cells (Ciechanover et al., 1980; Hershko et al., 1980). The mechanism of ubiquitylation, meaning the covalent ligation of the 76-amino-acid protein ubiquitin to a target protein, requires the sequential action of three enzymes (Figure 4). In the first, ATP-dependent step, ubiquitin is activated by the E1 activating enzyme, which forms a thioester linkage by binding to ubiquitin via a cysteine residue. In the second step, the activated ubiquitin is transferred to an active site cysteine residue within the E2 ubiquitin-conjugating enzyme. In the third step, an E3 ubiquitin ligase catalyzes the linkage of ubiquitin via its C-terminus to an amino group of lysine residues of the substrate protein (Hershko and Ciechanover, 1998). By the same cascade, one ubiquitin molecule can also be covalently attached to itself instead of the target protein directly, which leads to the formation of polyubiquitin chains. Within the ubiquitin chain, ubiquitin molecules can be conjugated through one of their seven lysine residues (K6, K11, K27, K29, K33, K48 and K63) or the N-terminal methionine residue (M1), resulting in numerous possibilities to assemble a ubiquitin chain

consisting of different linkage types. Ubiquitin chains comprised of only a single linkage type are referred to as homotypic, while heterotypic chains contain mixed linkages (Akutsu et al., 2016).

In vertebrates, the family of E1 enzymes consists of two members, UBA1 and UBA6, with UBA1 having an approximately tenfold higher abundance. The family of E2 enzymes consists of more than 40 members but the rate of ubiquitin transfer from E1 to E2 has been shown to be relatively independent of the specific identity of the E2 enzyme. However, the less abundant E1 enzyme UBA6 specifically activates the E2 enzyme UBE2Z (Use1), which only interacts with the N-recognin E3 ligase family members UBR1, 2 and 3 (Jin et al., 2007; Lee et al., 2011). Interestingly, when E2 enzymes are paired with E3 ligases from the RING family, the E2 partner determines ubiquitin chain specificity. While some E2 enzymes are restricted to adding ubiquitin to ubiquitin itself, thereby extending chains with a specific linkage type, other E2s are incapable of chain-building and limited to monoubiquitylation (Ye and Rape, 2009).

E3 ubiquitin ligases confer target specificity and mediate the transfer of ubiquitin from the E2 enzyme to the substrate to be targeted. More than 600 E3 ubiquitin ligases have been described, which can be categorized into different classes, defined by the presence of certain domains. The majority of E3 ubiquitin ligases belongs to the family of RING E3 ligases, which are conserved from yeast to humans and mediate direct transfer of ubiquitin from E2 to substrate. In contrast, for E3 ligases of the homologous to E6AP carboxyl terminus (HECT) family, ubiquitin transfer is not direct but involves a thioester intermediate formed between ubiquitin and the active site cysteine of the E3 ligase, before transferring the ubiquitin to the substrate (Metzger et al., 2012). RING-between-RING (RBR) E3 ligases constitute the smallest family of ubiquitin ligases with only 14 members and are also described as RING/HECT hybrid E3 ligases. The RBR RING1 domain binds the E2 enzyme analogous to RING-type E3s, however, the ubiquitin transfer does not occur directly but instead in two steps via an active site cysteine within the RING2 domain similarly to the mechanism of HECT-type E3 ligases (Wang et al., 2023). Ubiquitin modifications on target proteins can be removed by specialized proteases referred to as deubiquitinating enzymes (DUBs) (Komander et al., 2009).

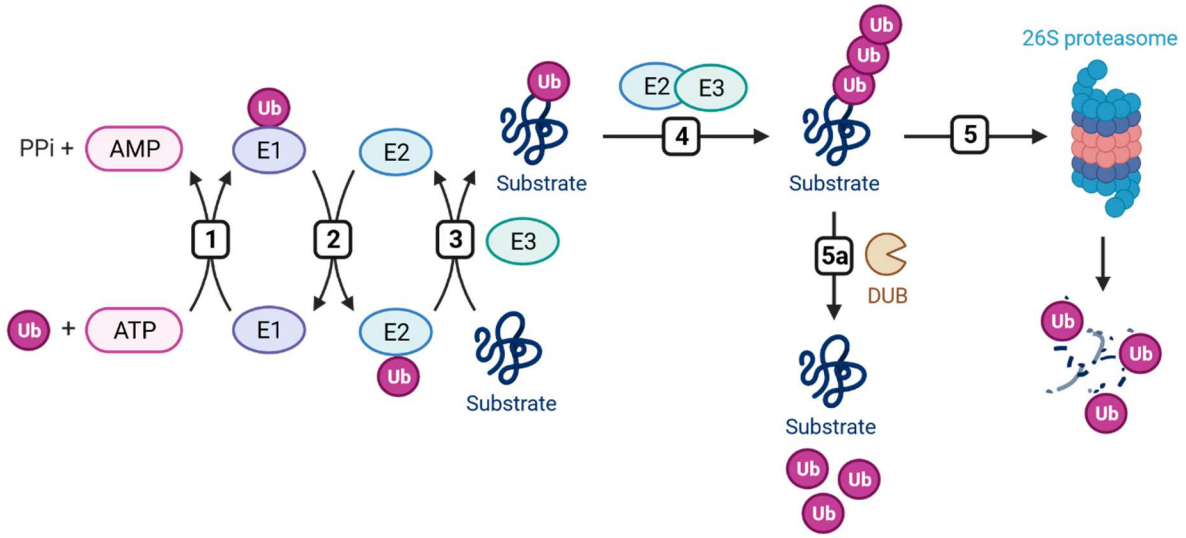

Figure 4: The ubiquitin-proteasome pathway.

(1) Ubiquitin (Ub) is activated by the E1 ubiquitin-activating enzyme in an ATP-dependent manner. (2) The activated ubiquitin is transferred to an E2 ubiquitin-conjugating enzyme. (3) An E3 ubiquitin ligase transfers ubiquitin from the E2 enzyme to a lysine residue of a substrate. (4) The monoubiquitylated substrate can be further modified by additional ubiquitin attachments in form of a ubiquitin chain. The chain can be assembled via different lysine residues of ubiquitin. (5) Lys48-linked ubiquitin chains target the substrate for degradation by the 26S proteasome. (5a) Alternatively, deubiquitinating enzymes (DUBs) can remove ubiquitin modifications from the substrate. Adapted from Deshaies and Joazeiro, 2009. Created with BioRender.com.

1.3.2 The ubiquitin code

The mechanism of ubiquitylation requires the sequential action of a cascade of different enzymes. Once attached to the substrate protein, ubiquitin is subjected to further modifications, such as the attachment of additional ubiquitin molecules resulting in polyubiquitin chains or other posttranslational modifications. The various ubiquitin modifications create a multitude of different signals with distinct cellular outcomes, referred to as the ubiquitin code.

Homotypic ubiquitin chains consist of several ubiquitin molecules linked via the same lysine residue. K48-linked chains have been identified as the predominant linkage type in cells and function to target proteins for proteasomal degradation. The second most abundant chain type, K63-linked chains, has been shown to be involved in non-degradative processes such as NFκB signaling or DNA damage pathways (Chen and Sun, 2009). In recent years, research has started to focus on the characterization of the remaining, unconventional ubiquitin chains. K6-linked ubiquitylation has been repeatedly shown to play a role in the DNA damage response (Wu-Baer et al., 2003;

Morris and Solomon, 2004) and autophagy of damaged mitochondria (Ordureau et al., 2015). Similarly, K11-linked chains play a role in the DNA damage response but are also generally associated with proteasomal degradation (Matsumoto et al., 2010). While K27-linked ubiquitin chains are involved in the innate immune response (Li et al., 2020), K29-linked chains have been implicated in neurodegenerative disorders and cellular signaling (Fei et al., 2013). K33-linked ubiquitylation remains the least studied ubiquitin linkage type (Akutsu et al., 2016). Another layer of complexity is added to the ubiquitin code by the formation of heterotypic chains consisting of mixtures of different lysine linkages within one polyubiquitin chain or the formation of branched ubiquitin chains.

Furthermore, ubiquitin can be modified by additional posttranslational protein modifications such as acetylation, deamidation or phosphorylation. Another protein modification system, which competes with ubiquitylation for the modification of lysine residues, is the small ubiquitin-like modifier (SUMO) system. Although the SUMO system, consisting of only one E1, one E2 and a few E3 enzymes, is less complex than the ubiquitin system, essential roles in several biological processes have been described (Flotho and Melchior, 2013). Interestingly, while SUMO forms chains that can be ubiquitylated, also ubiquitin can by SUMOylated, adding even more complexity to the ubiquitin code (Galisson et al., 2011). The final regulatory component of the ubiquitin code are deubiquitylating enzymes (DUBs), that control ubiquitin-dependent signaling by disassembling ubiquitin chains. Similar to ubiquitin ligases, they can be categorized into different families and display specificity towards a specific linkage type or target ubiquitin chains independently of the linkage (Komander and Rape, 2012). In recent years, much of the ubiquitin code has been unraveled and the ubiquitylation machinery and its involvement in nearly every cellular process is understood in more detail. This knowledge will provide opportunities to modulate the ubiquitin code therapeutically and develop novel ubiquitin-based therapies.

1.3.3 Protein degradation by the 26S proteasome

The best-known function of protein ubiquitylation is targeting the substrate protein for degradation by the 26S proteasome, the major protease in eukaryotic cells. Thereby, the 26S proteasome is involved in general protein homeostasis, cell cycle regulation and stress responses, but also responsible for degrading damaged or misfolded polypeptides (Coux et al., 1996; King et al., 1996a; Hershko and Ciechanover, 1998).

The 26S proteasome holoenzyme is composed of two functionally distinct subcomplexes; the 20S core protease (CP) which contains the proteolytic activity and the 19S regulatory particle (RP) which can be further separated into the base and lid subcomplexes and captures ubiquitylated substrates for degradation (Groll et al., 1997; Finley, 2009). The CP only degrades polypeptides that are deliberately recognized, previously unfolded and imported into its β-ring chamber. Therefore, the RP binds to either one or both ends of the CP in an ATP-dependent manner, recognizes ubiquitylated substrates, facilitates their unfolding, opens the α-ring pore, imports the unfolded substrates into the CP and releases ubiquitin prior to substrate degradation (Eytan et al., 1989; Bhattacharyya et al., 2014). Ubiquitylation alone is not sufficient for the critical decision to degrade a target protein. As a second prerequisite for the final degradation, an unstructured region near the end of the polypeptide to be degraded has to be recognized and bound by the RP base (Prakash et al., 2004; Peth et al., 2010). The proteasome itself is regulated at the level of controlled expression of the proteasome subunit genes and also at the level of subunit assembly into the holoenzyme complex (Marshall and Vierstra, 2019).

1.3.4 E3 ubiquitin ligase families

1.3.4.1 Cullin-RING E3 ubiquitin ligases (CRL)

Cullin (CUL)-RING ligases (CRLs) are multisubunit ubiquitin ligases, that are assembled on a Cullin scaffold and comprise the largest class of ubiquitin ligases. The RING subunit, a zinc-binding RING-H2 domain protein known as RBX1, ROC1 or HRT1, recruits the ubiquitin-conjugating enzyme (E2) to form an active ubiquitin ligase complex (Ohta et al., 1999) (Seol et al., 1999). The CRLs share a similar modular architecture, however the substrate binding unit varies (Figure 5). All cullins interact with the E2-binding RING domain protein via their C-terminus and with substrate receptors via their N-terminus (Zheng et al., 2002b). CUL1-based ligases, also named SKP1-CUL1-F-box (SCF) ubiquitin ligases, recruit substrates through the adaptor protein SKP1, which binds to the F-box protein substrate receptor (Tan et al., 1999). CUL7 also uses SKP1 as an adaptor, which in this case binds to the F-box protein FBXW8 as a substrate receptor. In contrast to SCF ligases, which can assemble with any of the known F-box proteins, CUL7 ligases are limited to FBXW8 (Hopf et al., 2022). Other cullins use other adaptor proteins to bind their substrate receptors, however, they show structural homology to SKP1. CUL2 and CUL5 recruit substrates

through an elongin B/C adaptor and von Hippel-Lindau (VHL)-box or suppressor of cytokine signaling (SOCS)-box proteins (Kamura et al., 2004). In CUL3 complexes Bric-a-brac/Tramtrack/Broad-complex (BTB) domain-containing proteins serve as both adaptors and substrate recognition factors (Furukawa et al., 2003). CUL9 is a poorly characterized member of the CRL family, but has been recently shown to ubiquitylate the substrates cytochrome c and survivin (Lopez and Tait, 2014; Yang et al., 2022). CUL4 ligases contain either CUL4A or CUL4B as a scaffold protein and use DNA damage binding protein 1 (DDB1) as an adaptor, which differs from the adaptors of other CUL complexes, as it is not related to SKP1, elongin B/C or BTB domains (Shiyanov et al., 1999). DDB1 has been initially identified as a protein to recognize DNA lesions and recruit the nucleotide excision repair machinery to remove DNA damage, but is also involved in a variety of other fundamental cellular processes such as transcription, cell cycle and cell death (Nichols et al., 2000; Higa et al., 2003; Cang et al., 2006). For a long time, it was unclear whether DDB1 directly recruits substrates to the CUL4 ubiquitin ligase or whether it depends on another distinct substrate receptor. More recent work revealed the presence of the family of WD40 repeat-containing DDB1-CUL4 associated factor (DCAF) proteins as substrate receptors of the CUL4-DDB1 ubiquitin ligase (He et al., 2006; Higa et al., 2006; Lee and Zhou, 2007). A conserved WDXR motif within DCAFs has been identified as critical for DDB1 binding (Angers et al., 2006).

The activity of all cullin-RING ligases is regulated by neddylation, a process which involves the covalent attachment of the ubiquitin-like protein NEDD8 to a conserved lysine residue within the cullin-homology domain. CUL4A was the first neddylation target to be identified but today, all members of the family of human cullin proteins have been shown to be covalently modified by neddylation (Osaka et al., 1998; Hori et al., 1999). For SCF ubiquitin ligase complexes, NEDD8 modification of the complex subunit CUL1 has been shown to activate ubiquitylation of the target proteins IκBα (Read et al., 2000) and $p27^{Kip1}$ (Morimoto et al., 2000), possibly due to enhanced recruitment of ubiquitin-linked E2 enzyme to the E3 ligase complex (Kawakami et al., 2001). The COP9 signalosome (CSN) counteracts the neddylation and activation of ubiquitin ligases by detaching NEDD8 that is conjugated to cullins, thereby decreasing the recruitment of E2s (Lyapina et al., 2001; Yang et al., 2002). Furthermore, non-neddylated cullins bind tightly to CAND1, which prevents the association between

CUL1 and SKP1/SKP2 and thereby regulates the formation of the SCF complex. Dissociation of CAND1 from CUL1 occurs upon neddylation of CUL1 and is coupled to binding of SKP1 and F-box proteins to CUL1 (Zheng et al., 2002a).

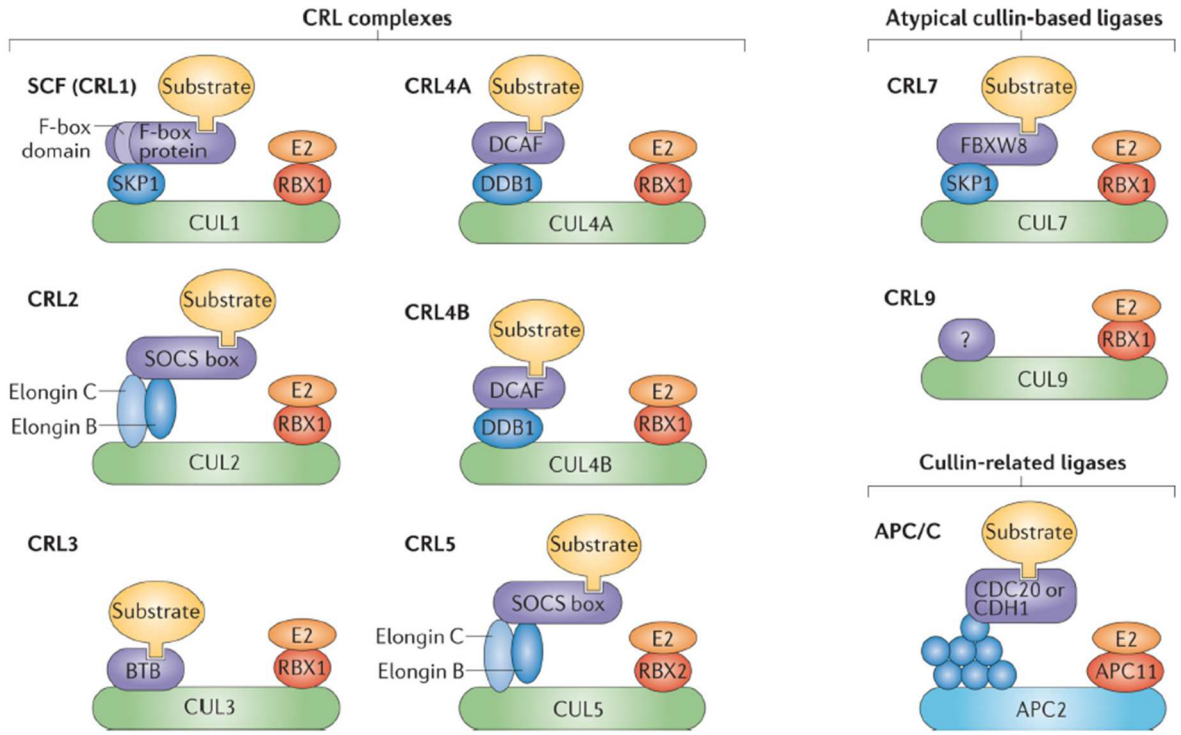

Figure 5: The cullin-RING E3 ligase family.

Cullin (CUL) proteins form the backbone of cullin-RING ligase (CRL) complexes. They bind to a catalytic RING-box protein (RBX1 or RBX2) with E3 ligase activity, which interacts with the E2 enzyme and a cullin-specific, variable substrate receptor module. CRL1, also known as SKP1-CUL1-F-box protein (SCF) complex, uses SKP1 and a variable F-box protein as substrate adaptors, while CRL2 and CRL5 complexes use elongin B, elongin C and SOCS box proteins. CRL3 contains BTB proteins as substrate adaptors and CRL4A and CRL4B use DDB1 as an adaptor which binds to a DCAF protein substrate receptor. CRL7 interacts with SKP1 and the specific F-box protein FBXW8, while the substrate adaptor of CRL9 remains unknown. The anaphase-promoting complex/cyclosome (APC/C) E3 ligase complex contains many more proteins than the CRL complexes but is related to CRLs by the CUL-like APC2 subunit. Adapted from Skaar et al., 2013.

1.3.4.2 HECT E3 ubiquitin ligases

Homologous to E6AP C-terminus (HECT) ubiquitin ligases are a small subfamily of E3 ligases, that ubiquitylate their substrates in a two-step process. All HECT E3 ligases present the catalytic HECT domain, consisting of a larger N-terminal lobe and a smaller C-terminal lobe connected by a short linker region allowing for flexibility, at their C-terminus. For substrate ubiquitylation, they first load activated ubiquitin from the E2 onto themselves through a ubiquitin-thioester intermediate at the active-site cysteine located in the HECT domain. Second, they transfer the ubiquitin to the substrate

(Huang et al., 1999; Verdecia et al., 2003). Based on the structural organization of their N-terminal protein-protein interaction domains for substrate binding, HECT-type E3 ligases can be further subdivided into three sub-families; the NEDD4 family consisting of nine members, the HERC family consisting of six members and the remaining 13 “other” HECT ligases that contain a variety of substrate-binding modules (Scheffner and Kumar, 2014; Weber et al., 2019). The activity of HECT E3 ligases is generally regulated by intra- or intermolecular interactions, which keep the E3 ligase in a catalytically inactive state until conformational changes relieve the inhibitory mechanism (Wiesner et al., 2007; Sander et al., 2017). Since ubiquitin ligases function in a wide range of cellular processes, they are also commonly involved in human pathologies such as cancer. E6AP is one example of a HECT-type E3 ubiquitin ligase reported to be associated with cancer. E6AP promotes human papilloma virus (HPV)-induced cervical cancer by associating with the viral protein E6, which binds to E6AP and its target protein p53, while acting as an allosteric activator of the E6AP ligase, resulting in rapid ubiquitin-dependent degradation of the tumor suppressor p53 (Huibregtse et al., 1993; Scheffner et al., 1993). Interestingly, the CRL4 E3 ligase substrate receptor DCAF1 (VprBP) can also assemble with a HECT-type E3 ubiquitin ligase and act as a substrate receptor of the EDD-DYRK2-DDB1 complex (Maddika and Chen, 2009).

1.3.5 PROTAC and GLUTAC technology for utilizing E3 ubiquitin ligases in cancer therapy

Proteolysis-targeting chimera (PROTAC) technology for targeted protein degradation in cancer therapy has made remarkable advances in recent years. In contrast to small molecule inhibitors, which are widely used in the clinics, PROTACs do not only inhibit the catalytic activity of their target proteins such as oncogenic kinases, but rather induce their degradation in a more specific and more effective manner. PROTAC technology has been first described by Sakamoto et al. in 2001 (Sakamoto et al., 2001). The heterobifunctional PROTAC molecule consists of a ligand which can bind to the target protein of interest and a ligand which binds to an E3 ubiquitin ligase, covalently connected with a small linker. By binding to the target protein and the E3 ubiquitin ligase simultaneously, the PROTAC brings both in close proximity, thereby inducing the ubiquitylation and subsequent proteasomal degradation of the target protein (Figure 6). In 2019, the first two heterobifunctional protein degraders targeting

the androgen and estrogen receptor have entered clinical trials. Today, several PROTACs based on different E3 ubiquitin ligases are used for clinical applications. A majority of these contain the Cullin-RING ubiquitin ligases VHL or CRBN as the recruiting ligase but the first PROTAC created used the $SCF^{\beta\text{-}TrCP}$ ubiquitin ligase to target methionine aminopeptidase-2 (METAP2) for degradation (Sakamoto et al., 2001). Next to PROTACs, there are other types of targeted protein degraders, such as molecular glues, also called GLUTACs. Compared to PROTACs, these are not large heterobifunctional molecules containing two ligands and a linker region, but smaller molecules that promote the ubiquitylation and degradation of the target protein by enhancing the protein-protein interaction between the ubiquitin ligase and the target. The most prominent examples for molecular glue degraders are thalidomide and lenalidomide which co-opt the ubiquitin ligase $CRL4^{CRBN}$ to target the transcription factors IKAROS family zinc finger 1 (IKZF1) and IKZF3 for degradation (Fischer et al., 2014; Krönke et al., 2014; Lu et al., 2014).

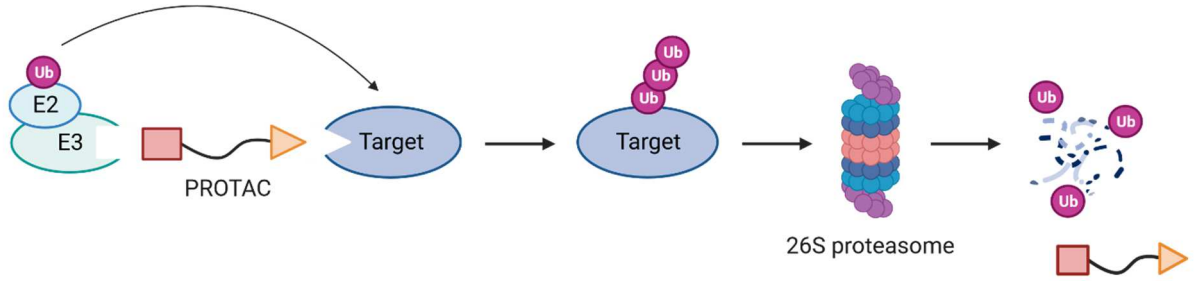

Figure 6: The mechanism of action of PROTACs.
PROTACs are chimeric molecules composed of an E3-binding ligand and a target-binding ligand, connected by a linker. By binding to the target protein and the E3 ubiquitin ligase simultaneously, the PROTAC induces formation of a ternary complex which brings both in close proximity and thereby facilitates the ubiquitylation and subsequent proteasomal degradation of the target protein. Created with BioRender.com.

1.4 SKP1-CUL1-F-box$^{\beta\text{-}TrCP}$ ($SCF^{\beta\text{-}TrCP}$) E3 ubiquitin ligase complex

1.4.1 General introduction to $SCF^{\beta\text{-}TrCP}$

SKP1-CUL1-F-box (SCF) ubiquitin ligases belong to the large family of CUL-RING ubiquitin ligases and are composed of SKP1, CUL1 and an F-box protein which confers substrate specificity (Bai et al., 1996; Skowyra et al., 1997). F-box proteins bind to the adaptor SKP1 via their F-box motif, allowing for their assembly into the complex. Simultaneously, they interact with the specific target protein via a second protein-

protein interaction domain (Bai et al., 1996). Many target proteins of SCF complexes have been identified. Typically, they are recognized by the F-box protein through degradation motifs (degrons or phosphodegrons) and targeted for ubiquitin-mediated degradation in a phosphorylation-dependent manner. Phosphodegrons are the most common mechanism of substrate recognition by F-box proteins but many other degron recognition mechanisms independent of phosphorylation or post-translational modifications are possible (Skaar et al., 2013). β-TrCP and its *Drosophila* homolog Slimb have been identified as F-box proteins of the SCF complex, recognizing destruction motifs in the target proteins in a phosphorylation-dependent manner (Winston et al., 1999). β-TrCP binds the consensus degron Asp-Ser-Gly-X-X-Ser within its substrates, where X represents any amino acid and both Ser residues are phosphorylated, but small variations from the consensus degron, such as a substitution of Ser and Thr residues, are also observed (Lau et al., 2012). Due to the variety of target proteins, the $SCF^{\beta\text{-}TrCP/Slimb}$ E3 ubiquitin ligase complex functions in diverse signaling pathways, such as the NFκB pathway by targeting IκBα (Winston et al., 1999), the Wnt signaling pathway by targeting β-catenin (Hart et al., 1999) or the Hedgehog signaling pathway by targeting the transcription factor Gli2 or its *Drosophila* homolog Cubitus interruptus (Ci) for ubiquitin-mediated degradation (Jiang and Struhl, 1998; Bhatia et al., 2006). Moreover, $SCF^{\beta\text{-}TrCP}$ has been implicated in cell cycle regulation. β-TrCP was shown to target the kinase Wee1 for ubiquitin-dependent degradation, which is essential for rapid activation of Cdc2 at the onset of mitosis (Watanabe et al., 2004) and the phosphatase Cdc25A, which dephosphorylates and activates cyclin-dependent kinases (CDKs) (Jin et al., 2003).

1.4.2 $SCF^{\beta\text{-}TrCP}$ in the regulation of PLK4

Involvement of the $SCF^{\beta\text{-}TrCP}$ ubiquitin ligase complex in regulating centrosome duplication was initially demonstrated by studies observing localization of the complex components SKP1 and CUL1 to the centrosome (Freed et al., 1999). Furthermore, expression of a dominant negative CUL1 mutant was shown to lead to the formation of supernumerary centrosomes in mammalian cells (Piva et al., 2002). Later, the $SCF^{\beta\text{-}TrCP/Slimb}$ E3 ubiquitin ligase has been identified as a critical regulator of PLK4 (Sak in *Drosophila*) protein levels to limit centriole duplication to exactly once per cell cycle (Cunha-Ferreira et al., 2009; Rogers et al., 2009). Human PLK4 dimerizes via its C-terminal coiled-coil region and autophosphorylates amino acid residues S285 and

T289 in *trans*, which allows for the interaction with β-TrCP, ubiquitylation by the $SCF^{β\text{-}TrCP}$ complex and subsequent proteasomal degradation (Guderian et al., 2010; Holland et al., 2010). Depletion of β-TrCP was shown to stabilize PLK4 protein levels and to induce centriole overduplication. Additionally, inhibition of proteasomal degradation by treatment of cells with the 26S proteasome inhibitor MG132 also increased PLK4 protein levels, as expected (Guderian et al., 2010). However, a PLK4 mutant which is not phosphorylatable at positions 285 and 289 due to serine/ threonine to alanine substitutions, was only partially stabilized, indicating that a second, β-TrCP-independent pathway might contribute to the regulation of PLK4 protein levels (Holland et al., 2010). Apart from that, the ubiquitin ligase Mind bomb 1 (MIB1) has been identified as an interaction partner of PLK4 and shown to ubiquitylate PLK4 to regulate its protein levels, however, the possibility that the observed effects are based on an indirect mechanism could not be excluded in this study (Čajánek et al., 2015).

1.5 DCAF1 – Substrate receptor of the CUL4-DDB1-DCAF1 ($CRL4^{DCAF1}$) E3 ubiquitin ligase complex

1.5.1 General introduction to DCAF1

DCAF1, also known as Vpr binding protein (VprBP), was originally identified by co-immunoprecipitation experiments as an interaction partner of the human immunodeficiency virus (HIV) viral protein Vpr (Zhao et al., 1994; Zhang et al., 2001). Various functions of Vpr have been reported, among them mediating nuclear import of the viral preintegration complex (Connor et al., 1995), inducing cell cycle arrest in G2 phase (He et al., 1995; Re et al., 1995; Bartz et al., 1996) and inducing apoptosis (Stewart et al., 1997; Jacotot et al., 2000). Vpr was shown to coprecipitate with DCAF1 and DDB1, components of the CUL4A/B-DDB1-DCAF1 E3 ubiquitin ligase complex, which was further demonstrated to be involved in the Vpr-induced G2 phase arrest (Tan et al., 2007). DCAF1 belongs to the DDB1-CUL4 associated factors (DCAFs), a family of WD40 repeat proteins which confer substrate specificity to the ubiquitin ligase complex (Angers et al., 2006). DDB1 specifically attaches to CUL4 and can bind numerous different DCAFs (He et al., 2006; Higa et al., 2006). Examples for DCAF proteins are DCAF5, which specifically targets the DNA methyltransferase DNMT1 and the transcription factor E2F1 for proteolysis (Leng et al., 2018) or DCAF12, which recognizes a specific degron motif within its substrates (Pla-Prats et al., 2023). The

substrate receptor DCAF1 is attached to the CUL4-DDB1 ubiquitin ligase machinery via the so-called double DxR motif within its WD40 domain (Angers et al., 2006) (Figure 7). The activity of the $CRL4^{DCAF1}$ complex is regulated by its oligomerization state; upon neddylation the tetrameric, auto-inhibited complex switches to a dimeric, active conformation (Mohamed et al., 2021).

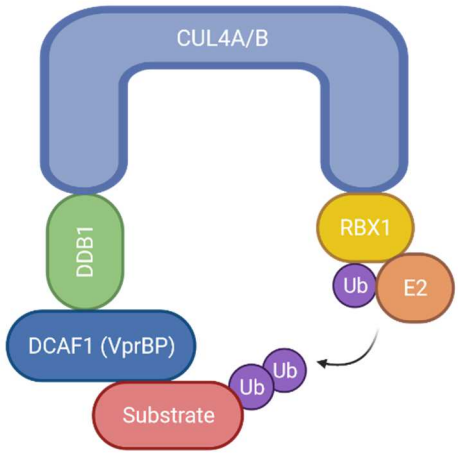

Figure 7: Composition of the CUL4A/B-DDB1-DCAF1 complex.
CUL4A/B forms the scaffold protein and binds to both RING-box protein 1 (RBX1), which recruits the E2-ubiquitin complex, as well as to the substrate recognition unit consisting of DNA damage binding protein 1 (DDB1) and the DDB1-CUL4 associated factor (DCAF) protein DCAF1, also referred to as Vpr-binding protein (VprBP). Adapted from Zhou et al., 2020b. Created with BioRender.com.

Interestingly, DCAF1 can also function as a substrate receptor of the HECT-type E3 ubiquitin ligase complex EDD(UBR5)-DYRK2-DDB1-DCAF1. In this complex, the dual specificity tyrosine-phosphorylation regulated kinase 2 (DYRK2) functions as an adaptor connecting EDD to the DDB1-DCAF1 complex (Maddika and Chen, 2009). Katanin p60 was identified as a downstream substrate of the complex, which is phosphorylated by DYRK2 and subsequently ubiquitylated by the EDD E3 ubiquitin ligase (Maddika and Chen, 2009). Another substrate targeted for ubiquitin-dependent degradation is the telomerase subunit telomerase reverse transcriptase (TERT). The viral protein Vpr promotes binding of the substrate receptor DCAF1 to the substrate TERT, which facilitates EDD-mediated ubiquitylation and subsequent proteasomal degradation of TERT, resulting in loss of telomerase activity (Wang et al., 2013).

1.5.2 DCAF1 domain organization

While most DCAFs consist primarily of a WD40 domain for mediating protein-protein interactions (Higa et al., 2006), DCAF1 demonstrates a complex domain architecture

(Figure 8). It is comprised of an N-terminal armadillo domain (Arm), a central Lissencephaly type-1-like homology motif (LisH) domain, a helix-loop-helix (HLH) and WD40 domain closer to the C-terminus and a highly acidic C-terminal tail (Higa et al., 2006; Jin et al., 2006). The HLH and WD40 domain together have been shown to mediate DDB1 binding, which in turn bridges DCAF1 to the cullin scaffold (Mohamed et al., 2021). The LisH domain has been implicated in DCAF1 dimerization (Ahn et al., 2011). The WD40 domain was shown to be essential for formation of the tetrameric, auto-inhibited CRL4^{DCAF1} complex which counteracts neddylation. Substrate binding works hand-in-hand with neddylation and induces and maintains a dimeric conformation of the complex, which represents the active state of the ubiquitin ligase (Mohamed et al., 2021). DCAF1 binds its substrates and other interaction partners that are either regulated by DCAF1 or act as regulators of the E3 ligase, such as p53, MCM10, Merlin or CEP78, via the C-terminal WD40 or Acidic domain (Li et al., 2010; Kaur et al., 2012; Wang et al., 2016; Hossain et al., 2017).

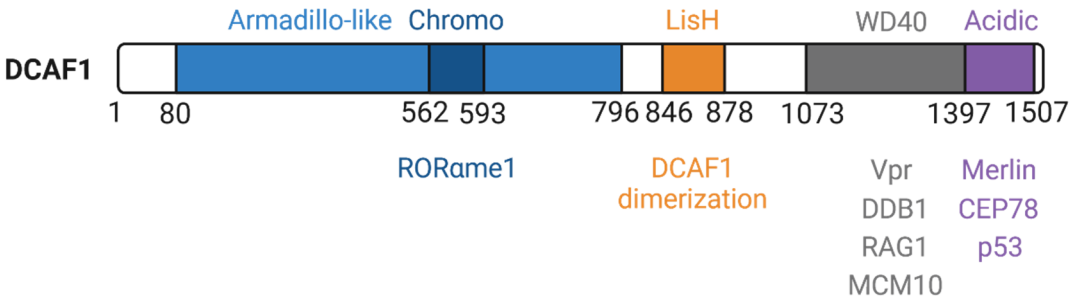

Figure 8: Domain organization of human DCAF1.
Isoform 1 of human DCAF1 is a 1507 amino acid protein with distinct domains, marked by the numbers of amino acids. Domain features and DCAF1-interacting proteins are color-coded and shown below the domain mediating the association. Adapted from Nakagawa et al., 2013 and Schabla et al., 2019. Created with BioRender.com.

1.5.3 Functions of DCAF1 in physiology and cancer

The CRL4^{DCAF1} complex is the second most abundant ubiquitin ligase complex among all CRL4 complexes, rendering DCAF1 a critical substrate receptor of the CUL-RING ubiquitin ligase system (Reichermeier et al., 2020). Germline depletion of *Dcaf1* was shown to be embryonically lethal before embryonic day 7.5 (E7.5) in mice (McCall et al., 2008). While DCAF1 is highly evolutionary conserved in mammals, *Drosophila*, *Xenopus* and *Caenorhabditis elegans* and ubiquitously expressed in all tissues and organs, there is no homolog in yeast (Zhang et al., 2001). Via targeting numerous

substrate proteins, DCAF1 is involved in the regulation of fundamental cellular processes and DCAF1 deficiency has been associated with defects in cell cycle, cell division and cell survival (Schabla et al., 2019). The tumor suppressor p53 has been shown to be negatively regulated by DCAF1, however, the exact mechanism by which DCAF1 ubiquitylates p53 and whether it cooperates with the E3 ligase MDM2 remains unclear (Guo et al., 2016). Another tumor suppressor protein linked to DCAF1 activity is Merlin, encoded by the neurofibromatosis type II (NF2) gene, which is mutated in several glial cancers (Ammoun and Hanemann, 2011). However, instead of being a substrate of the $CRL4^{DCAF1}$ E3 ubiquitin ligase, Merlin was shown to inhibit $CRL4^{DCAF1}$ and thereby exert its tumor-suppressive function (Li et al., 2010). The exact mechanism how Merlin interferes with substrate ubiquitylation of $CRL4^{DCAF1}$ and whether the degradation of only certain or all DCAF1 substrates is inhibited by Merlin, remains unclear. DCAF1 is further involved in cell cycle progression and cell proliferation by regulating the transcription factor FoxM1 (Wang et al., 2017). Interestingly, DCAF1 was shown to not only ubiquitylate and degrade FoxM1 mainly during S phase of the cell cycle, but also to transcriptionally co-activate FoxM1 during G2/ M phase. In this context, DCAF1 was found to be upregulated in human high-grade serous ovarian cancer (HGSOC) samples, which correlates with the increased expression of FoxM1 target genes driving cell proliferation (Wang et al., 2017). Interestingly, DCAF1 was also shown to possess serine/threonine kinase activity and phosphorylate histone H2A at threonine 120. Increased DCAF1 expression and kinase activity were associated with tumor growth and accordingly, a small molecule inhibitor of DCAF1 kinase activity, demonstrating tumoristatic effects in mice, has been developed (Kim et al., 2013a).

1.6 Objectives

Centrosome duplication is a tightly controlled process, as centrosome amplification has been associated with cancer. PLK4 is known as the master regulator of centrosome duplication and its activity as well as its protein abundance are tightly regulated to ensure correct centriole and centrosome numbers. The $SCF^{\beta\text{-TrCP}}$ E3 ubiquitin ligase has been shown to recognize PLK4 upon trans-autophosphorylation of a degron motif and regulate its protein levels by ubiquitylation and proteasomal degradation. However, it was also shown that a β-TrCP binding mutant of PLK4, which is non-phosphorylatable within the β-TrCP recognition motif, was still ubiquitylated and partly degraded, indicating that other ubiquitin ligases might be involved in the regulation of PLK4 ubiquitylation and degradation (Rogers et al., 2009; Holland et al., 2010; Klebba et al., 2013). In a previous immunoprecipitation- and mass spectrometry-based screening approach, DCAF1 has been identified as a novel interaction partner of PLK4. DCAF1 serves as a substrate recognition factor in the cullin-RING E3 ubiquitin ligase complex CUL4-DDB1-DCAF1 ($CRL4^{DCAF1}$), suggesting that this might be a second ubiquitin ligase involved in the regulation of PLK4 protein levels.

In the presented thesis, I aim at characterizing the $CRL4^{DCAF1}$ ubiquitin ligase as a novel regulator of PLK4. This contributes to a more detailed understanding of the regulation of PLK4 protein abundance and thereby centriole duplication and might pave the way for the development of $CRL4^{DCAF1}$-based PROTAC or GLUTAC technology for the targeted degradation of overexpressed PLK4 as a novel approach for cancer therapy. First, I investigate the interaction between PLK4 and the substrate receptor DCAF1 in detail and identify the interacting domains of both proteins. By either overexpression or depletion of proteins in immortalized human cell lines or cancer cell lines, I analyze whether PLK4 is a ubiquitylation target of $CRL4^{DCAF1}$ and whether DCAF1 is thereby involved in the regulation of PLK4 protein levels. Finally, I investigate the function of $CRL4^{DCAF1}$ in the centriole duplication process downstream of PLK4, by analyzing its involvement in the interaction between PLK4 and its substrate STIL and in the process of centriole disengagement at the onset of centriole biogenesis.

2. Materials and Methods

2.1 Materials

2.1.1 Chemicals and reagents

Table 1: Chemicals and reagents

Chemical/ Reagent	Source
0.05 % Trypsin-EDTA	Gibco
1 kb DNA ladder	Thermo Fisher Scientific
100 bp DNA ladder	Thermo Fisher Scientific
3x Flag peptide	Thermo Fisher Scientific
Acrylamide solution	Sigma-Aldrich
Agarose	VWR Chemicals
Ammonium persulfate (APS)	Carl Roth
Ampicillin	AppliChem
Aprotinin	Roche
Bio-Rad Protein Assay	Bio-Rad
Bovine Serum Albumin (BSA)	Sigma-Aldrich
Cycloheximide	Santa Cruz Biotechnology
Dimethylsulfoxide (DMSO)	Sigma-Aldrich
Dithiothreitol (DTT)	Carl Roth
DNA polymerase GoTaq MasterMix	Promega
Doxycycline	Sigma-Aldrich
DPBS	Gibco
Dulbecco’s Modified Eagle’s Medium (DMEM)	Gibco
EGTA	Sigma-Aldrich
Ethanol	Sigma-Aldrich
Ethylenediaminetetraacetic acid (EDTA)	Carl Roth
Fetal bovine serum (FBS)	Gibco
Flag M2 affinity gel	Sigma-Aldrich
Formaldehyde solution	Sigma-Aldrich

Ganciclovir	Alpha Diagnostic Intl. Inc.
GFP-trap agarose	I. Hoffmann, DKFZ
Glutathione, reduced	Sigma-Aldrich
Glycerol	Thermo Fisher Scientific
Glycine	Carl Roth
HA beads	Thermo Fisher Scientific
HA peptide	MedChemExpress
Imidazole	Sigma-Aldrich
Immobilized reduced glutathione CL-4B sepharose	Sigma-Aldrich
IPTG	Biomol
Isopropanol	VWR Chemicals
Kanamycin	AppliChem
LB medium	Carl Roth
LB-Agar	Carl Roth
LDS sample buffer 4x	Invitrogen
Leupeptin	Roche
Lipofectamine 2000	Invitrogen
Lysozyme	Carl Roth
Magnesium chloride	Merck
Methanol	Sigma-Aldrich
MG132 (Z-Leu-Leu-Leu-al)	Sigma-Aldrich
Milk powder	Gerbu
MLN4924	Cell Signaling Technology
N-ethylmaleimide (NEM)	Sigma-Aldrich
N,N,N',N'-Tetramethylethylenediamine (TEMED)	Carl Roth
Ni-NTA agarose	Qiagen
Nocodazole	Merck
Nonidet NP40 (Igepal)	MP Biochemicals
Nuclease-free water	Dharmacon
OptiMEM	Gibco

Penicillin-Streptomycin	Sigma-Aldrich
PIN	Roche
PIPES	Sigma-Aldrich
Poly-D-Lysine	Gibco
Polyethylenimine linear 25000 Da	Polysciences
Ponceau S solution	Serva
ProLong Gold Antifade Mountant	Invitrogen
Protein G sepharose	GE Healthcare
Protein ladder prestained	neoLab
Puromycin	Sigma-Aldrich
RO-3306	Merck
ROTI®Quant	Carl Roth
Rotiphorese Gel 30 acrylamide/bisacrylamide 37.5:1	Carl Roth
Sodium azide	Merck
Sodium chloride	Sigma-Aldrich
Sodium dodecyl sulfate (SDS)	Carl Roth
Sodium fluoride	Merck
Sodium hydroxide	J. T. Baker
Sodium vanadate	Sigma-Aldrich
StainIN RED Nucleic Acid Stain	HighQu
T4 DNA ligase	Thermo Fisher Scientific
Thymidine	Santa Cruz Biotechnology
TLCK	Roche
TPCK	Roche
TRIS base	Serva
Triton X-100	Sigma-Aldrich
Tween 20	Sigma-Aldrich
Urea	Thermo Fisher Scientific
Western Chemiluminescence HRP-substrate	Merck
β-Glycerophosphate	Sigma-Aldrich

β-Mercaptoethanol	Sigma-Aldrich

2.1.2 Laboratory equipment

Table 2: Laboratory equipment

Name	Specification	Source
Cell culture dishes	Cellstar	Greiner Bio-One
Cell culture incubator	CO_2 Incubator	Sanyo
Centrifuges	5415 R 5810 R RC5C	Eppendorf Eppendorf Sorvall
Coverslips		NeoLab
DNA gel electrophoresis	Mini-Sub Cell	Bio-Rad
Electrotransfer unit	Transblot Turbo	Bio-Rad
Fluorescence microscope	Cell Observer Z1	Zeiss
Freezer (- 20 °C)	MEDLine	Liebherr
Freezer (- 80 °C)	Ultralow	Sanyo
Fridge (4 °C)	ProfiLine	Liebherr
Gel documentation	Gelstick	Intas
Glassware	Glass pipettes, measuring cylinders, flasks, bottles	Brand, Schott
Heat block	Thermomixer comfort Digital Heatblock	Eppendorf VWR
Incubation shaker	Minitron	Infors HT
Laboratory balance	Extend	Sartorius
Light microscope	Axio Vert.A1	Zeiss
Live-cell imaging dish	x-well cell culture chamber	Sarstedt
Luminescent image analyzer	ImageQuant LAS 4000	GE Healthcare
Magnet stirrers	Ikamag RTC	IKA Labortechnik
Microplate absorbance reader	SPECTROstar Nano	BGM Labtech
Microscope slides		Thermo Fisher Scientific
Microwave		Sharp
NanoDrop spectrophotometer	ND-1000	Peqlab

Nitrocellulose membrane	Amersham Protran 0.45 µM	GE Healthcare
PAGE system	Mini Protean III	Bio-Rad
Parafilm	Laboratory film M	Bemis
PCR thermocycler	Mastercycler nexus GX2	Eppendorf
pH meter	Seven Easy	Mettler Toledo
Pipettes	Pipetman	Gilson
Pipettor	Pipetboy	Integra
Plasticware	Reaction tubes, falcon tubes, pipette tips, PCR tubes, petri dishes	Eppendorf, Nerbe, Falcon, Biozym, Greiner Bio-One, TPP
Power supply	PowerPac 200	Bio-Rad
Rocking platform shaker	Rocker 25	Labnet
Rotating wheel	Test tube rotator	Snijders
Sonifier	Sonifier 250	Branson
Sterile workbench	SterilGARD Hood	Baker Company
Vortex shaker	VF2	IKA Labortechnik
Water bath	12B	Julabo EM

2.1.3 Buffers

Table 3: Buffers

Name	Composition
4x Laemmli buffer	0.1 M Tris-HCl pH 6.8 4 % SDS 20 % glycerol 0.1 M DTT 0.02 % bromophenol blue
BRB80 pre-extraction buffer	80 mM PIPES pH 6.8 1 mM $MgCl_2$ 1 mM EGTA 0.1 % Triton X-100

In vitro ubiquitylation assay buffer	50 mM Tris-HCl pH 7.5 100 mM NaCl 10 mM $MgCl_2$ 0.05 % NP-40 Added before use: 1 mM DTT 0.1 mM Na_3VO_4 1 µg/ml Aprotinin 1 µg/ml Leupeptin 10 µg/ml Trypsin inhibitor from soybean
NP-40 buffer	40 mM Tris-HCl pH 7.5 150 mM NaCl 5 mM EDTA 10 mM β-glycerophosphate 5 mM NaF 0.5 % NP-40 Added before use: 1 mM DTT 10 µg/ml TPCK 5 µg/ml TLCK 0.1 mM Na_3VO_4 1 µg/ml Aprotinin 1 µg/ml Leupeptin 10 µg/ml Trypsin inhibitor from soybean
PBS	137 mM NaCl 2.7 mM KCl 1.8 mM KH_2PO_4 10 mM Na_2HPO_4 pH 7.4
PBST	0.1 % Tween-20 in PBS
Protein purification bacteria lysis buffer	50 mM Tris-HCl pH 7.0 300 mM NaCl 0.1 % NP-40 5 % Glycerol 5 mM EDTA Added before use: 1 mg/ml lysozyme 5 mM β-Mercaptoethanol 10 µg/ml TPCK

	5 µg/ml TLCK 0.1 mM Na_3VO_4 1 µg/ml Aprotinin 1 µg/ml Leupeptin 10 µg/ml Trypsin inhibitor from soybean
Protein purification dialysis buffer	Bacteria lysis buffer without lysozyme 1 mM DTT
Protein purification elution buffer	Bacteria lysis buffer without lysozyme 10 mM reduced glutathione
Protein purification washing buffer	Bacteria lysis buffer without lysozyme
RIPA buffer	50 mM Tris-HCl pH 7.4 150 mM NaCl 2 mM EDTA 50 mM NaF 1 % NP-40 0.5 % Na-deoxycholate 0.1 % SDS Added before use: 1 mM DTT 10 µg/ml TPCK 5 µg/ml TLCK 0.1 mM Na_3VO_4 1 µg/ml Aprotinin 1 µg/ml Leupeptin 10 µg/ml Trypsin inhibitor from soybean
SDS running buffer	25 mM Tris-HCl pH 8.3 190 mM glycine 0.1 % SDS
TAE buffer	40 mM Tris-HCl pH 7.6 20 mM acetic acid 1 mM EDTA
TBS	50 mM Tris-HCl pH 7.4 150 mM NaCl
TBST	0.05 % Tween-20 in TBS
U-ExM denaturation buffer	50 mM Tris-HCl pH 9.0 200 mM NaCl 200 mM SDS

U-ExM monomer solution	23 % w/v Sodium acrylate 10 % w/v Acrylamide 0.1 % w/v Bisacrylamide in PBS
Urea buffer	8 M Urea 0.1 M potassium phosphate pH 8.0 Added before use: 30 mM imidazole 20 mM N-ethylmaleimide 1 mM DTT 10 µg/ml TPCK 5 µg/ml TLCK 0.1 mM Na_3VO_4 1 µg/ml Aprotinin 1 µg/ml Leupeptin 10 µg/ml Trypsin inhibitor from soybean
Western blot blocking solution	5 % milk powder in PBST

2.1.4 Antibodies

2.1.4.1 Primary antibodies

Table 4: Primary antibodies

Target protein	Origin	Dilution	Clone	Source
Acetyl. Tubulin	mouse	1:500 (U-ExM)	6-11B-1	Sigma-Aldrich
Centrin	mouse	1:500 (IF)	20H5	Merck
CEP152	mouse	1:750 (WB)	P1285	Thermo Fisher
CEP192	rabbit	1:500 (WB)	A302-324A	Bethyl
CUL4	mouse	1:500 (WB)	H-11	Santa Cruz
Cyclin B1	rabbit	1:1000 (WB)		(Hoffmann et al., 1993)
Cyclin E1	mouse	1:1000 (WB)	HE12	Santa Cruz
DCAF1	mouse	1:1000 (WB)	C-8	Santa Cruz
DCAF5	rabbit	1:500 (WB)		Innovagen AB, Lund, Sweden
DDB1	rabbit	1:1000 (WB)	A300-462A	Bethyl
EDD	mouse	1:500 (WB)	B-11	Santa Cruz

Flag	mouse	1:5000 (WB)	M2 (F3165)	Sigma-Aldrich
H3 pS10	rabbit	1:1000 (WB)	06-570	Merck
HA-tag	mouse	1:1000 (WB)	16B12	Babco
NEDD1	mouse	1:500 (IF)	H-3	Santa Cruz
Normal mouse IgG	mouse	4 µg (IP)		Santa Cruz
Pericentrin	rabbit	1:2000 (IF)	ab4448	Abcam
PLK4	mouse	1:500 (WB)		Cizmecioglu et al., 2010
PLK4 pS305	rabbit	1:250 (WB)		Park et al., 2014
STIL	rabbit	1:1000 (WB)	A302-442A	Bethyl
α-Tubulin	mouse	1:10000 (WB), 1:1000 (IF)	B-5-1-2	Sigma-Aldrich
α-Tubulin	rabbit	1:500 (U-ExM)		Proteintech
β-TrCP	rabbit	1:1000 (WB)	D13F10	Cell Signaling
β-Tubulin	rabbit	1:500 (U-ExM)		Proteintech
γ-Tubulin	mouse	1:1000 (IF)	GTU-88	Sigma-Aldrich

2.1.4.2 Secondary antibodies

Table 5: Secondary antibodies

Antibody	Origin	Dilution	Source
Anti-mouse IgG HRP	goat	1:5000 (WB)	Novus
Anti-rabbit IgG HRP	donkey	1:5000 (WB)	Jackson Laboratories
Anti-mouse IgG Alexa 488	goat	1:1000 (U-ExM) 1:2000 (IF)	Invitrogen
Anti-rabbit IgG Alexa 488	goat	1:2000 (IF)	Invitrogen
Anti-mouse IgG Alexa 594	goat	1:2000 (IF), 1:1000 (U-ExM)	Invitrogen
Anti-rabbit IgG Alexa 594	goat	1:1000 (U-ExM) 1:2000 (IF)	Invitrogen
Anti-mouse IgG_{2a} Alexa 594	goat	1:2000 (IF)	Invitrogen
Anti-mouse IgG_1 Alexa 488	goat	1:2000 (IF)	Invitrogen

2.1.5 Small interfering RNAs (siRNAs)

Table 6: Small interfering RNAs

Name	Sequence sense (5' – 3')	Source
siGL2	CGUACGCGGAAUACUUCGAdTdT	Wang et al., 2006
siDCAF1 #1	UCACAGAGUAUCUUAGAGAdTdT	Nakagawa et al., 2015
siDCAF1 #2	CGGAGUUGGAGGAGGACGAUUdTdT	Hakata et al., 2014
siDCAF5	GCAGAAACCUCUACAAGAAdTdT	Ambion
siPLK4	GGUAGUACUAGUUCACCUAdTdT	Ambion

2.1.6 Primers

Table 7: Primers

Name	Sequence (5' – 3')	No.
DCAF1_miRNA_sense	GCGATCACAGAGTATCTTAGAGATTCTGTGAAGCCACAG ATGGGAATCTCTAAGATACTCTGTGA	1
DCAF1_miRNA_antisense	GCAGTCACAGAGTATCTTAGAGATTCCCATCTGTGGCTTC ACAGAATCTCTAAGATACTCTGTGA	2
PLK4_flank_A	GATAAAGCCCGGGCGGGATCCGGAAATATGG	3
PLK4_flank_D	GCCCCCCCTCGAGGGCTCAATGAAAAT	4
PLK4_I602E_mut_B	GGTTTTCTGTCTCTCTGGTTTTAACCTGTGAGC	5
PLK4_I602E_mut_C	GCTCACAGGTTAAAACCAGAGAGACAGAAAACC	6
PLK4_K608A_mut_B	GCTCACCACAGCCGCTTTGGTTTTCTGTCTG	7
PLK4_K608A_mut_C	CAGACAGAAAACCAAAGCGGCTGTGGTGAGC	8
PLK4_R691A_mut_B	CTTACAAGCTGTACAAACGCGGAAGCATATTG	9
PLK4_R691A_mut_C	CAATATGCTTCCGCGTTTGTACAGCTTGTAAG	10
PLK4_K699A_mut_B	GTGATTTTGGGAGATGCAGATCTTACAAGCTG	11
PLK4_K699A_mut_C	CAGCTTGTAAGATCTGCATCTCCCAAAATCAC	12
PLK4_K748A_mut_B	CTTTTTAAAGTGTAAGACGCCCCTGTCTTTTCAATCACC	13
PLK4_K748A_mut_C	GGTGATTGAAAAGACAGGGGCGTCTTACACTTTAAAAAG	14
PLK4_K753A_mut_B	CTTCACTTTCACTTGCTAAAGTGTAAGACTTCCCTGTC	15
PLK4_K753A_mut_C	GACAGGGAAGTCTTACACTTTAGCAAGTGAAAGTGAAG	16

2.1.7 Plasmids

Plasmids that were provided are listed below.

Table 8: Provided plasmids

Plasmid name	Source
pCMV-3Tag2A	Agilent Technologies
pPK-CMV-HA-UbiquitinC	F. Rösl, DKFZ Heidelberg
pCMV-3Tag1A	Agilent Technologies
pCMV-3Tag1A-PLK4	Cizmecioglu et al., 2010
pCMV-3Tag1A-PLK4_K41R	Cizmecioglu et al., 2010
pCMV-3Tag1A-PLK4_AA	A. Kratz, DKFZ Heidelberg
pCMV-3Tag1A-PLK4_ ΔPEST	A. Kratz, DKFZ Heidelberg
pCMV-3Tag1A-PLK4_1-285	Cizmecioglu et al., 2010
pCMV-3Tag1A-PLK4_1-580	Cizmecioglu et al., 2010
pCMV-3Tag1A-PLK4_581-879	Cizmecioglu et al., 2010
pCMV-3Tag1A-PLK4_581-971	Cizmecioglu et al., 2010
pCMV-3Tag1A-PLK4_1-879	Cizmecioglu et al., 2010
pCMV-3Tag1A-PLK4_286-971	Cizmecioglu et al., 2010
pCMV-3Tag1C-DCAF1	A. Kratz, DKFZ Heidelberg
pCMV-Sport6-Flag-DCAF1	V. Planelles, University of Utah
pCMV-Sport6-Flag-DCAF1_Arm	V. Planelles, University of Utah
pCMV-Sport6-Flag-DCAF1_ΔArm	V. Planelles, University of Utah
pCMV-Sport6-Flag-DCAF1_WD40-Acidic	V. Planelles, University of Utah
pCMV-Sport6-Flag-DCAF1_ΔWD40-ΔAcidic	V. Planelles, University of Utah
pCMV-Sport6-Flag-DCAF1_WD40	V. Planelles, University of Utah
pCMV-Sport6-Flag-DCAF1_Acidic	V. Planelles, University of Utah
pCMV-Sport6-Flag-DCAF1_ΔAcidic	V. Planelles, University of Utah
pBi9	O. Gruss, ZMBH Heidelberg
pCAGGS-flpE	Addgene #20733
pcDNA3.1(+)-HA	F. Settele, DKFZ Heidelberg

pcDNA3.1(+)-HA-DCAF1	Vector and Clone Repository, DKFZ Heidelberg
pSG5-His-Myc-Ubiquitin	M. Scheffner, University of Konstanz
pGEX-4T3-DCAF1	S. Suzuki, DKFZ Heidelberg

Plasmids that were generated in the presented thesis are listed below.

Table 9: Plasmids generated in this thesis

Plasmid name	Template	Primers	Enzymes
pBi9-miRNA-DCAF1	pBI9	1, 2	BsaI
pCMV-3Tag1A-PLK4_I602E	pCMV-3Tag1A-PLK4	3 – 6	BamHI, XhoI
pCMV-3Tag1A-PLK4_K608A	pCMV-3Tag1A-PLK4	3, 4, 7, 8	BamHI, XhoI
pCMV-3Tag1A-PLK4_R691A	pCMV-3Tag1A-PLK4	3, 4, 9, 10	BamHI, XhoI
pCMV-3Tag1A-PLK4_K699A	pCMV-3Tag1A-PLK4	3, 4, 11, 12	BamHI, XhoI
pCMV-3Tag1A-PLK4_K748A	pCMV-3Tag1A-PLK4	3, 4, 13, 14	BamHI, XhoI
pCMV-3Tag1A-PLK4_K753A	pCMV-3Tag1A-PLK4	3, 4, 15, 16	BamHI, XhoI

2.1.8 Bacterial strains

Table 10: Bacterial strains

Strain	Genotype	Source
E. coli XL1-Blue	*recA1 endA1 gyrA96 thi-1 hsdR17 supE44 relA1 lac* [F' *proAB lacI*^{q}ZΔ*M15* Tn*10* (Tet^r)]	Agilent Technologies
E. coli Top10 One Shot	F-*mcrA* Δ(*mrr-hsd*RMS-*mcr*BC) Φ80*Lac*ZΔM15 Δ *Lac*X74 *rec*A1 *ara*D139 Δ(*araleu*) 7697 *gal*U *gal*K *rps*L (StrR) *end*A1 *nup*G	Thermo Fisher Scientific
E. coli DH5α MAX Efficiency	F$^-$ Φ80*lac*ZΔM15 Δ(*lac*ZYA-*arg*F) U169 *rec*A1 *end*A1 *hsd*R17 (rk$^-$, mk$^+$) *pho*A *sup*E44 λ$^-$*thi*$^-$1 *gyr*A96 *rel*A1	Thermo Fisher Scientific
E. coli Rosetta (DE3)	F$^-$*ompT hsDS*$_B$(r$_B^-$m$_B^-$) *gal dcm* (DE3= pRARE2 (Cam^R)	Merck

2.1.9 Cell lines

Table 11: Cell lines

Name	Cell type	Source
HEK293T	Human epithelial embryonic kidney cells expressing the SV-40 large T-antigen	DSMZ, Braunschweig
HeLa	Human epithelial cervix adenocarcinoma cells transformed by HPV18	ATCC
HeLa S/A	Modified HeLa cell line, contains a silent but activatable (S/A) locus, which is active in the presence of doxycycline and can be used to insert gene of interest	O. Gruss, ZMBH Heidelberg
HeLa tet-on shDCAF1	Stable HeLa cell line with doxycycline-inducible knockdown of DCAF1	This work
HeLa tet-on GFP-PLK4	Stable HeLa cell line with doxycycline-inducible overexpression of GFP-PLK4	T. Mayer, University of Konstanz
U2OS	Human osteosarcoma cells	ATCC

2.1.10 Kits

Table 12: Kits

Name	Source
GenElute HP Plasmid Miniprep Kit	Sigma-Aldrich
GenElute HP Plasmid Midiprep Kit	Sigma-Aldrich
GenElute HP Plasmid Maxiprep Kit	Sigma-Aldrich
NucleoSpin Gel and PCR Clean-up Kit	Macherey-Nagel

2.1.11 Antibiotics

Table 13: Antibiotics

Antibiotic	Stock concentration	Working concentration
Ampicillin	100 mg/ml	100 µg/ml
Kanamycin	50 mg/ml	50 µg/ml
Puromycin	2.5 mg/ml	2.5 µg/ml
Doxycycline	2 mg/ml	2 µg/ml

2.2 Methods

2.2.1 Methods in molecular biology

2.2.1.1 Polymerase chain reaction (PCR) and site-directed mutagenesis

DNA sequences were amplified by polymerase chain reaction (PCR) for cloning or in order to introduce mutation sites. For subcloning into a different backbone vector, forward and reverse primers containing restriction enzyme sites were used to attach these sites to the amplified DNA sequence and allowing for the insertion of this sequence into the target backbone after restriction digest. Site-directed mutagenesis was performed according to the protocol by Heckman and Pease (Heckman and Pease, 2007). Briefly, two overlapping fragments were generated using a forward and reverse primer each. Mutations were introduced within the overlapping part in each fragment, by one primer containing the desired mutation. The products were then used as templates for an overlapping PCR, resulting in one DNA fragment carrying the desired mutation.

PCR reactions were performed using the GoTaq G2 Hotstart Green Master Mix (Promega) and were set-up as shown below:

GoTaq G2 Hotstart Green Master Mix (Promega)	25 µl
Template DNA	200 ng
Forward primer	300 nM
Reverse primer	300 nM
Nuclease-free H_2O	ad 50 µl

PCR reactions were carried out in a thermocycler (Eppendorf) with the following settings:

Initial denaturation	95 °C	4 min	
Denaturation	95 °C	1 min	x 30
Annealing	50 – 72 °C	45 s	
Elongation	72 °C	1 min/ kb	
Final elongation	72 °C	5 min	
Cooling	4 °C		

The annealing temperature was adjusted for each PCR, depending on the melting temperatures of the primers. The elongation time was adjusted to the length of the final

PCR product. PCR products were analyzed by agarose gel electrophoresis and purified using the NucleoSpin Gel and PCR Clean-up Kit (Macherey-Nagel) as described in 2.2.1.2 and 2.2.1.3.

2.2.1.2 Agarose gel electrophoresis

Agarose gel electrophoresis was performed to separate DNA according to size. 0.8 – 2 % agarose gels were prepared by boiling agarose in 1x TAE buffer. 0.05 % StainIN RED Nucleic Acid Stain was added in order to visualize DNA fragments. The agarose solution was poured into a gel chamber and once polymerized, transferred to an electrophoresis chamber (Bio-Rad) and covered with 1x TAE buffer. DNA samples were prepared by addition of 6x DNA sample buffer and loaded to the wells of the gel. A 100 bp or 1 kb DNA ladder was used as a size reference. Agarose gels were run at 80 – 100 V for 45 – 60 min. DNA separated in the agarose gel was visualized under UV light at 366 nm wavelength.

2.2.1.3 Extraction of DNA fragments from agarose gels

Correct DNA fragments were identified under UV light at 366 nm, cut out from the agarose gel using a scalpel and transferred to a reaction tube. DNA was purified from the agarose gel using the NucleoSpin Gel and PCR Clean-up Kit (Macherey-Nagel) according to the manufacturer´s instructions. DNA was eluted with 20 – 30 µl ddH_2O and the DNA concentration was determined using the NanoDrop spectrophotometer as described in 2.2.1.7.

2.2.1.4 Restriction digest of DNA

For further cloning purposes, plasmid DNA or purified PCR products were digested with different combinations of two restriction enzymes (NEB). 1 – 4 µg of plasmid DNA or PCR product were digested using 1 – 2 µl of each restriction enzyme in a total reaction volume of 20 – 40 µl. Digestion reactions were incubated at 37 °C for 2 h and inactivated at 65 °C for 20 min. Digested DNA fragments were separated by agarose gel electrophoresis as described in 2.2.1.2 and the correct fragments were extracted from the agarose gel as described in 2.2.1.3.

2.2.1.5 Ligation of DNA fragments

Following restriction digestion and purification of DNA fragments, they were combined by DNA ligation. 100 ng of linearized backbone and threefold molar amounts of insert

were added to the ligation reaction, which was performed in a total volume of 20 µl using 1 U of T4 DNA ligase (Thermo Fisher Scientific). The reactions were incubated for 1 h at 22 °C and inactivated at 65 °C for 10 min. 10 µl of the final ligation reactions were used to transform chemically competent *E. coli* as described in 2.2.1.6.

2.2.1.6 Transformation of chemically competent *E. coli*

For plasmid amplification and cloning, chemically competent *E. coli* XL1-Blue/Top10/DH5α were transformed with plasmid DNA or ligations. 60 µl of competent *E. coli* were mixed with either 100 ng of plasmid DNA or 10 µl of ligation reactions. Following an incubation on ice for 20 min, bacteria were heat-shocked for 90 s at 42 °C and immediately placed back on ice for another 3 min. 800 µl of LB medium was added and the bacteria were incubated for 1 h at 37 °C with shaking at 400 rpm. For plasmid amplification, 100 µl of the bacteria suspension were spread on an LB agar plate containing the appropriate antibiotic. For cloning, the bacteria were first pelleted at 4000 g for 2 min, the pellet was resuspended in 100 µl of the supernatant and then spread on an LB agar plate. The plate was incubated overnight at 37 °C. For plasmid amplification or cloning purposes, single colonies were picked and used to inoculate LB medium and grow overnight cultures.

2.2.1.7 Plasmid DNA preparation from *E. coli*

Cultures of *E. coli* XL1-Blue/Top10/DH5α bacteria containing plasmid DNA were grown in LB medium supplemented with the appropriate antibiotic at 37 °C and 180 rpm overnight. Bacteria cells were pelleted at 3200 – 5000 g and 4 °C for 20 min. Plasmid DNA was isolated using GenElute HP Plasmid Mini/Midi/Maxiprep Kits (Sigma-Aldrich), depending on the volume of the overnight culture, according to the manufacturer´s instructions. Elutions were performed with ddH_2O. DNA concentration and quality of plasmid DNA were determined using a NanoDrop ND-1000 spectrophotometer (Peqlab). ddH_2O was used as a blank and the optical density of the sample was measured at 230 nm, 260 nm and 280 nm wavelength. The DNA concentration was determined based on the absorbance at 260 nm, while $OD_{260\ nm}$ = 1 corresponds to a DNA concentration of 50 µg/ml. Ratios of $OD_{260\ nm}$ /$OD_{280\ nm}$ ~ 1.8 and $OD_{260\ nm}$ /$OD_{230\ nm}$ between 1.8 and 2.2 indicated high purity of the DNA solution. Plasmid DNA from cloning was sequenced at LGC Genomics, Berlin, Germany.

2.2.2 Methods in cell biology

2.2.2.1 Cell culture

HEK293T, HeLa, HeLa tet-on shDCAF1, HeLa tet-on GFP-PLK4 and U2OS cells were cultured in Dulbecco´s Modified Eagle´s Medium (DMEM) containing 4.5 g/l glucose supplemented with 10 % fetal bovine serum (FBS) and 1 % penicillin/ streptomycin. Cells were grown in a humidified atmosphere at 37 °C and 5 % CO_2. For passaging of cells, the medium was aspirated and cells were washed once with PBS. In order to detach the cells from the cell culture dish, they were incubated with 0.05 % Trypsin-EDTA solution at 37 °C for 3 – 5 min and then resuspended in fresh growth medium and diluted to the desired ratio in a fresh cell culture dish. All cell culture work was performed under sterile conditions. Cell line identities were confirmed by cell line authentication regularly (Multiplexion, Heidelberg).

2.2.2.2 Freezing and harvesting of cells

In order to freeze cells in cryo vials, medium was aspirated, cells were washed once with PBS and detached from the cell culture dish by incubation with 0.05 % Trypsin-EDTA. Detached cells were pelleted by centrifugation at 330 g for 5 min. Cell pellets were resuspended in growth medium supplemented with additional 10 % FBS and 10 % DMSO. Cell suspensions were transferred to 1.5 ml cryo vials and frozen in a freezing container (Nalgene, Thermo Fisher Scientific) at – 80 °C. For short term storage, cryo vials were kept at – 80 °C; for long term storage they were transferred to liquid nitrogen.

In order to harvest cells, medium was aspirated, cells were washed with PBS, detached with 0.05 % Trypsin-EDTA and resuspended in growth medium. HEK293T cells were harvested by scraping cells off the cell culture dish in PBS. Cells were pelleted by centrifugation at 330 g for 5 min. Cell pellets were used for the preparation of cell lysates immediately or stored at – 80 °C.

2.2.2.3 Transfection of mammalian cells

2.2.2.3.1 Plasmid DNA transfection using polyethylenimine (PEI)

HEK293T cells were transiently transfected with plasmid DNA in 15 cm cell culture dishes using polyethylenimine (PEI, Polysciences). Cells were seed 1 – 2 days prior to transfection so that they reached a confluency of 70 – 80 % on the day of

transfection. The transfection mixture was prepared by diluting 10 – 20 µg plasmid DNA in 4.6 ml DMEM without FBS and adding 92.5 µl of a 1 mg/ml PEI stock solution. The mixture was vortexed and incubated for 10 min at room temperature (RT), before 13.9 ml DMEM supplemented with 5 % FBS were added and mixed by vortexing shortly. Medium was aspirated from the prepared cell cultures and the transfection mix was added. Transfected cells were incubated for 24 – 48 h at 37 °C before harvesting.

2.2.2.3.2 Plasmid DNA and siRNA transfection using Lipofectamine 2000

HeLa cells were transfected with plasmid DNA using Lipofectamine 2000 (Invitrogen). Cells were seeded in 6-well plates 1 day prior to transfection so that they reached a confluency of 70 – 80 % on the day of transfection. Two separate mixtures were prepared by diluting 2.8 µg plasmid DNA in 200 µl Opti-MEM (Gibco) and 5 µl Lipofectamine 2000 in 200 µl Opti-MEM. Both mixtures were vortexed and incubated for 5 min at RT separately, before they were combined, vortexed again and incubated for another 15 min at RT. Medium was aspirated from the prepared cell cultures and replaced with 2 ml DMEM supplemented with 5 % FBS. The transfection mix was added dropwise. 6 h after transfection, the transfection medium was replaced with fresh complete medium (10 % FBS, 1 % P/S) and 24 h after transfection, cells were passaged or harvested.

HeLa, U2OS and HEK293T cells were transfected with siRNA using Lipofectamine 2000. Cells were seeded in 6-well plates one day prior to transfection so that they reached a confluency of 50 – 60 % on the day of the first transfection. Two separate mixtures were prepared by diluting 2 µl siRNA from 20 µM stocks in 150 µl DMEM without FBS and 5 µl Lipofectamine 2000 in 150 µl DMEM without FBS. Both mixtures were vortexed and incubated for 5 min at RT separately, before they were combined, vortexed again and incubated for another 15 min at RT. Medium was aspirated from the prepared cell cultures and replaced with 700 µl fresh complete medium. The transfection mix was added dropwise giving a final siRNA concentration of 40 nM. The siRNA transfection was repeated 24 h after the first siRNA transfection. Either 6 h or 24 h after the second siRNA transfection, cells were passaged and 48 h after the second transfection, cells were harvested.

2.2.2.4 Generation of a stable HeLa cell line for inducible knockdown of DCAF1

For the generation of a stable cell line for conditional DCAF1 knockdown, HeLa S/A cells (O. Gruss, ZMBH Heidelberg, Germany) were seeded in 6-well plates. One day after seeding, cells were transfected with 1.3 µg pCAGGS-flpE recombinase (O. Gruss, ZMBH Heidelberg, Germany) and 1.5 µg pBi9-shDCAF1 using Lipofectamine 2000, as described in 2.2.2.3.2. Cells were incubated for 24 h after transfection and then passaged from 6-well plates to 10 cm dishes. Puromycin selection was started by addition of 2.5 µg/ml puromycin to the cell culture medium. After 24 h, puromycin was washed out and fresh complete medium was added to the cells. 10 µM ganciclovir was added to the medium and cells were incubated for 4 days. Remaining cells were released from ganciclovir treatment and cultured in fresh complete medium for 5 days. Single colonies were picked by scraping with a pipette tip and transferred to 24-well plates. Cells were cultured in normal growth medium and passaged to larger cell culture dishes at 70 – 80 % confluency. DCAF1 knockdown was induced by addition of 2 µg/ml doxycycline for 72 h before harvesting.

2.2.2.5 Treatment of cells with MG132, MLN4924 and cycloheximide

HEK293T cells were treated with 10 µM proteasome inhibitor MG132 (Sigma-Aldrich) for 5 h before harvesting or with 5 µM NAE inhibitor MLN4924 for 4 h before harvesting. Cycloheximide chase assays were performed in U2OS cells using 100 µg/ml cycloheximide for the indicated time periods.

2.2.2.6 Cell cycle synchronization

HEK293T cells were synchronized in G1/S phase by double thymidine arrest. Cells were treated with 2 mM thymidine (Santa Cruz Biotechnology) for 18 h, released for 9 h and arrested again for 16 h. For single thymidine and nocodazole arrest in mitosis, cells were treated with 2 mM thymidine for 20 h, released for 2 h and treated with 100 ng/ml nocodazole (Merck) for 16 - 17 h. For G2 phase arrest of HeLa or HEK293T cells, cells were treated with 10 µM RO-3306 for 18 h.

2.2.2.7 Live cell imaging

Cell division of HeLa shDCAF1 cells with or without doxycycline-induced knockdown of DCAF1 was analyzed by live cell imaging. 48 h after doxycycline induction, cells were seeded to 8-well imaging dishes (Sarstedt) at 40 % confluency and cultivated in the presence of 2 µg/ml doxycycline for another 24 h. For imaging, the dish was placed

in a microscopy incubation chamber at 37 °C and 5 % CO_2 and cells were monitored using the Zeiss Observer.Z1 inverted motorized microscope and a 10/0.3 EC PlnN Ph1 DICI objective. Phase-contrast images were taken at multiple positions in each well every 10 min for up to 60 h. Images were analyzed using Fiji software.

2.2.2.8 Immunofluorescence staining and microscopy

HeLa cells grown on glass coverslips were washed with PBS and fixed with ice-cold methanol for 10 min at – 20 °C. To improve the staining quality for centrosomal proteins, for some experiments a pre-extraction step with BRB80 buffer for 1 min at RT was included prior to fixation. After fixation, cells were washed with PBS again and blocked with 3 % BSA and 0.05 % Triton X-100 in PBS (PBS-BT) for 30 min at room temperature. Primary and secondary antibodies were diluted in PBS-BT and the antibody incubations were performed for 1 h at room temperature with three washing steps with PBS in between. After washing with PBS another three times, coverslips were mounted onto glass microscope slides using ProLong™ Gold Antifade (Molecular Probes by Life Technologies) with DAPI. Cells were imaged using the Zeiss Observer.Z1 inverted motorized microscope and images were processed using Fiji software with maximum intensity projection of z-stack images.

2.2.2.9 Ultrastructure expansion microscopy (U-ExM)

Expansion microscopy was performed according to the protocol by Gambarotto et al., 2019. Cells on coverslips were fixed using ice-cold methanol for 10 min at – 20 °C. Cells were washed with PBS and incubated in a 0.7 % formaldehyde and 1 % acrylamide solution for 4 h at 37 °C. Gel polymerization on the coverslips was performed using a gelation solution (23 % w/v sodium acrylate, 10 % w/v acrylamide, 0.1 % w/v BIS, 0.5 % TEMED, 0.5 % ammonium persulfate in PBS). Gels were allowed to polymerize for 5 min on ice before coverslips were transferred to 37 °C for 1 h. After complete polymerization, coverslips with gels were incubated in denaturation buffer (200 mM SDS, 200 mM NaCl, 50 mM Tris in ddH_2O) for 15 min at room temperature to detach the gels from the coverslips. Gels were transferred to 1.5 ml microcentrifuge tubes filled with denaturation buffer and incubated for 90 min at 95 °C. Following denaturation, gels were transferred to beakers filled with ddH_2O and washed with ddH_2O additional two times for 10 min each, allowing for gel expansion. Before antibody labeling, ddH_2O was replaced with PBS, the gels were washed twice with

PBS for 15 min each, allowing the gels to shrink again and then transferred into a six-well plate. Primary antibodies were diluted in 2 % BSA in PBS and added to the gels. Primary antibody staining was performed in the six-well plate overnight at 4 °C with agitation. Gels in the six-well plate were washed three times for 10 min each with 0.1 % Tween-20 in PBS (PBST) at RT with agitation. Secondary antibodies were diluted in 2 % BSA in PBS, added to the gels and incubated for 2.5 h at 37 °C with agitation and protected from light. Gels were washed in the six-well plate as before, transferred to beakers filled with 1000 ml ddH_2O allowing for the second round of gel expansion and incubated in the dark until mounting and imaging. For mounting, 35 mm cell imaging dishes with a glass bottom were prepared by coating with 0.1 mg/ml poly-lysine solution. The expanded gel was cut into pieces and a piece of gel was transferred to a non-coated imaging dish first in order to identify the side of the gel where cells are located. Once identified, the piece of gel was transferred to the poly-lysine coated imaging dish with the cells facing the glass bottom of the dish. Images were acquired using the Zeiss Observer.Z1 inverted motorized microscope and images were processed using ImageJ Fiji software with maximum intensity projection of z-stack images.

2.2.3 Methods in protein biochemistry

2.2.3.1 Preparation of protein extracts from cells

For the preparation of protein extracts, cells were harvested as described in 2.2.2.2. Cell pellets were resuspended in 3 – 5 volumes of NP-40 buffer for immunoprecipitations or RIPA buffer for direct SDS-PAGE and Western blot analysis. Cells were lysed by incubation for 30 min on ice. Lysates were cleared by centrifugation for 20 min at 16100 g and 4 °C and supernatants were transferred to fresh tubes. For Ni-NTA pulldown, cell pellets were resuspended in 8 M urea buffer and cells were lysed by sonication using a Branson Sonifier 250 at output 3 and 50 % cycle duty for 10 pulses. Lysates were cleared by centrifugation for 20 min at 16100 g and 4 °C. Protein concentrations were determined by Bradford assay as described in 2.2.3.2. For SDS-PAGE and Western blot analysis, samples of cell lysates were mixed with 2x Laemmli buffer and incubated for 5 min at 95 °C.

2.2.3.2 Determination of protein concentration by Bradford assay

Protein concentrations of cell lysates were determined by Bradford assay using the Bio-Rad Protein Assay. 1 µl of protein extract were diluted in 800 µl ddH_2O. For the standard curve, different amounts of a 1 mg/ml stock solution of BSA standard were diluted in 800 µl ddH_2O. 200 µl of assay dye were added to all samples. After mixing by inverting the tubes, samples were incubated for 5 min at RT. 200 µl of each sample were transferred to a 96-well plate and the $OD_{595\ nm}$ was determined using a SPECTROstar Nano microplate reader (BMG Labtech). All samples were measured in triplicates. Protein concentrations of the cell lysates were calculated based on the BSA standard curve.

2.2.3.3 SDS polyacrylamide gel electrophoresis (SDS-PAGE)

SDS polyacrylamide gel electrophoresis (SDS-PAGE) was used to separate protein samples according to their molecular weight. Polyacrylamide gels consisting of a separating gel and a stacking gel on top, were prepared using the Mini-Protean vertical electrophoresis system (Bio-Rad). Depending on the size of the proteins to be separated, the separating gel contained 7 – 15 % acrylamide/bisacrylamide, 375 mM Tris-HCl pH 8.8, 0.1 % SDS, 0.1 % APS and 0.1 % TEMED. The stacking gel contained 5 % acrylamide/bisacrylamide, 125 mM Tris-HCl pH 6.8, 0.1 % SDS, 0.1 % APS and 0.1 % TEMED. After polymerization, gels were assembled in the SDS-PAGE chamber and 500 ml SDS running buffer was added to the chamber. Protein samples were prepared as described previously and loaded on to the gel. 3 µl of a molecular weight marker (neoLab) was loaded as a size reference. Gels were run at 80 – 110 V for 2 h.

2.2.3.4 Western blot

Following SDS-PAGE, proteins were transferred to nitrocellulose membranes by Western blot using the Trans-Blot Turbo semi-dry system (Bio-Rad). Semi-dry blots were run at 2.5 A for 15 – 20 min depending on the size of the proteins to be transferred. After transfer, proteins on the nitrocellulose membrane were stained with Ponceau S solution in order to assess the quality of the transfer. Membranes were blocked by incubation in 5 % milk powder in PBST for at least 30 min at RT with shaking in order to reduce unspecific binding of the antibodies. Primary antibodies against target proteins were diluted in 5 % milk powder in PBST and membranes were incubated with antibodies overnight at 4 °C with shaking. After washing with PBST three times for

10 min each, membranes were incubated with species-specific horseradish peroxidase (HRP)-conjugated secondary antibodies diluted in blocking solution for 1 h at RT with shaking. Membranes were washed another three times with PBST for 10 min each, before signals were detected using Immobilon Western Chemiluminescence HRP-substrate (Merck) and the ImageQuant LAS 4000 (GE) imager. Image processing and quantifications were performed using ImageJ Fiji software.

2.2.3.5 Immunoprecipitation assays

2.2.3.5.1 Immunoprecipitation of Flag-tagged proteins using Flag M2 affinity beads

For immunoprecipitation (IP) of Flag-tagged proteins, α-Flag M2 beads (Sigma-Aldrich) were used. Cell lysates were prepared using NP-40 buffer as described in 2.2.3.1. 10 µl bed volume of affinity beads were used for each sample and prepared in batch by washing twice with TBS, once with 0.1 M glycine-HCl pH 3.5 and twice with TBS. The centrifugation steps were performed at 5400 g and 4 °C for 2 min each. The prepared beads were resuspended in NP-40 buffer and added to 3 – 12 mg of each protein extract. Sample volumes were equalized by addition of NP-40 buffer and the IPs were incubated for 3 h or overnight at 4 °C on a rotating wheel. Following incubation, beads were washed 3 – 4 times in NP-40 buffer. For elution of bound proteins, beads were incubated with 50 µl of 200 ng/µl 3x Flag peptide (Thermo Fisher Scientific) diluted in NP-40 for 30 min on ice with short vortexing every 5 – 10 min. Beads were pelleted by centrifugation for 2 min at 5400 g and 4 °C, supernatants were transferred to fresh tubes, mixed with 4x Laemmli buffer and incubated for 5 min at 95 °C. IP samples were analyzed by SDS-PAGE and Western blot.

2.2.3.5.2 Double immunoprecipitation of Flag- and HA-tagged proteins using Flag M2 affinity beads and HA beads

In order to analyze if three proteins are part of the same complex, two sequential IPs were performed. First, the Flag-tagged protein was immunoprecipitated using α-Flag M2 beads as described in 2.2.3.5.1. Bound proteins were eluted by incubation with 100 µl of 200 ng/µl 3x Flag peptide. The eluates were used for a second IP against the HA-tag of another protein using α-HA beads (Thermo Fisher Scientific). 15 µl bed volume of affinity beads were used for each sample and prepared in batch by washing

once in TBS. The prepared beads were resuspended in NP-40 buffer and added to the eluates. NP-40 buffer was added to the samples to reach equal volumes of 500 µl each. The IPs were incubated for 3 h at 4 °C on a rotating wheel. Following incubation, beads were washed 3 – 4 times in 0.05 % Tween-20 in TBS (TBST). For elution of bound proteins, beads were incubated with 50 µl of 1 mg/ml HA peptide (MedChemExpress) diluted in NP-40 for 15 min at 30 °C. Beads were pelleted by centrifugation, supernatants were transferred to fresh tubes, mixed with 4x Laemmli buffer and incubated for 5 min at 95 °C. Double IP samples were analyzed by SDS-PAGE and Western blot.

2.2.3.5.3 Immunoprecipitation of GFP-tagged proteins using GFP-trap affinity beads

For IP of GFP-tagged proteins, GFP-trap affinity beads were used. Cell lysates were prepared using NP-40 buffer as described in 2.2.3.1. 10 µl bed volume of affinity beads were used for each sample and prepared in batch by washing once with ddH_2O and twice with NP-40 buffer. The centrifugation steps were performed at 5000 g and 4 °C for 2 min each. The prepared beads were resuspended in NP-40 buffer and added to 2 – 8 mg of each protein extract. Sample volumes were equalized by addition of NP-40 buffer and the IPs were incubated for 3 h at 4 °C on a rotating wheel. Following incubation, beads were washed 3 – 4 times in NP-40 buffer. For elution of bound proteins, beads were incubated with 50 µl 2x Laemmli buffer for 10 min at 95 °C. After centrifugation, supernatants were transferred to fresh tubes and analyzed by SDS-PAGE and Western blot.

2.2.3.5.4 Immunoprecipitation of endogenous proteins using protein G sepharose

The endogenous proteins PLK4 or DCAF1 were immunoprecipitated using specific antibodies and protein G sepharose beads (GE). 10 – 15 mg protein extracts from HEK293T cells were prepared as described in 2.2.3.1 and incubated with either 5 µg mouse anti-PLK4 or mouse anti-DCAF1 antibody at 4 °C overnight on a rotating wheel. 5 µg of non-specific mouse IgG was used as control. Beads were prepared in batch by incubation in 0.1 % BSA in PBS overnight at 4 °C on a rotating wheel, followed by washing twice in ddH_2O and twice in NP-40 buffer. Centrifugation steps were performed at 4000 g and 4 °C for 2 min each. 15 µl bed volume of beads were used

for each sample and incubated together with the protein extract-antibody mixtures at 4 °C for 2 h on a rotating wheel. Following incubation, beads were washed 3 – 4 times in NP-40 buffer. For elution of bound proteins, beads were incubated with 50 µl 2x Laemmli buffer for 10 min at 95 °C. After centrifugation, supernatants were transferred to fresh tubes and analyzed by SDS-PAGE and Western blot.

2.2.3.6 *In vivo* ubiquitylation assays

Ubiquitylation of PLK4 by DCAF1 in mammalian cells was analyzed by either Flag-IP or Ni-NTA pulldown and subsequent Western blot detection. For the Flag-IP assay, Flag-tagged PLK4, Myc-tagged DCAF1 and HA-tagged Ubiquitin were co-expressed in HEK293T cells for 24 h. Cells were transfected with plasmid DNA as described in 2.2.2.3.1 and treated with 10 µM MG132 (Sigma-Aldrich) for 5 h before harvesting. Protein extracts were prepared as described in 2.2.3.1 using NP-40 buffer supplemented with 10 mM N-ethylmaleimide (NEM). Flag-tagged PLK4 was immunoprecipitated as described in 2.2.3.5.1. NP-40 buffer supplemented with 10 mM NEM was used for all washing steps. Eluted proteins were mixed with 4x Laemmli buffer and incubated for 5 min at 95 °C. Samples were analyzed by SDS-PAGE and Western blot.

For the Ni-NTA pulldown assay, Flag-tagged PLK4, Myc-tagged DCAF1 and His-tagged Ubiquitin were co-expressed in HEK293T cells for 24 h. Cells were transfected with plasmid DNA as described in 2.2.2.3.1 and treated with 10 µM MG132 (Sigma-Aldrich) for 5 h before harvesting. Protein extracts were prepared as described in 2.2.3.1 using 8 M Urea buffer and sonication. 40 µl suspension of Ni-NTA beads was used per sample and prepared in batch by washing once with ddH_2O and twice with Urea buffer. The centrifugation steps were carried out at 7000 g and 4 °C for 2 min. The prepared beads were resuspended in Urea buffer and added to 3 – 8 mg of each protein extract. Sample volumes were equalized by addition of Urea buffer and incubated for 3 – 4 h at RT on a rotating wheel. Following incubation, beads were washed 3 times in Urea buffer supplemented with 0.1 % Triton X-100. For elution, beads were incubated with 50 µl 2x Laemmli buffer supplemented with 200 mM imidazole for 10 min at RT. After centrifugation, supernatants were transferred to fresh tubes and incubated for 5 min at 95 °C. Samples were analyzed by SDS-PAGE and Western blot.

2.2.3.7 *In vitro* ubiquitylation assay

In vitro ubiquitylation assays were performed with purified recombinant proteins and Flag-DCAF1/ Myc-CUL4 complexes precipitated from HEK293T cells to analyze the ubiquitylation of MBP-tagged PLK4. Flag-DCAF1 or Flag-DCAF1 Δacidic were co-expressed with Myc-CUL4 in HEK293T cells as described in 2.2.2.3.1. Protein extracts were prepared as described in 2.2.3.1 and Flag-DCAF1 was immunoprecipitated as described in 2.2.3.5.1 but no elution step was performed. Following 3 – 4 washing steps in NP-40 buffer, beads were washed once in ubiquitin assay buffer. For the ubiquitylation reactions, Flag-DCAF1/ Myc-CUL4 complexes immobilized on α-Flag M2 beads were combined with 200 nM MBP-PLK4, 170 nM UBA1, 1 µM UBCH5C, 30 µM Ubiquitin and 5 mM ATP in 20 µl total volume assay buffer. Samples were incubated for 90 min at 37 °C and 400 rpm. Reactions were terminated by the addition of 2x LDS buffer and incubation for 10 min at 72 °C. Samples were analyzed by SDS-PAGE and Western blot.

2.2.3.8 Bacterial expression and purification of recombinant GST-DCAF1

E. coli Rosetta (DE3) cells were transformed with pGEX-4T3-DCAF1 as described in 2.2.1.6. A single colony was picked and used to inoculate 10 ml LB medium with ampicillin. The culture was grown at 37 °C and 180 rpm overnight and then used to inoculate 400 ml LB medium with ampicillin by 1:100 dilution on the next day. The culture was again grown at 37 °C and 180 rpm until it reached a density of $OD_{600} = 0.5$. Protein expression was induced by adding 400 µM IPTG and the bacteria culture was further cultivated at 18 °C and 180 rpm overnight. Bacteria were harvested by centrifugation at 5000 rpm and 4 °C for 30 min using a Sorvall RC5C centrifuge with an F10-6x500Y rotor (Piramoon Technology). Supernatants were discarded and pellets were frozen at – 80 °C for at least 4 h. For protein purification, bacteria pellets were thawed, resuspended in 20 ml lysis buffer and lysed by sonication using a Branson Sonifier 250 at 30 % output and 50 % cycle duty for ten rounds of 20 pulses each. After each round, the bacteria suspension was cooled on ice for 20 s. Lysates were cleared by centrifugation at 13000 rpm and 4 °C for 30 min using a Sorvall F-28/50 rotor. Cleared bacteria supernatants were transferred to fresh reaction tubes. Immobilized glutathione CL-4B beads (Sigma-Aldrich) were prepared by centrifugation at 500 g and 4 °C for 5 min, discarding the supernatant and washing once with 10 ml lysis buffer. 600 µl bed volume of beads were used per sample. The equilibrated beads were added

to the bacteria supernatant and incubated on a rotating wheel at 4 °C for 2 h. Following incubation, the beads were collected in a Poly-Prep chromatography column (Bio-Rad) and washed three times with 10 ml washing buffer. Several elutions were performed at 4 °C with 600 µl elution buffer each and all elution fractions were pooled. Dialysis of the eluate was performed overnight in 1 l dialysis buffer using a 0.5 kDa MW cut-off dialysis membrane at 4 °C with gentle stirring. Dialyzed samples were cleared by centrifugation at 16100 g and 4 °C for 20 min. Protein concentration was determined by Bradford assay as described in 2.2.3.2. Aliquots were frozen in liquid nitrogen and stored at – 80 °C.

2.2.3.9 GST pull-down assay

GST pull-down assays were performed to analyze the direct interaction between GST-DCAF1 and MBP-PLK4 in vitro. 10 µg of MBP-PLK4 and 10 µg of GST-DCAF1 or an equimolar amount of GST as control were combined and incubated in 200 µl NP-40 buffer on a rotating wheel at 4 °C for 1 h. 10 µl of each reaction were taken as input samples. Immobilized glutathione CL-4B beads were prepared by washing once in NP-40 buffer and added in 200 µl NP-40 buffer to the pre-incubated protein mixture. 10 µl bed volume of beads were used for each pull-down. Proteins were bound to the beads by incubation on a rotating wheel at 4 °C for 2 h. Following incubation, beads were washed four times with NP-40 buffer. Bound proteins were eluted with 25 µl 2x Laemmli buffer at 95 °C for 5 min. Input and pull-down samples were analyzed by SDS-PAGE and Western blot.

2.2.4 Statistical analysis

All statistical analyses were performed with GraphPad Prism, version 9 (GraphPad Software, Inc). Data were collected from at least three independent experiments and represented as individual values or as mean ±SD. For statistical analysis of fold change data, values were normalized to a control group and a logarithmic transformation was performed in order to ensure that the data is normally distributed. Statistical significance of this data was analyzed by one sample, two-tailed t test against the mean of the control group, which was set to 1.0, or by paired, two-tailed t test for comparisons among the test groups. Statistical significance of normally distributed data, that was not normalized to a control group, was analyzed by unpaired, two-tailed, Student's t test with Welch's correction. P values below 0.05 were considered statistically

significant (ns $p > 0.05$, * $p < 0.05$, ** $p < 0.01$, *** $p < 0.001$ and **** $p < 0.0001$).

3. Results

3.1 Characterization of DCAF1 as a novel interaction partner of PLK4

DCAF1 has been identified as a potential novel interaction partner of PLK4 in asynchronous HEK293T cells by a mass spectrometry (MS)-based approach performed by Anne-Sophie Kratz in collaboration with the DKFZ protein analysis facility. PLK4 is a protein kinase known as the master regulator of centriole duplication, while DCAF1 has been first identified as a binding partner of the HIV-1 viral protein Vpr and later as a substrate receptor of an E3 ubiquitin ligase complex. A direct correlation between both proteins is not known, however, it seems worth investigating, since the interaction between PLK4 and another E3 ligase substrate receptor, β-TrCP, is well established and unraveled the complex mechanism of PLK4 autoregulation in centriole duplication.

3.1.1 PLK4 and DCAF1 interact *in vivo* and *in vitro*

I used Flag-immunoprecipitation (IP) to confirm the *in vivo* interaction between PLK4 and DCAF1 by two different approaches. First, HEK293T cells were transfected with Flag-PLK4 or Flag-empty vector as control and cell lysates were subjected to IP against the Flag-tag. I could confirm that endogenous DCAF1 co-precipitates with overexpressed wild-type Flag-PLK4 (Figure 9 A). Next, HEK293T cells were transfected with Flag-DCAF1 or Flag-empty vector as control. By performing Flag-IP, I could show that also endogenous PLK4 co-precipitates with overexpressed wild-type DCAF1, confirming the interaction between both proteins, reciprocally (Figure 9 B). In addition, I immunoprecipitated endogenous DCAF1 from HEK293T cell lysates using specific antibodies or unspecific mouse IgG as control. Input and eluate samples were subjected to Western blot analysis, which confirmed that PLK4 specifically interacts with DCAF1 at the endogenous level (Figure 9 C) (Grossmann et al., 2024).

In order to confirm that both proteins interact directly and that the interaction is not mediated by another unknown mediator component present in cells, I performed *in vitro* binding assays. I expressed recombinant GST-DCAF1 in *E. coli* Rosetta and purified the protein from the lysate. Purified GST-DCAF1 or GST as a control were incubated with recombinant MBP-PLK4 and GST pulldown assays were performed. Analysis of pulldown samples by Western blot revealed that MBP-PLK4 interacts directly with GST-DCAF1 (Figure 9 D) (Grossmann et al., 2024).

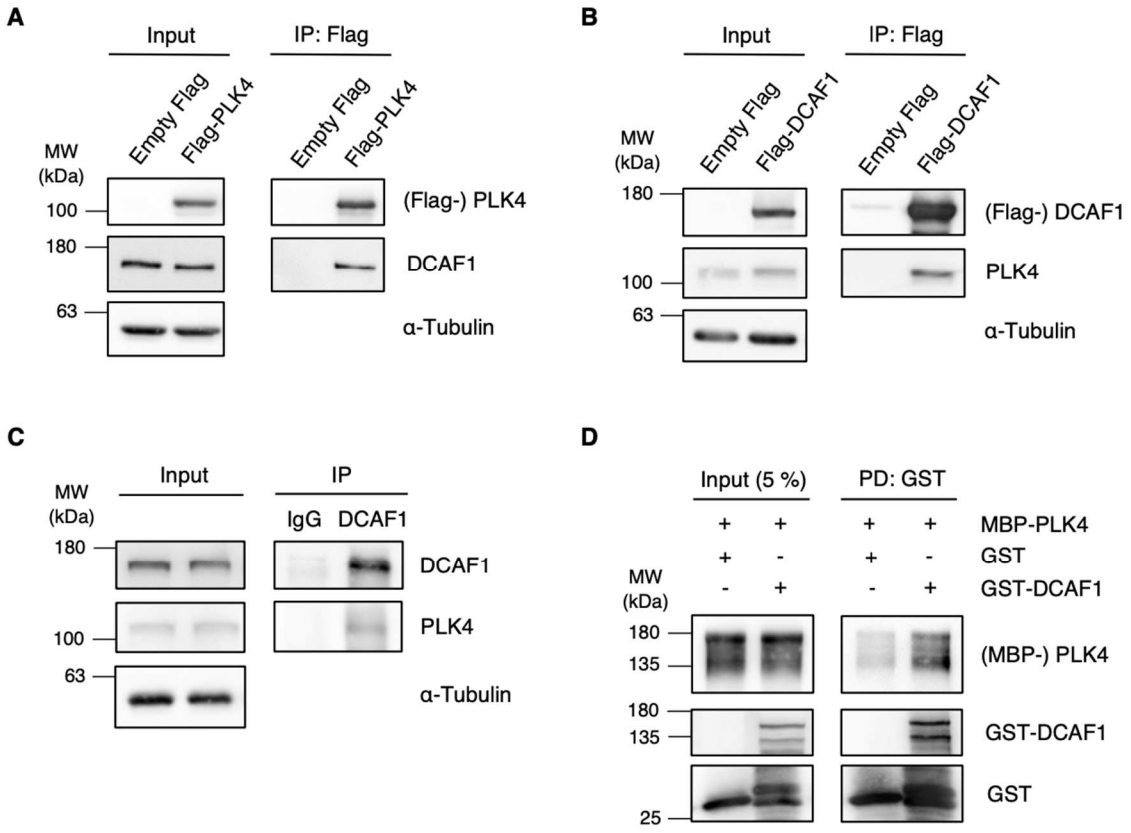

Figure 9: PLK4 interacts with DCAF1 *in vivo* and *in vitro*.

(A) Empty Flag or Flag-PLK4 was overexpressed in HEK293T cells for 48 h. Cells were harvested and cell lysates were subjected to Flag IP. Input and eluate samples were analyzed by Western blot. **(B)** Empty Flag or Flag-DCAF1 was overexpressed in HEK293T cells for 48 h. Cells were harvested and cell lysates were subjected to Flag IP. Input and eluate samples were analyzed by Western blot. **(C)** Endogenous DCAF1 was immunoprecipitated from HEK293T cell lysates using unspecific IgG control or specific DCAF1 antibodies and protein G sepharose. Input and eluate samples were analyzed by Western blot. **(D)** Purified recombinant GST-DCAF1 or empty GST were combined with MBP-PLK4 and GST pull-down assays were performed using glutathione CL-4B sepharose beads. Input and eluate samples were analyzed by Western blot (Grossmann et al., 2024).

3.1.2 PLK4 polo-boxes 1 and 2 mediate binding to DCAF1

The domain organization of PLK4 has been well described. PLK4 contains an N-terminal kinase domain and three polo-box domains towards the C-terminus. The two more central, tandem homodimerized polo-boxes PB1 and PB2 are also referred to as the cryptic polo-box (CPB). The PLK4 PB domains are known to be involved in homodimer formation and mediation of protein-protein interactions (Slevin et al., 2012).

In order to characterize the interaction between PLK4 and DCAF1 in more detail, I aimed at identifying the PLK4 domain, which mediates binding to DCAF1. Truncated,

Flag-tagged fragments of PLK4 have been generated previously in order to map the binding site between PLK4 and CEP152 by Flag-IP (Cizmecioglu et al., 2010) (Figure 10 A). I used the same constructs to transfect HEK293T cells and performed Flag-IP from the cell lysates in order to identify the minimal region that is sufficient to mediate binding to endogenous DCAF1. Western blot analysis of eluate samples revealed that full-length PLK4 as well as all PLK4 fragments containing the cryptic polo-box domain PB1-PB2 interact with endogenous DCAF1 (Figure 10 B). Presence or absence of the C-terminal PB3 does not affect the binding. However, N-terminal fragments of PLK4 containing the kinase domain but lacking the polo-box domains are not able to interact with DCAF1. The interaction mapping clearly demonstrates that the cryptic polo-box PB1-PB2 of PLK4 mediates binding to DCAF1. Thus, the binding site for DCAF1 on PLK4 is distinct from the binding site for β-TrCP, which binds to a more N-terminal region on PLK4 (Grossmann et al., 2024). Interestingly, the interaction between DCAF1 and the short PLK4 PB1-PB2 fragment is even stronger than the interaction with full-length PLK4, probably due to a different protein folding and easier accessibility of the binding site.

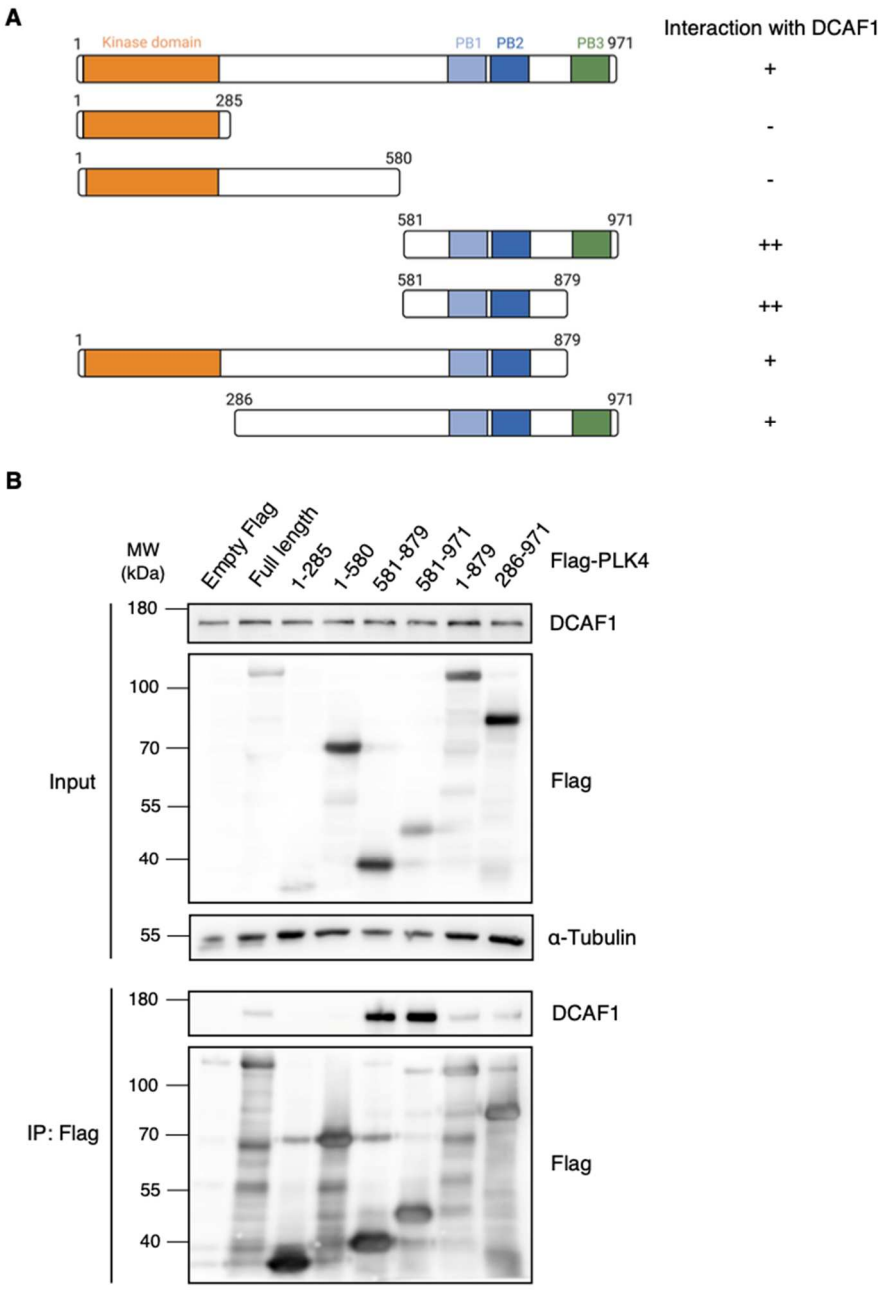

Figure 10: PLK4 polo-boxes 1 and 2 mediate binding to DCAF1.

(A) Overview of full-length and different truncated PLK4 fragments used in (B). Interaction of the fragments with endogenous DCAF1 is indicated on the right (-, + and ++). **(B)** Flag-PLK4 full length or different truncated fragments were overexpressed in HEK293T cells for 48 h. Cells were harvested and cell lysates were subjected to Flag IP. Input and eluate samples were analyzed by Western blot (Grossmann et al., 2024).

For a more detailed analysis of the binding interface, I generated several mutants of PLK4 containing point mutations of critical amino acids within the cryptic polo-box domain. Analysis of the PLK4-DCAF1 complex structure performed with AlphaFold2.0 by Gali Prag (Tel Aviv University, Israel) revealed, that PLK4 presents a positively

charged binding surface which allows for electrostatic interactions with DCAF1 (Grossmann et al., 2024). By overexpression of the PLK4 mutants in HEK293T cells and subsequent Flag-IP assays, I could confirm that the interaction between PLK4 and DCAF1 is disrupted upon mutation of any of these amino acids, underlining their critical function at the binding interface (Figure 11 A). To confirm that mutations within the PB1-PB2 domain do not disrupt the structure of the domain and thereby would prevent any protein-protein interaction, I generated two additional negative control PLK4 PB1-PB2 mutations, K748A and K753A, which are located in vicinity but not directly within the PLK4-DCAF1 interaction interface. As expected, these mutations do not abolish the interaction between PLK4 and DCAF1 (Figure 11 B) (Grossmann et al., 2024).

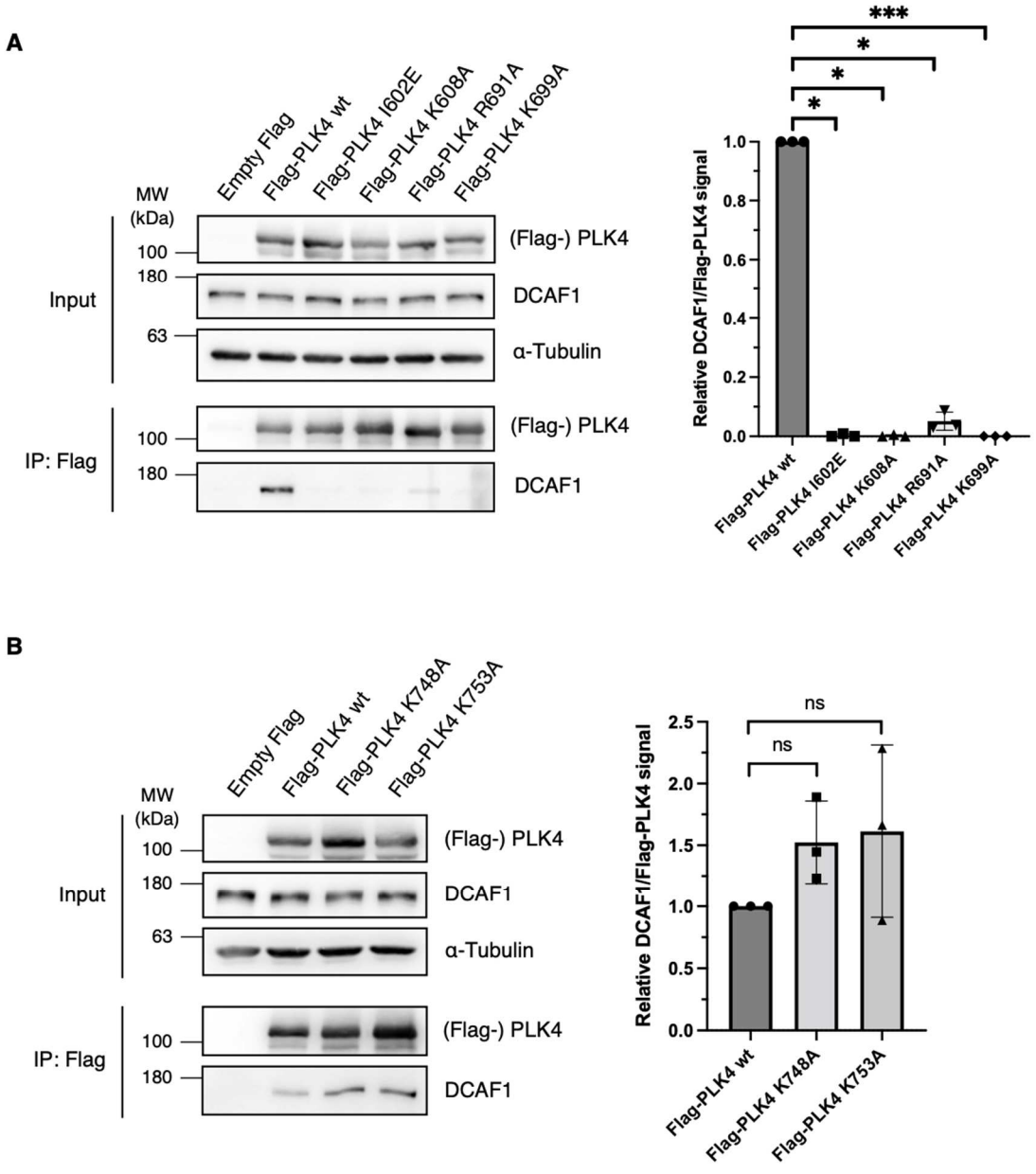

Figure 11: Amino acids in PLK4 PB1-PB2 are critical for binding to DCAF1.
(A) Different Flag-tagged PLK4 mutants containing point mutations within the PLK4-DCAF1 binding interface were generated and overexpressed in HEK293T cells for 48 h. Cells were harvested and cell lysates were subjected to Flag IP. Input and eluate samples were analyzed by Western blot. Quantification of relative DCAF1/ Flag-PLK4 signal normalized to Flag-PLK4 wt, N = 3. *** $p < 0.001$, * $p < 0.05$. Data are presented as mean ±SD. **(B)** Two different Flag-tagged PLK4 mutants containing point mutations in vicinity to the PLK4-DCAF1 binding interface were generated and overexpressed in HEK293T cells for 48 h. Cells were harvested and cell lysates were subjected to Flag IP. Input and eluate samples were analyzed by Western blot. Quantification of relative DCAF1/ Flag-PLK4 signal normalized to Flag-PLK4 wt, N = 3. ns $p > 0.05$. Data are presented as mean ±SD (Grossmann et al., 2024).

3.1.3 DCAF1 acidic domain mediates binding to PLK4

Interaction sites between DCAF1 and certain substrates or regulators have been characterized and functions of individual domains of DCAF1 have been identified already. Especially the DCAF1 C-terminus, consisting of the WD40 domain and the acidic tail, has been implicated in substrate binding or protein-protein interactions in general. Additionally, the WD40 domain has been shown to be necessary for formation of the tetrameric, auto-inhibited state of the complex, while the LisH domain has been implicated in DCAF1 dimerization (Ahn et al., 2011; Mohamed et al., 2021).

In order to identify the minimal region required to mediate binding to PLK4, I used different truncated, Flag-tagged DCAF1 fragments. These constructs were kindly provided by Vicente Planelles (University of Utah, USA) (Cassiday et al., 2015) (Figure 12 A). I transfected HEK293T cells and performed Flag-IP experiments from cell lysates. Western blot analysis of eluate samples revealed, that the C-terminal acidic domain of DCAF1 is sufficient to mediate binding to endogenous PLK4 (Figure 12 B). All fragments lacking the acidic domain, fail to interact with PLK4. A slightly larger fragment containing both the WD40 and the acidic domain interacts stronger with PLK4 than the acidic domain alone, suggesting that the acidic domain is indispensable but both domains contribute to the binding (Grossmann et al., 2024).

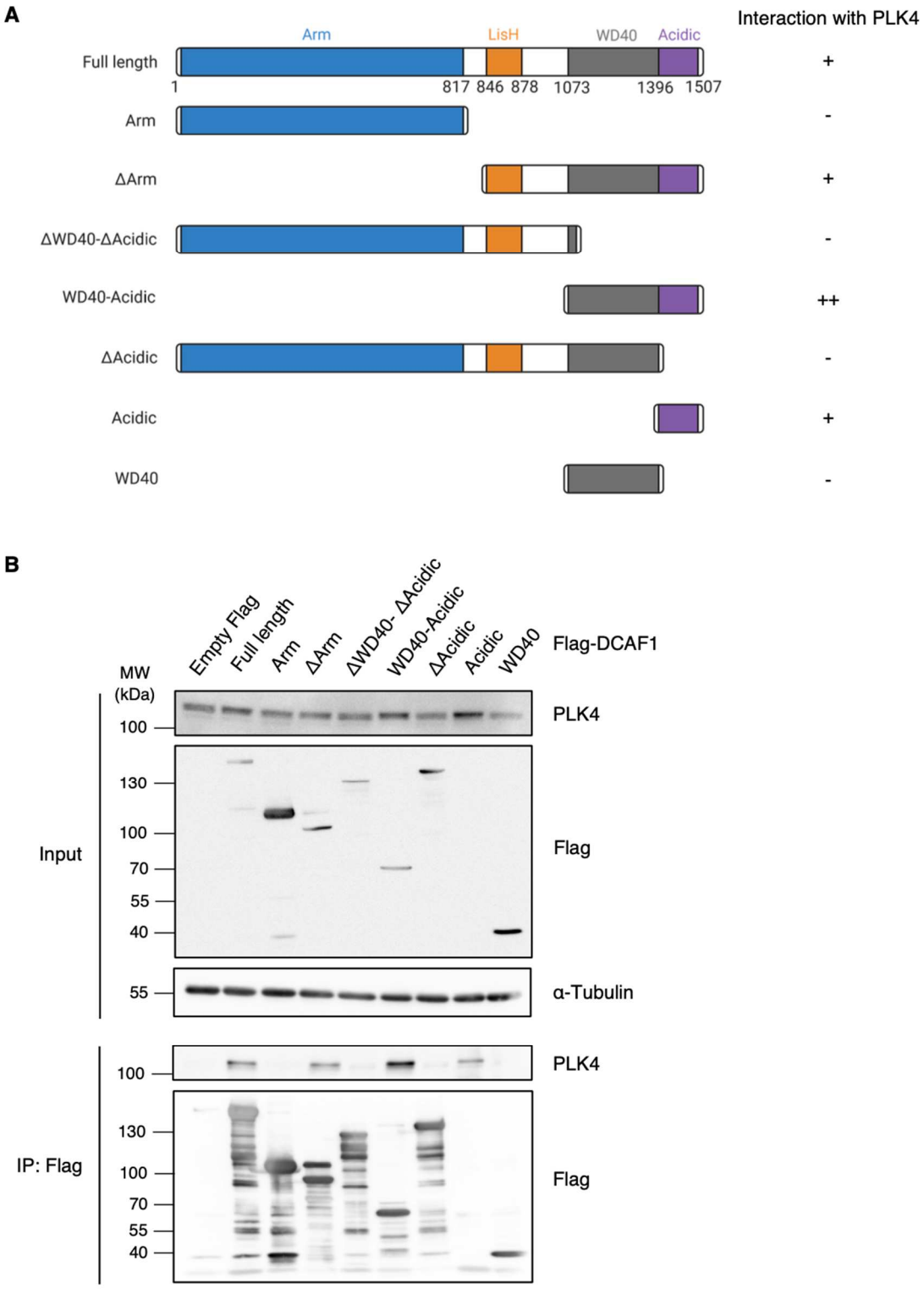

Figure 12: DCAF1 acidic domain mediates binding to PLK4.

(A) Overview of full-length and different truncated DCAF1 fragments used in (B). These constructs were kindly provided by Vicente Planelles, University of Utah. Interaction of the fragments with endogenous PLK4 is indicated on the right (-, + and ++). This figure was generated with BioRender.com. **(B)** Flag-DCAF1 full length or different truncated fragments were overexpressed in HEK293T cells for 48 h. Cells were harvested and cell lysates were subjected to Flag IP. Input and eluate samples were analyzed by Western blot (Grossmann et al., 2024).

3.1.4 Correlation between CEP152, CEP192 and DCAF1 at the PLK4 PB1-PB2 domain

CEP152 and CEP192 are two centriolar proteins which have been previously shown to interact with the PB1-PB2 domain of PLK4 (Cizmecioglu et al., 2010; Hatch et al., 2010; Sonnen et al., 2013). In order to compare the interaction between PLK4 and DCAF1 to the interaction between PLK4 and CEP152/CEP192 and investigate a potential correlation between all four proteins, I overexpressed the PLK4 PB1-PB2 mutants in HEK293T cells and assessed their ability to interact with CEP152 and CEP192 by Flag-IP and Western blot analysis. Compared to the interaction between PLK4 and DCAF1, similar but not identical amino acids within the PLK4 PB1-PB2 domain are critical for CEP152/CEP192 binding (Figure 13 A). Especially the PLK4 R691A mutation, which completely abolished the interaction with DCAF1, does not affect the interaction with CEP152 and CEP192. To investigate a potential competition between DCAF1 and CEP152/CEP192 for PLK4 binding, I overexpressed increasing amounts of DCAF1 in HEK293T cells and tested by Flag-IP and Western blot analysis how this would affect the interaction between PLK4 and CEP152/CEP192. While the interaction between PLK4 and CEP192 is unaffected by increasing amounts of DCAF1, the interaction between PLK4 and CEP152 is slightly but not significantly decreased (Figure 13 B). DCAF1 cannot completely outcompete and prevent CEP152 and CEP192 from binding to PLK4, indicating that all of these proteins can interact with the PB1-PB2 domain of PLK4 simultaneously (Grossmann et al., 2024).

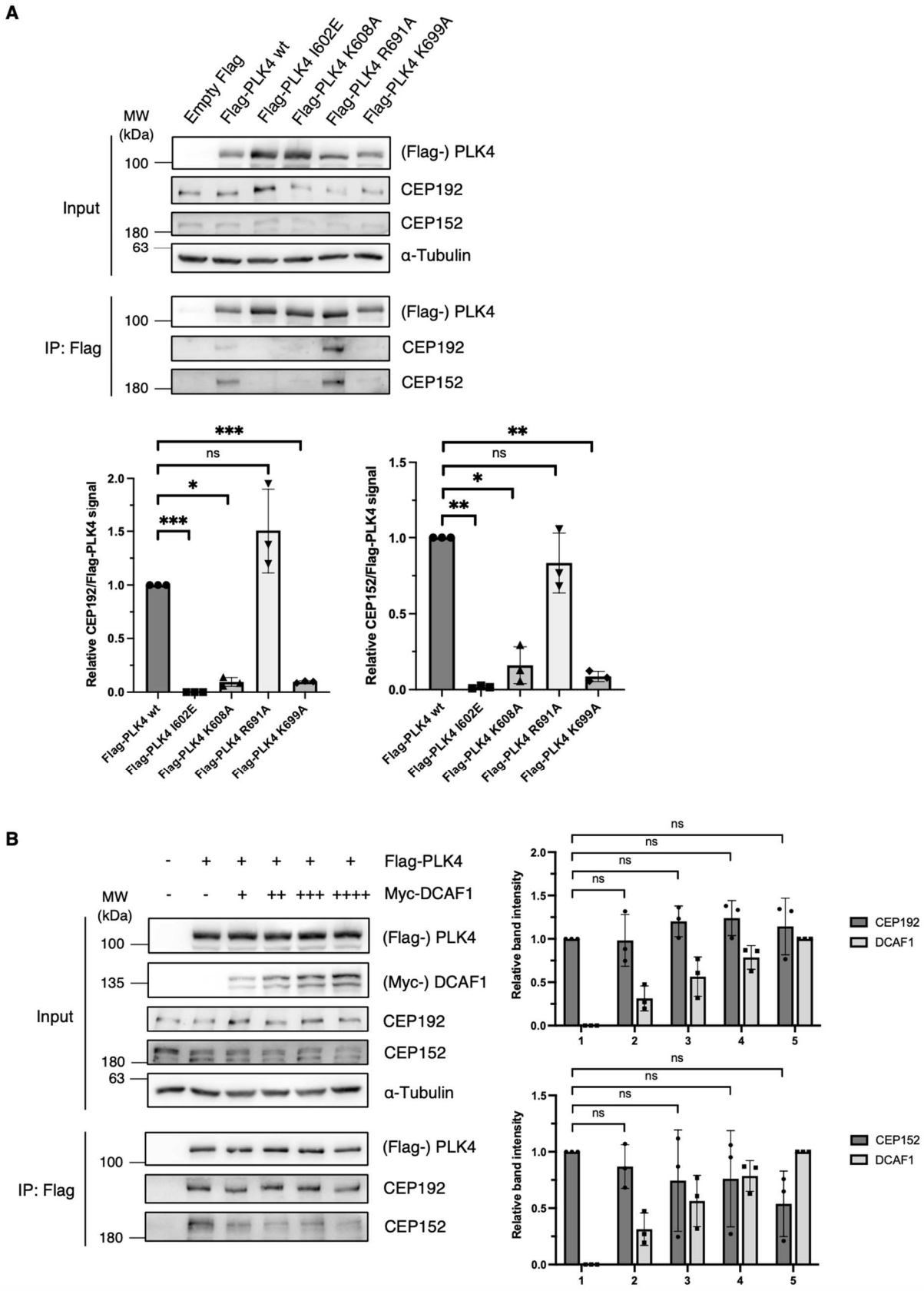

Figure 13: CEP152, CEP192 and DCAF1 interact with PLK4 PB1-PB2 simultaneously

(A) Indicated Flag-PLK4 mutants were overexpressed in HEK293T cells for 48 h. Cells were harvested and cell lysates were subjected to Flag IP. Input and eluate samples were analyzed by Western blot.

Quantification of relative CEP192/ Flag-PLK4 and CEP152/Flag-PLK4 signal normalized to Flag-PLK4 wt, N = 3. *** $p < 0.001$, ** $p < 0.01$, * $p < 0.05$, ns $p > 0.05$. Data are presented as mean ±SD. **(B)** Flag-PLK4 was overexpressed in HEK293T cells together with different amounts of Myc-DCAF1 in different samples (+, ++, +++, ++++) for 48 h. Co-precipitated CEP192 and CEP152 were detected by IP against the Flag tag and subsequent Western blot analysis. Quantification of relative CEP192/ Flag-PLK4, CEP152/ Flag-PLK4 and Myc-DCAF1 signal, N = 3. ns $p > 0.05$. Data are presented as mean ±SD (Grossmann et al., 2024).

3.1.5 The interaction between PLK4 and DCAF1 is independent of phosphorylation

DCAF1 functions as a substrate receptor of an E3 ubiquitin ligase complex, similar to β-TrCP, substrate receptor of the $SCF^{β\text{-}TrCP}$ complex, which has already been shown to be involved in the regulation of PLK4 protein levels. β-TrCP interacts with an N-terminal region of PLK4 upon trans-autophosphorylation of two amino acid residues, S285 and T289, within the β-TrCP recognition motif (Guderian et al., 2010; Holland et al., 2010).

Since the interaction mapping revealed that the DCAF1 binding site is distinct from the β-TrCP binding site, I aimed at investigating whether the interaction between DCAF1 and PLK4 is also dependent on PLK4 kinase activity and phosphorylation, similar to the interaction with β-TrCP. I used several PLK4 mutants that have been generated previously; first, a kinase-dead version of PLK4 generated by a point mutation within the kinase domain (K41R), second, a version of PLK4 which is non-phosphorylatable at the β-TrCP recognition site (S285A + T289A) and third, a PLK4 ΔPEST mutant which lacks the PEST destruction motif which is normally bound by β-TrCP (Figure 14 A). I overexpressed these mutants in HEK293T cells and performed Flag-IP experiments to analyze the interaction of the PLK4 mutants with DCAF1 compared to β-TrCP. While the interaction between PLK4 and β-TrCP is abolished when PLK4 is kinase-dead or mutated in the β-TrCP recognition motif, DCAF1 interacts with all phosphorylation mutants to a similar level as with wild-type PLK4 (Figure 14 B). Thus, trans-autophosphorylation of PLK4 is not required to allow for the interaction with DCAF1, which is in stark contrast to the interaction with β-TrCP (Grossmann et al., 2024).

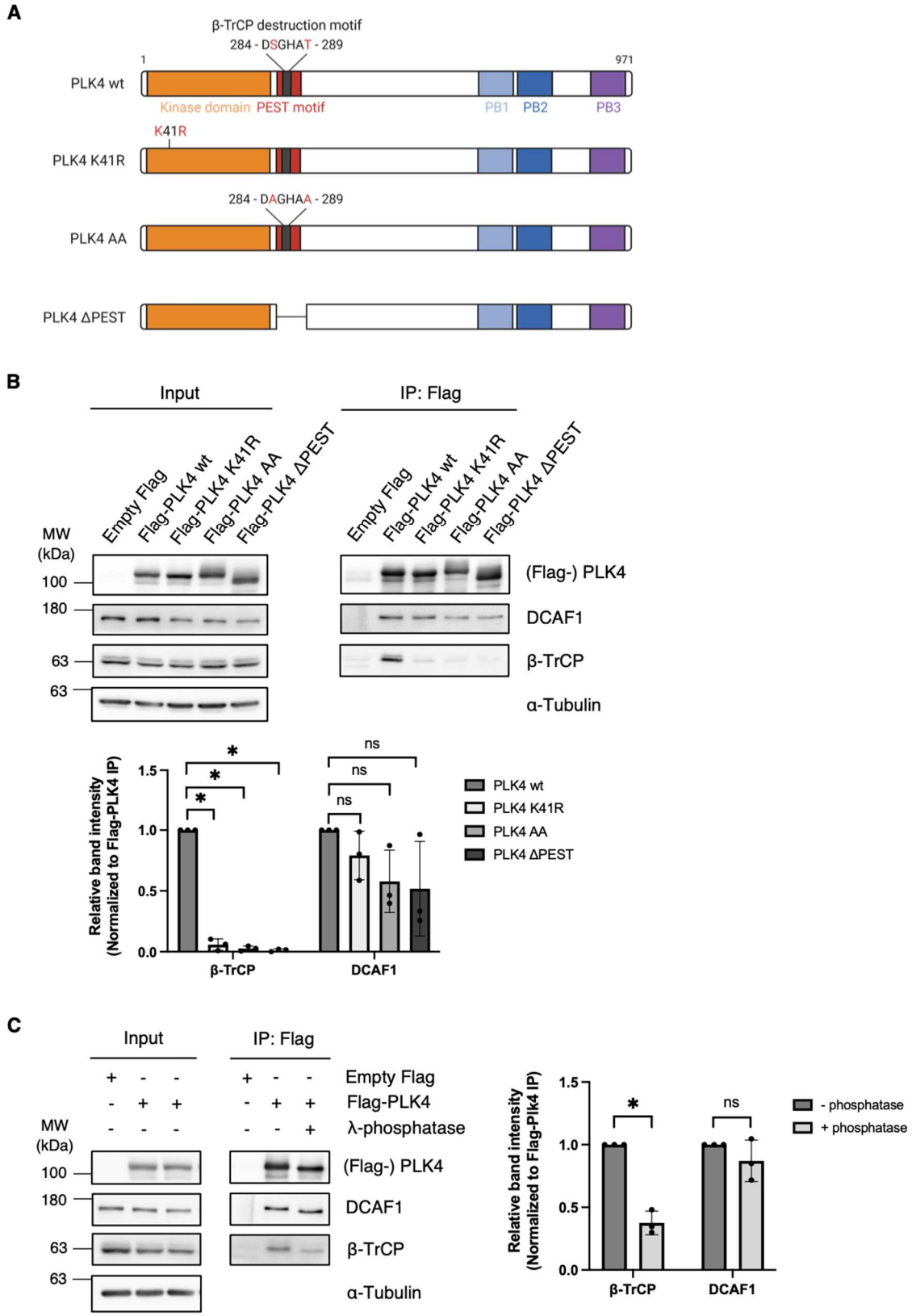

Figure 14: The interaction between PLK4 and DCAF1 is independent of PLK4 kinase activity and phosphorylation.

(A) Overview of PLK4 wild-type and different phosphorylation mutants used in (B). This figure was generated with BioRender.com. **(B)** Flag-PLK4 wt or Flag-PLK4 mutants (K41R, AA, ΔPEST) were overexpressed in HEK293T cells for 48 h. Cells were harvested and cell lysates were subjected to Flag

IP. Input and eluate samples were analyzed by Western blot. Quantification of relative β-TrCP/ Flag-PLK4 or DCAF1/ Flag-PLK4 signal normalized to Flag-PLK4 wt, N = 3. * $p < 0.05$, ns $p > 0.05$. Data are presented as mean ±SD. **(C)** Flag-PLK4 was overexpressed in HEK293T cells for 48 h. Cells were harvested and cell lysates were subjected to Flag IP with or without dephosphorylation of protein samples using λ-phosphatase. Input and eluate samples were analyzed by Western blot. Quantification of relative β-TrCP/ Flag-PLK4 or DCAF1/ Flag-PLK4 signal, N = 3. * $p < 0.05$, ns $p > 0.05$. Data are presented as mean ±SD (Grossmann et al., 2024).

However, additional unknown kinases might be involved in the regulation of the PLK4-DCAF1 interaction by potential phosphorylation of the DCAF1 binding site on PLK4. To exclude this possibility, I performed Flag-IP experiments after overexpression of wild-type Flag-PLK4 in HEK293T cells and subsequent treatment of samples with λ-phosphatase. While dephosphorylation of PLK4 strongly diminished the interaction with β-TrCP as expected, the effect on the interaction with DCAF1 is negligible (Figure 14 C). Together, these results indicate that DCAF1 binds to PLK4 independently of the kinase activity of PLK4 and its autophosphorylation mechanism and also independently of phosphorylation by any other unknown kinase (Grossmann et al., 2024).

3.2 Characterization of the CUL4-DDB1-DCAF1 ($CRL4^{DCAF1}$) ubiquitin ligase complex as a novel regulator of PLK4

DCAF1 functions as the substrate receptor of the CUL4-DDB1-DCAF1 ($CRL4^{DCAF1}$) E3 ubiquitin ligase complex, which belongs to the large family of cullin-RING ligases, just like the $SCF^{\beta\text{-}TrCP}$ complex. As it is already well established that PLK4 protein levels are regulated by ubiquitylation and proteasomal degradation, the interaction between PLK4 and DCAF1 might suggest an involvement of the $CRL4^{DCAF1}$ ubiquitin ligase in the regulation of PLK4. Thus, I focus on investigating a potential function of $CRL4^{DCAF1}$ in the ubiquitylation and proteasomal degradation of PLK4, as a second regulatory mechanism for tightly controlled PLK4 levels and a strict limitation of centriole duplication to exactly once per cell cycle.

3.2.1 The cullin-RING E3 ubiquitin ligase components CUL4, DDB1 and DCAF1 form a complex with PLK4

DCAF1 has been identified as a novel PLK4 interaction partner by mass spectrometry analysis. In the same screen also the cullin-RING E3 ubiquitin ligase complex component DDB1 has been identified as an interaction partner of PLK4. To confirm the interaction between PLK4 and DDB1, but also between PLK4 and the cullin-RING ligase scaffold protein CUL4, I overexpressed Flag-PLK4 in HEK293T cells and performed Flag-IP experiments. Endogenous DCAF1, as well as DDB1 and CUL4 co-precipitated with PLK4 (Figure 15 A) (Grossmann et al., 2024).

However, DDB1 and DCAF1 are also components of the HECT type E3 ubiquitin ligase complex EDD(UBR5)-DYRK2-DDB1-DCAF1 (Maddika and Chen, 2009) and the scaffold protein EDD (UBR5) has also been identified as a PLK4 interaction partner in the mass spectrometry screen. In order to identify whether PLK4 interacts with DCAF1 as part of the CUL4-DDB1 complex or the EDD-DYRK2-DDB1 E3 ubiquitin ligase complex, I performed sequential Flag- and HA-IP experiments to identify proteins present in the same complex. I co-expressed Flag-tagged PLK4 and HA-tagged DCAF1 in HEK293T cells and subjected cell lysates to Flag-IP in the first step. Flag-IP eluates were then used for HA-IP in the second step. Input samples and eluate samples after the second IP were analyzed by Western blot, revealing proteins that interact with both PLK4 and DCAF1 in the same complex (Figure 15 B). In contrast to EDD, CUL4 was detected in the sequential IP experiments, indicating that the cullin-

RING E3 ubiquitin ligase complex CRL4^{DCAF1} interacts with PLK4 (Grossmann et al., 2024). These results suggest PLK4 as an interaction partner of CRL4^{DCAF1}, however, whether PLK4 is a downstream substrate or an upstream regulator of the complex, remains to be deciphered.

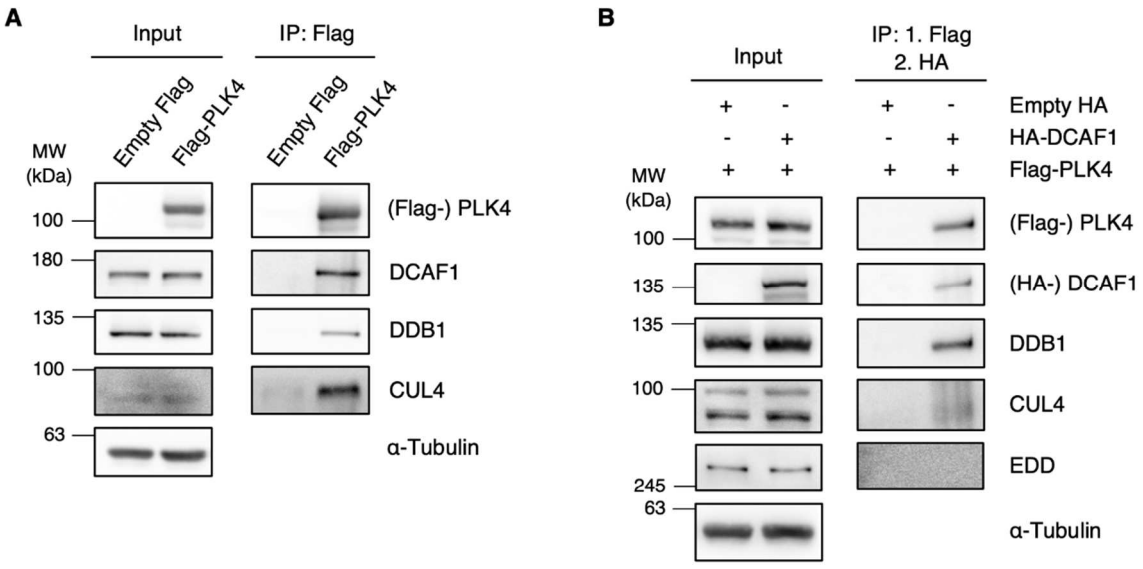

Figure 15: PLK4 forms a complex with the E3 ligase components CUL4, DDB1 and DCAF1.
(A) Empty Flag or Flag-PLK4 was overexpressed in HEK293T cells for 48 h. Cells were harvested and cell lysates were subjected to Flag IP. Input and eluate samples were analyzed by Western blot. **(B)** Flag-PLK4 and HA-DCAF1 were overexpressed in HEK293T cells for 48 h. Cells were harvested and cell lysates were subjected to Flag IP, followed by Flag peptide elution and subsequent IP against the HA tag using the eluates. Input and final eluate samples were analyzed by Western blot (Grossmann et al., 2024).

3.2.2 CRL4^{DCAF1} regulates PLK4 protein levels

It is known that PLK4 protein levels are regulated through ubiquitylation and proteasomal degradation mediated by the SCF$^{β\text{-}TrCP}$ E3 ubiquitin ligase (Rogers et al., 2009; Holland et al., 2010; Klebba et al., 2013). Since CRL4^{DCAF1} is another E3 ligase which can target its substrates for proteasomal degradation through ubiquitylation and my results clearly show that PLK4 interacts with the CRL4^{DCAF1} complex components (Figure 15), it is conceivable that this interaction implicates the regulation of PLK4 protein levels, which I investigated further.

If CRL4^{DCAF1} is a negative regulator of PLK4, its absence should cause elevated PLK4 levels. Depletion of DCAF1 by two different siRNAs in U2OS cells and analysis of cell lysates by Western blot, revealed significantly increased PLK4 protein levels compared to control (Figure 16 A). Further, I investigated how the absence of DCAF1 affects

PLK4 protein stability over time. I depleted DCAF1 in U2OS cells using siRNA and blocked protein translation by treatment with the ribosomal inhibitor cycloheximide (CHX). Analysis of protein levels by Western blot revealed a decrease in PLK4 levels over time in control as well as DCAF1-depleted cells, however in the absence of DCAF1, PLK4 levels were slightly stabilized and the protein half-life was increased from 1.02 h in control cells to 1.70 h upon DCAF1 depletion (Figure 16 B). Thus, DCAF1 seems to be necessary for a rapid and efficient PLK4 degradation, which is decelerated in the absence of DCAF1 (Grossmann et al., 2024).

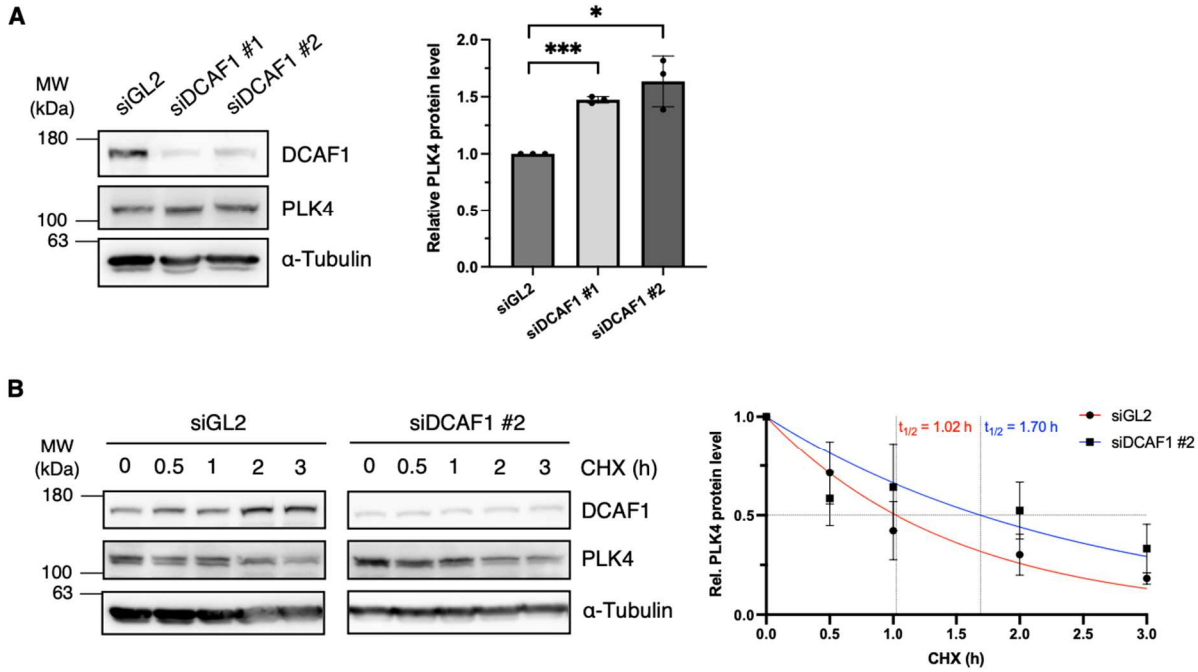

Figure 16: DCAF1 regulates PLK4 protein levels.

(A) U2OS cells were transfected twice with siRNA against either GL2 (control) or DCAF1 and harvested 72 h after the first transfection. Protein levels were determined by Western blot analysis. Quantification of relative PLK4/ α-Tubulin signal normalized to siGL2, N = 3. *** $p < 0.001$, * $p < 0.05$. Data are presented as mean ±SD. **(B)** U2OS cells were transfected twice with siRNA against either GL2 (control) or DCAF1 and protein synthesis was blocked 72 h after the first transfection by treatment with 100 µg/ml cycloheximide (CHX) for the indicated durations prior to harvest. Protein half-lives were determined by nonlinear fit to a one-phase decay model. N = 3 (Grossmann et al., 2024).

In addition, I generated a stable HeLa cell line for doxycycline-inducible knockdown of DCAF1. These cells express an shRNA targeting DCAF1 under control of a doxycycline-inducible promoter (Tet-On system). The shRNA sequence was generated based on the siRNA sequence siDCAF1 #1, as this siRNA gave the strongest knockdown of DCAF1, as well as the most significant effect on PLK4 levels in siRNA

experiments (Figure 16 A). Using the doxycycline-inducible HeLa cell line, I could confirm that the downregulation of DCAF1 leads to a simultaneous upregulation of PLK4 levels (Figure 17 A). The effect is detectable after 24 h of doxycycline treatment, already. The strongest downregulation of DCAF1, accompanied by the strongest upregulation of PLK4, is observed after 72 h of doxycycline treatment. The treatment for additional 24 h, reaching a total time of 96 h, does not increase the effects on neither DCAF1 nor PLK4 protein levels further. Thus, for all following experiments conducted with the stable HeLa cell line, DCAF1 knockdown is induced by doxycycline treatment for 72 h.

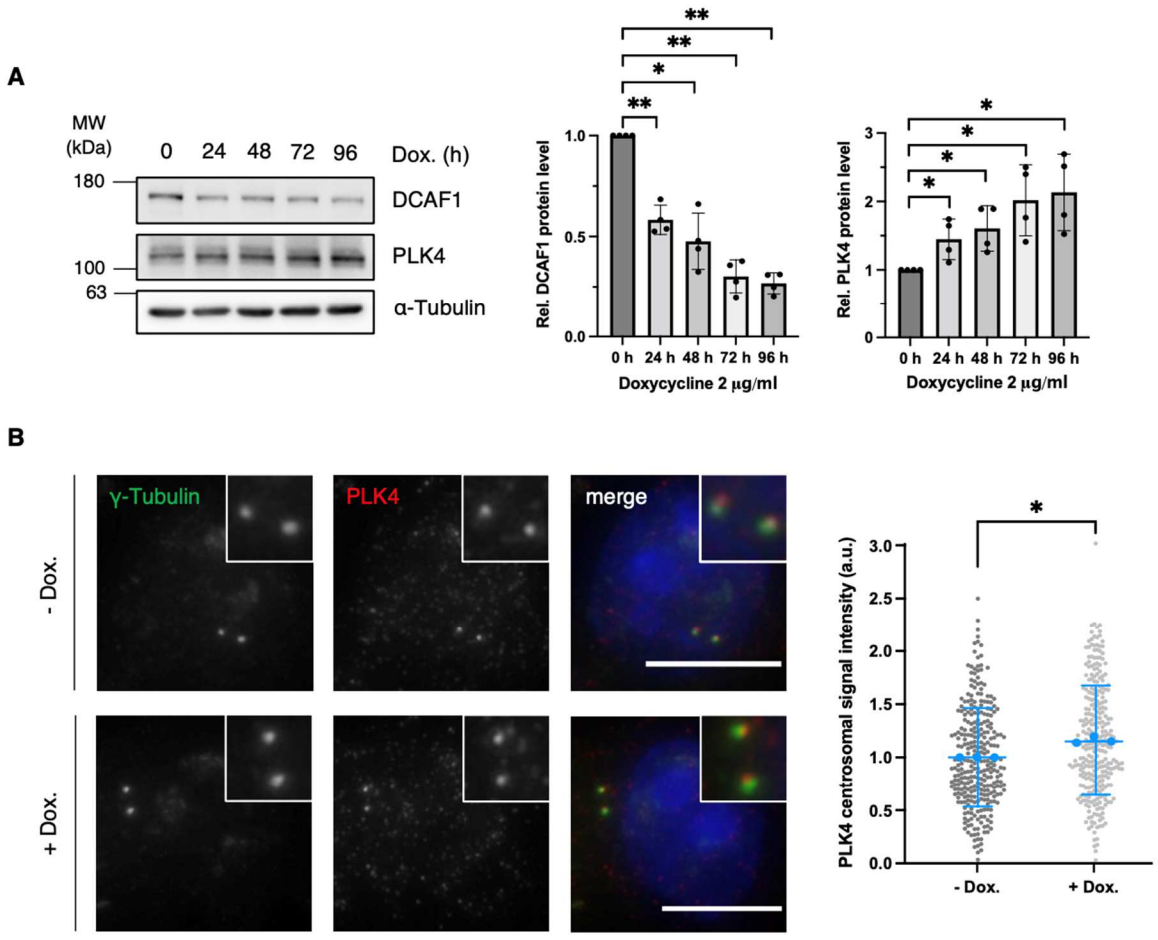

Figure 17: DCAF1 knockdown increases PLK4 protein levels.

(A) Knockdown of DCAF1 was induced in HeLa tet-on shDCAF1 cells by treatment with 2 µg/ml doxycycline for the indicated durations prior to harvest. Protein levels were determined by Western blot analysis. Quantification of relative DCAF1/ α-Tubulin and PLK4/ α-Tubulin signal normalized to 0 h time point, N = 4. ** $p < 0.01$, * $p < 0.05$. Data are presented as mean ±SD. **(B)** For knockdown of DCAF1, HeLa tet-on shDCAF1 cells were treated with 2 µg/ml doxycycline for 72 h prior to fixation. For immunofluorescence analysis, cells were stained with antibodies against γ-tubulin and PLK4. Scale bar: 10 µm. Centrosomal signal intensities were quantified and background fluorescence intensity was subtracted. Values were normalized to the untreated control. Individual values are presented with mean

±SD. In total, n = 300 centrosomes per condition were analyzed in N = 3 independent experiments. Statistical analysis of the mean values of three experiments. * p < 0.05 (Grossmann et al., 2024).

Since PLK4 is a centrosomal protein, I performed immunofluorescence stainings to specifically quantify PLK4 levels at the centrosome. Downregulation of DCAF1 by doxycycline treatment in the inducible HeLa cell line revealed that PLK4 levels are not only elevated at the general protein level but also at the centrosome specifically (Figure 17 B). Thus, DCAF1 might have a specific regulatory function at the centrosome in controlling PLK4 and thereby potentially also other proteins involved in the centrosome duplication cycle (Grossmann et al., 2024).

DCAF5, another substrate receptor of CUL-RING ubiquitin ligases (Zhang et al., 2019a), was also identified as a PLK4 interaction partner in the mass spectrometry screen and also co-precipitated with PLK4, when I performed Flag-IP from HEK293T cell lysates (Figure 18 A). However, I could show that DCAF5 is not involved in the regulation of PLK4, since its depletion in HEK293T cells using siRNA did not increase PLK4 protein levels (Figure 18 B) (Grossmann et al., 2024).

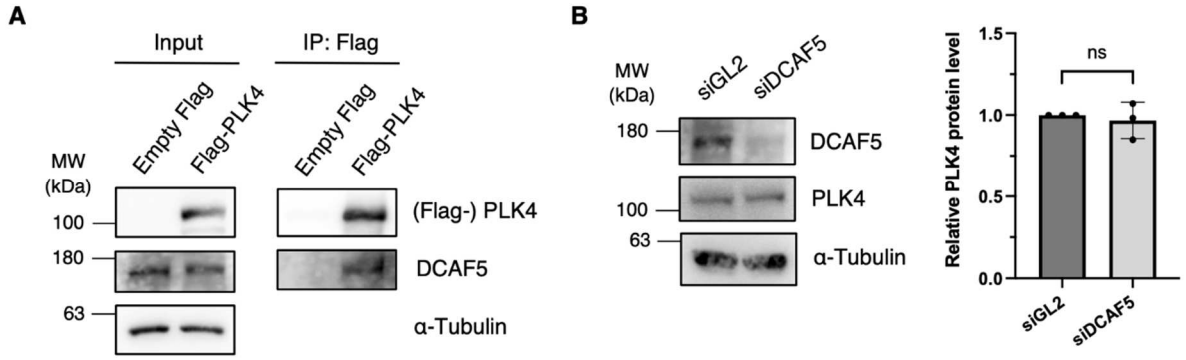

Figure 18: DCAF5 does not regulate PLK4 protein levels.
(A) Empty Flag or Flag-PLK4 was overexpressed in HEK293T cells for 48 h. Cells were harvested and cell lysates were subjected to Flag IP. Input and eluate samples were analyzed by Western blot. **(B)** HEK293T cells were transfected twice with siRNA against either GL2 (control) or DCAF5 and harvested 72 h after the first transfection. Protein levels were determined by Western blot analysis. Quantification of relative PLK4/ α-Tubulin signal normalized to siGL2, N = 3. ns p > 0.05. Data are presented as mean ±SD (Grossmann et al., 2024).

Taken together, these results indicate that the $CRL4^{DCAF1}$ E3 ubiquitin ligase interacts with PLK4 and is involved in the regulation of PLK4 protein levels, suggesting a second mechanism in addition to the $SCF^{\beta\text{-}TrCP}$ ubiquitin ligase for controlling PLK4 levels.

3.2.3 DCAF1 localizes to the centrosome

By complementary, mass spectrometry-based proteomics methods, Jakobsen et al. analyzed the components of human centrosomes and identified 126 known and 22 novel centrosomal proteins (Jakobsen et al., 2011). Although DCAF1 was not identified as a centrosomal protein candidate, it was a few years later shown to colocalize with centrin in immunofluorescence stainings of RPE-1 cells (Hossain et al., 2017). To confirm the centrosomal localization of DCAF1, which would support the hypothesis that the $CRL4^{DCAF1}$ ubiquitin ligase is involved in the regulation of the centrosomal protein PLK4, I performed ultrastructure expansion microscopy (U-ExM). This technique allows to physically magnify the centrosome approximately 4-fold and obtain high resolution images using a conventional microscope. Centrioles were visualized by staining microtubules for α-/β-tubulin, using a combination of two different antibodies. Immunofluorescence images revealed that DCAF1 colocalizes with centriolar α-/β-tubulin (Figure 19). This further indicates a potential regulatory function of the $CRL4^{DCAF1}$ ubiquitin ligase at the centrosome.

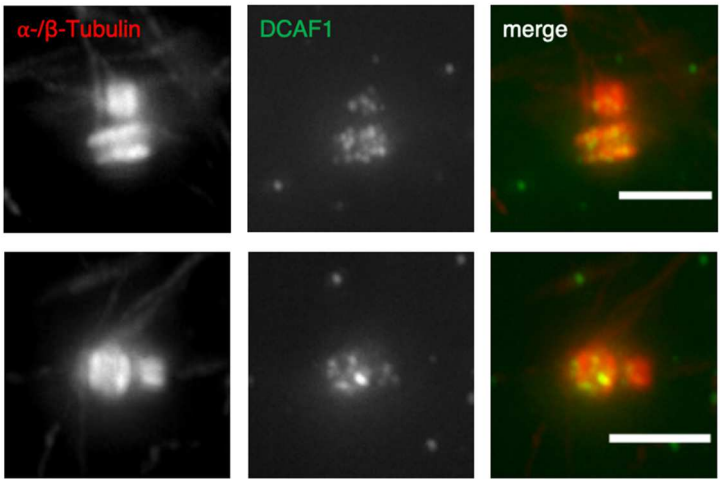

Figure 19: DCAF1 colocalizes with α-/β-tubulin at the centrosome.
Ultrastructure expansion microscopy (U-ExM) images of centrioles from HeLa cells stained against α-/β-Tubulin and DCAF1. Scale bar: 3 µm (physical scale), 0.68 µm (biological scale).

3.2.4 $CRL4^{DCAF1}$ ubiquitylates PLK4 *in vivo* and *in vitro*

To investigate whether the interaction between the E3 ubiquitin ligase complex $CRL4^{DCAF1}$ and its potential substrate PLK4 leads to enhanced ubiquitylation of PLK4 and whether the regulation of PLK4 protein levels by $CRL4^{DCAF1}$ is due to ubiquitylation and proteasomal degradation, I performed *in vivo* as well as *in vitro* ubiquitylation

assays. While *in vivo* experiments performed in living cells are more physiological but at the same time more variable, as they depend on many external factors such as cell density or cell cycle state and are influenced by all other components present in cells in addition to the proteins of interest, *in vitro* experiments exclude external influences as they are limited to the components of interest that are added to the reaction.

For the *in vivo* experiments, I used two different assays to study the ubiquitylation of PLK4 in HEK293T cells. First, I co-expressed HA-ubiquitin together with Flag-PLK4 and Myc-DCAF1 and treated cells with the 26S proteasome inhibitor MG132 to prevent proteasomal degradation and cause the accumulation of ubiquitylated proteins. Flag-PLK4 was immunoprecipitated and analyzed by Western blot. PLK4 was already slightly ubiquitylated without additional overexpression of DCAF1, however co-expression of DCAF1 strongly increased PLK4 ubiquitylation (Figure 20 A). This effect was reversed by inhibition of cullin-RING E3 ubiquitin ligases with the small-molecule neddylation inhibitor MLN4924, indicating that the cullin-RING ligase $CRL4^{DCAF1}$ contributes to PLK4 ubiquitylation (Grossmann et al., 2024).

To confirm this result, I performed a second *in vivo* ubiquitylation assay where I overexpressed His-ubiquitin together with Flag-PLK4 and Myc-DCAF1 in HEK293T cells. Proteins bound to His-ubiquitin were precipitated using Ni-NTA beads and analyzed by Western blot. Again, PLK4 was already slightly ubiquitylated without additional overexpression of DCAF1 but co-expression of DCAF1 clearly increased PLK4 ubiquitylation, which was reversible by treatment of cells with the cullin-RING E3 ligase inhibitor MLN4924 (Figure 20 B).

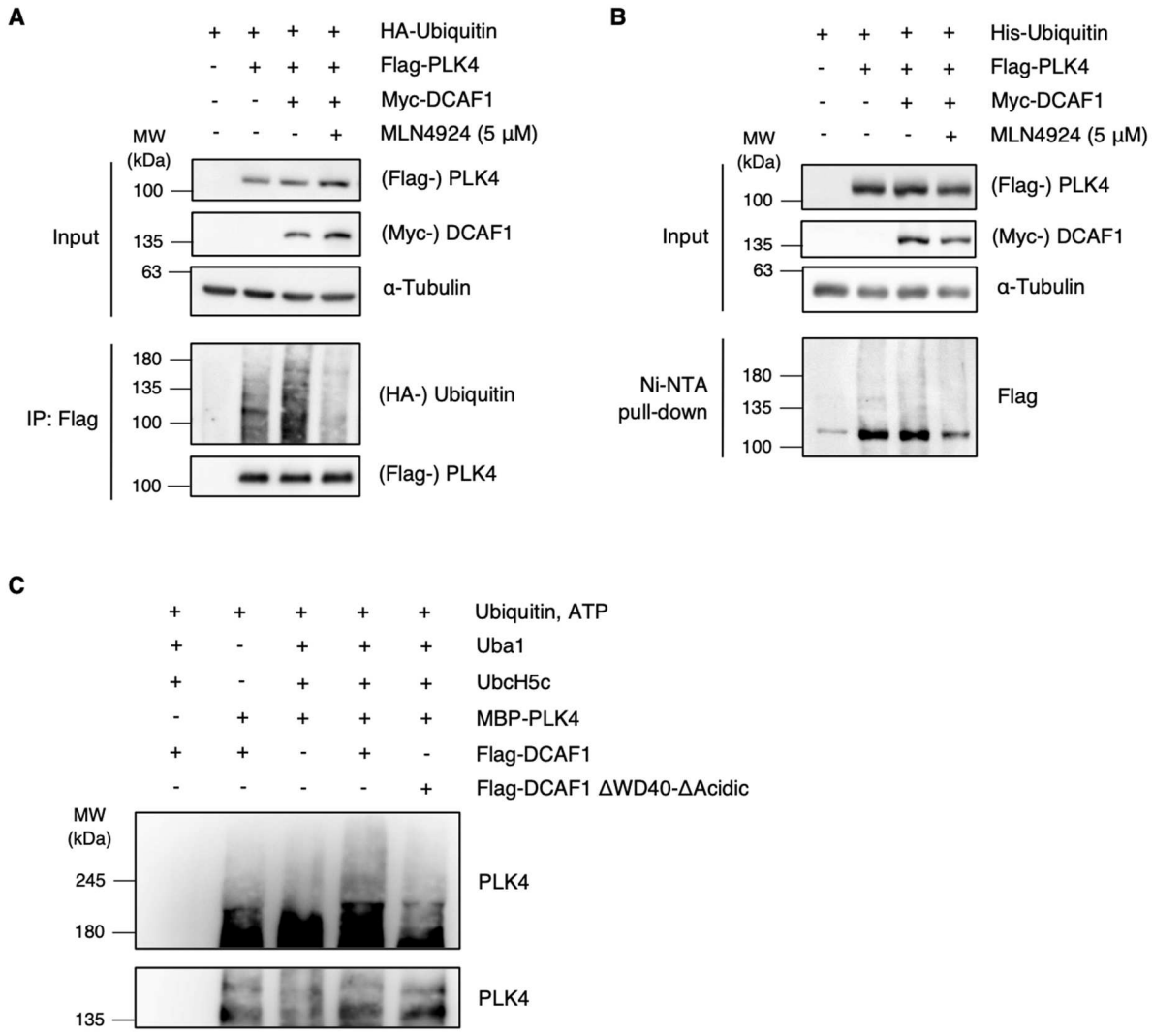

Figure 20: DCAF1 ubiquitylates PLK4 *in vivo* and *in vitro*.

(A) HA-Ubiquitin, Flag-PLK4 and Myc-DCAF1 were overexpressed in HEK293T cells for 24 h with or without inhibition of Cullin-RING E3 ligases by treatment with 5 µM MLN4924 for 5 h prior to harvest. The 26S proteasome was blocked by 10 µM MG132 for 5 h prior to harvest. Flag-PLK4 was immunoprecipitated from cell lysates in the presence of 10 mM *N*-ethylmaleimide using α-Flag M2 beads. Input and eluate samples were analyzed by Western blot. **(B)** His-Ubiquitin, Flag-PLK4 and Myc-DCAF1 were overexpressed in HEK293T cells for 24 h with or without inhibition of Cullin-RING E3 ligases by treatment with 5 µM MLN4924 for 5 h prior to harvest. The 26S proteasome was blocked by 10 µM MG132 for 5 h prior to harvest. Cells were harvested and cell lysates were subjected to Ni-NTA pulldown. Input and eluate samples were analyzed by Western blot. **(C)** Flag-DCAF1/ Myc-CUL4 complexes were expressed in HEK293T cells for 48 h and immobilized on α-Flag M2 beads. In vitro ubiquitylation assays were performed with 200 nM MBP-PLK4, 170 nM UBA1, 1 µM UBCH5C, 30 µM Ubiquitin, 5 mM ATP and immobilized Flag-DCAF1 complexes for 90 min at 37 °C. Samples were analyzed by Western blot (Grossmann et al., 2024).

To confirm these results *in vitro,* I performed *in vitro* ubiquitylation assays of recombinant MBP-PLK4. I co-expressed Myc-CUL4 together with Flag-DCAF1 or Flag-DCAF1$^{\Delta WD40\text{-}\Delta Acidic}$, which lacks the PLK4 binding domain, in HEK293T cells and

immobilized the complexes on α-Flag M2 beads. Using these E3 ligase complexes, I analyzed the ubiquitylation of recombinant MBP-PLK4 in presence of the E1 enzyme UBA1, the E2 enzyme UBCH5C, ubiquitin and ATP. The $CRL4^{DCAF1}$ E3 ligase has been previously shown to cooperate with the specific E1 enzyme UBA1 and the E2 enzyme UBCH5C in the ubiquitylation of its substrates (Han et al., 2020). Purified E1, E2 and ubiquitin were kind gifts from Frauke Melchior (ZMBH, Heidelberg). Western blot analysis revealed that PLK4 is strongly ubiquitylated by wild-type DCAF1 but not by the $DCAF1^{\Delta WD40\text{-}\Delta Acidic}$ mutant lacking the PLK4 binding domain (Figure 20 C) (Grossmann et al., 2024).

Taken together, these results indicate that the $CRL4^{DCAF1}$ E3 ubiquitin ligase complex interacts with PLK4 and regulates its protein levels by ubiquitylation and proteasomal degradation.

3.3 The CRL4^{DCAF1} ubiquitin ligase regulates PLK4-dependent centriole duplication

My results indicate that PLK4 might be a novel substrate of the CRL4^{DCAF1} E3 ubiquitin ligase, which is bound by the substrate receptor DCAF1 in a phosphorylation-independent manner and thereby targeted for ubiquitylation and subsequent proteasomal degradation. PLK4 is a low-abundance protein with tightly controlled protein levels throughout the cell cycle and also known as the master regulator of centriole duplication (Bettencourt-Dias et al., 2005). Since centriole duplication is a very complex and critical process for cell division, it is plausible that several distinct regulatory mechanisms exist and that CRL4^{DCAF1} might be second ubiquitin ligase, in addition to SCF$^{\beta\text{-TrCP}}$, required for the regulation of PLK4 protein levels. Therefore, I further investigated the potential involvement of the CRL4^{DCAF1} ubiquitin ligase in centriole duplication.

3.3.1 CRL4^{DCAF1} regulates PLK4 predominantly in G2 phase of the cell cycle

In the mammalian cell cycle, PLK4 is recruited to the centrosome and binds to the centriolar proteins CEP152 and CEP192 at the G1/S phase transition (Kim et al., 2013b; Sonnen et al., 2013). Upon interaction with STIL, PLK4 autophosphorylation is initiated which allows for the recognition by SCF$^{\beta\text{-TrCP}}$ and triggers the proteasomal degradation of PLK4. As the interaction between PLK4 and CRL4^{DCAF1} occurs at a different binding site and in a different, phosphorylation-independent manner compared to SCF$^{\beta\text{-TrCP}}$, I further investigated whether CRL4^{DCAF1} might also regulate PLK4 in a different phase of the cell cycle.

I overexpressed Flag-PLK4 in HEK293T cells that were subsequently synchronized either at the G1/S phase transition by double thymidine arrest, in G2 phase by treatment with the CDK1 inhibitor RO-3306 or in mitosis by single thymidine and nocodazole arrest. Performing Flag-IP experiments from cell lysates of synchronized cells, I found that the interaction between PLK4 and DCAF1 is significantly stronger in interphase compared to mitosis (Figure 21). The strongest interaction was observed in G2 phase (Grossmann et al., 2024). In general, the DCAF1 expression in synchronized HEK293T cells was slightly stronger in interphase compared to mitosis.

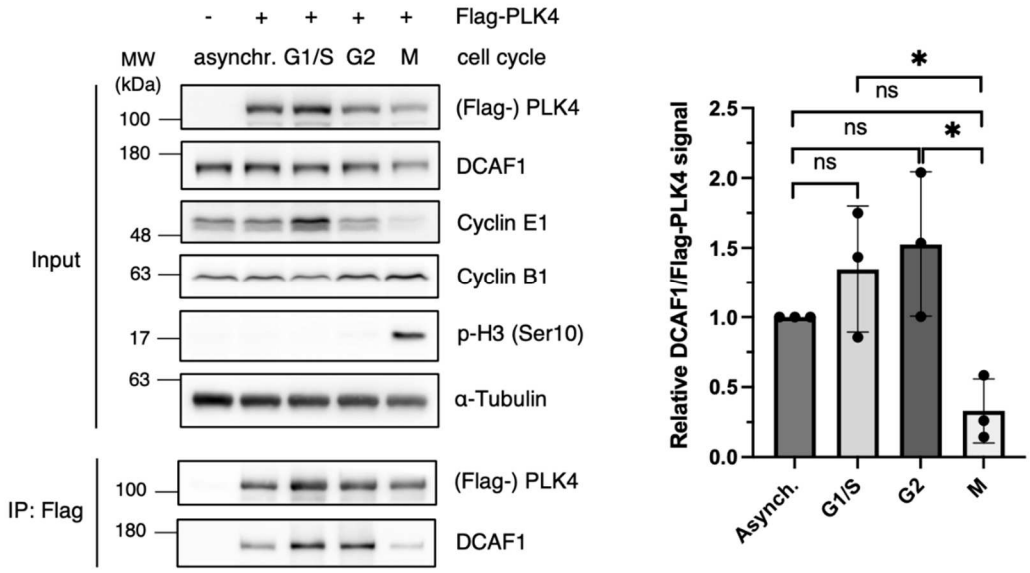

Figure 21: DCAF1 interacts with PLK4 predominantly in G2 phase of the cell cycle.
Flag-PLK4 was overexpressed in HEK293T cells for 48 h. Cells were synchronized in G1/S phase by double thymidine arrest, in G2 phase by CDK1 inhibition with RO-3306 or in M phase by single thymidine and nocodazole arrest, as indicated. Flag-PLK4 was immunoprecipitated from cell lysates using α-Flag M2 beads. Quantification of relative DCAF1/ Flag-PLK4 signal normalized to asynchronous cells, N = 3. * $p < 0.05$, ns $p > 0.05$. Data are presented as mean ±SD (Grossmann et al., 2024).

To further investigate whether the strong interaction also correlates with a strong ubiquitylation of PLK4 by DCAF1, I performed *in vivo* ubiquitylation assays in synchronized HEK293T cells. I co-expressed HA-ubiquitin together with Flag-PLK4 and Myc-DCAF1, synchronized cells as described previously and treated cells with the 26S proteasome inhibitor MG132 before harvesting to prevent proteasomal degradation and cause the accumulation of ubiquitylated proteins. Flag-PLK4 was immunoprecipitated from cell lysates. Western blot analysis revealed that PLK4 is ubiquitylated by DCAF1 predominantly in G2 phase, correlating with the strong interaction in this phase of the cell cycle (Figure 22 A). Consistent with the weak interaction between PLK4 and DCAF1 in mitosis, also the ubiquitylation of PLK4 in mitosis is weak. Quantification of the PLK4 ubiquitylation in G2 phase with and without overexpression of DCAF1 confirmed that the significantly increased ubiquitylation in G2 can be clearly attributed to DCAF1 (Figure 22 B) (Grossmann et al., 2024).

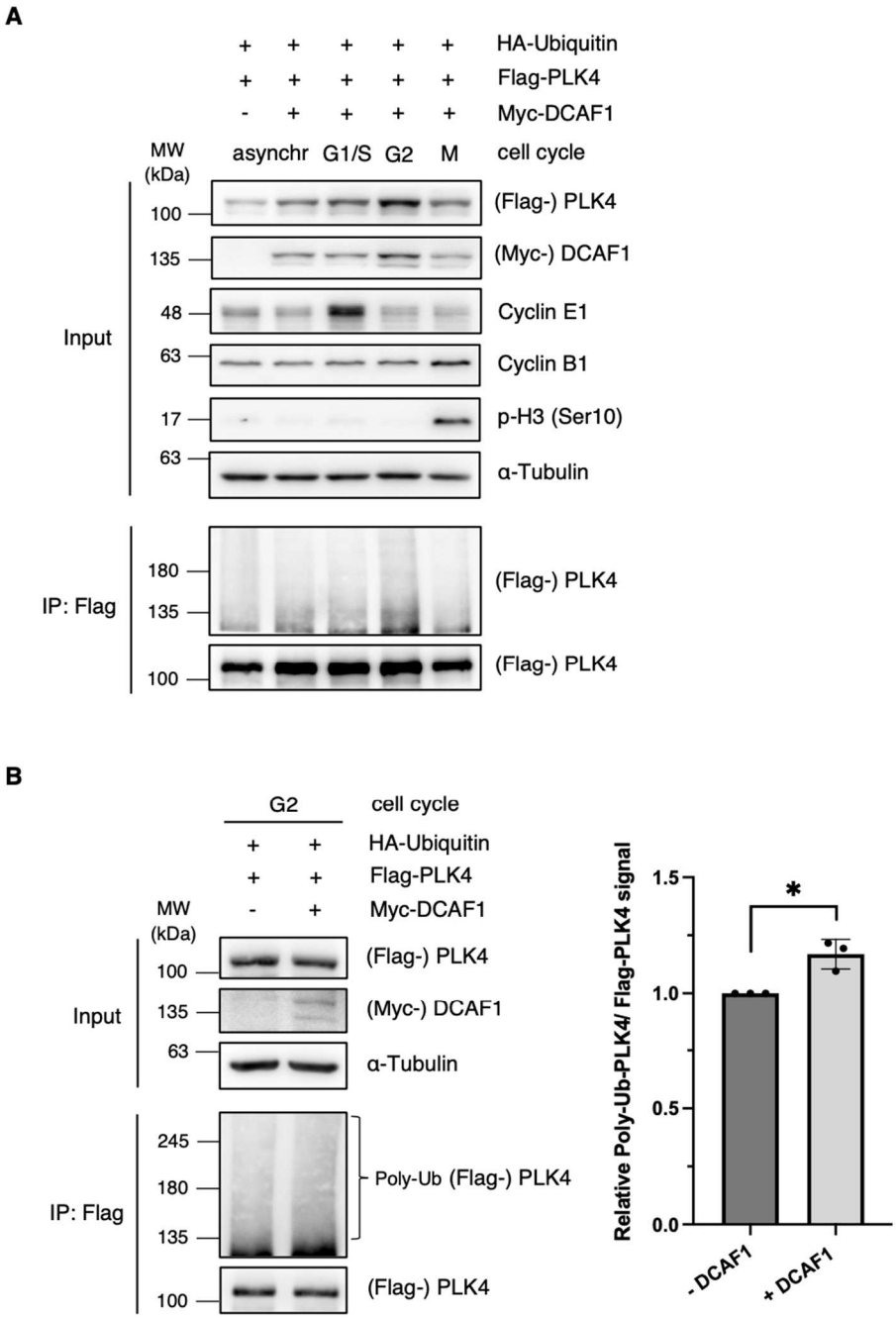

Figure 22: DCAF1 ubiquitylates PLK4 predominantly in G2 phase of the cell cycle.

(A) HA-Ubiquitin, Flag-PLK4 and Myc-DCAF1 were overexpressed in HEK293T cells for 24 h. Cells were synchronized in G1/S phase by double thymidine arrest, in G2 phase by CDK1 inhibition with RO-3306 or in M phase by single thymidine and nocodazole arrest, as indicated. To inhibit the 26S proteasome, cells were treated with 10 µM MG132 for 5 h prior to harvest. Flag-PLK4 was immunoprecipitated from cell lysates in the presence of 10 mM *N*-ethylmaleimide using α-Flag M2 beads. **(B)** HA-Ubiquitin, Flag-PLK4 and Myc-DCAF1 were overexpressed in HEK293T cells for 24 h. Cells were synchronized in G2 phase by CDK1 inhibition with RO-3306. To inhibit the 26S proteasome, cells were treated with 10 µM MG132 for 5 h prior to harvest and Flag-PLK4 was immunoprecipitated from cell lysates in the presence of 10 mM *N*-ethylmaleimide using α-Flag M2 beads. Quantification of relative Poly-Ub-Flag-PLK4/ Flag-PLK4 signal normalized to the – DCAF1 control, N = 3. * $p < 0.05$. Data are presented as mean ±SD (Grossmann et al., 2024).

Together, these results demonstrate that the $CRL4^{DCAF1}$ ubiquitin ligase complex regulates PLK4 protein levels in G2 phase, indicating a complementary function in addition to $SCF^{\beta\text{-}TrCP}$, as the activity of the $SCF^{\beta\text{-}TrCP}$ E3 ligase was shown to be low in G2 phase (Paul et al., 2022).

3.3.2 Absence of DCAF1 causes formation of supernumerary centrioles in mitosis

Overexpression of PLK4 has been shown to cause centriole overduplication and the formation of multipolar spindles in mitosis (Habedanck et al., 2005; Coelho et al., 2015). If the $CRL4^{DCAF1}$ ubiquitin ligase complex is an important regulator of PLK4 and depletion of DCAF1 causes elevated PLK4 protein levels as indicated by my previous results, absence of DCAF1 should also cause the formation of supernumerary centrioles in mitosis.

I induced knockdown of DCAF1 in doxycycline-inducible HeLa cells and analyzed the centriole numbers in mitotic cells by immunofluorescence staining of the centriolar protein centrin. In a wild-type cell forming a regular bipolar spindle in mitosis, one centrosome, consisting of two centrioles, is expected to be present at each of both spindle poles, resulting in a total of four centrin foci per cell. Compared to control cells, DCAF1-depleted cells revealed a higher percentage of mitotic cells with supernumerary, meaning more than four, centrioles leading to the formation of multipolar spindles (Figure 23). While mitotic cells with zero or one centriole were not observed under the analyzed conditions, numbers of cells with two or three centrioles were similar in DCAF1-depleted cells compared to control cells. Elevated PLK4 protein levels and the formation of supernumerary centrioles observed in the absence of DCAF1, confirm the important role of the $CRL4^{DCAF1}$ ubiquitin ligase in the regulation of PLK4 levels and the prevention of centriole overduplication (Grossmann et al., 2024).

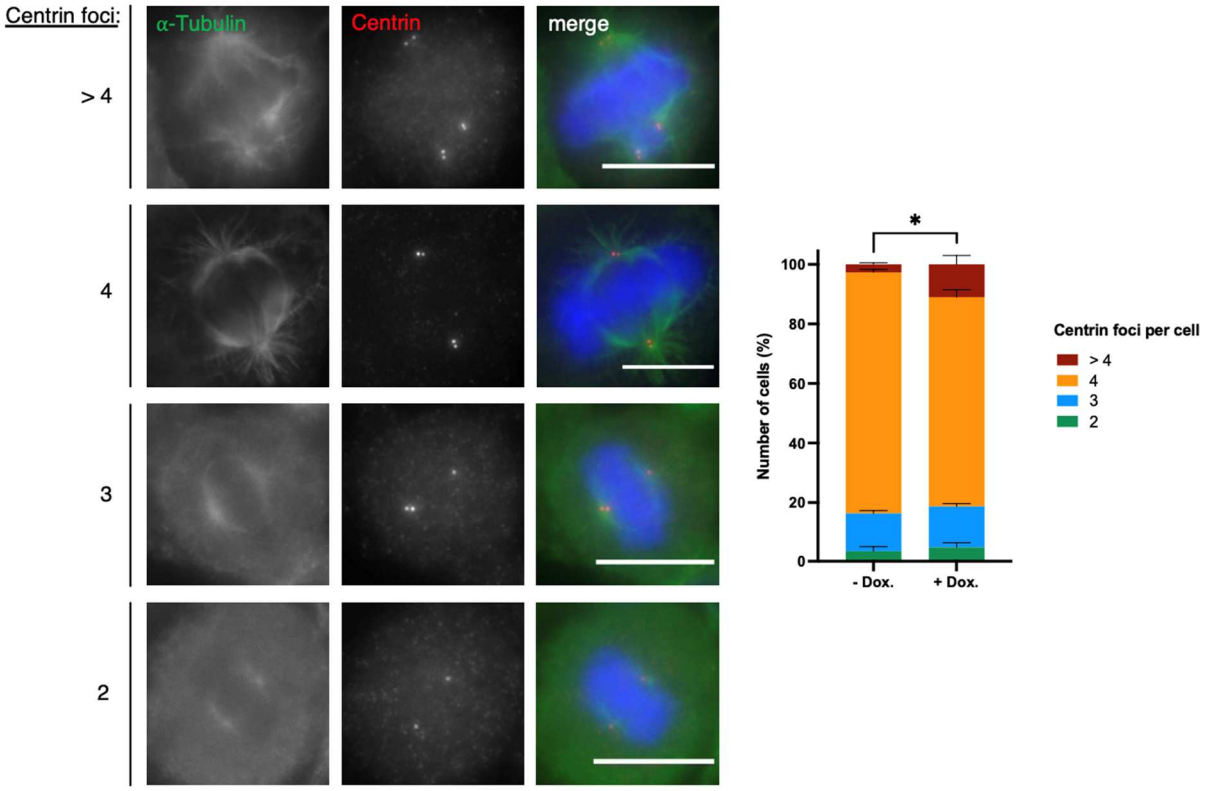

Figure 23: Absence of DCAF1 causes formation of supernumerary centrioles in mitosis.
For knockdown of DCAF1, HeLa tet-on shDCAF1 cells were treated with 2 µg/ml doxycycline for 72 h prior to fixation. For knockdown of β-TrCP, cells were transfected twice every 24 h with 40 nM siRNA. For immunofluorescence analysis, cells were stained with antibodies against α-Tubulin and centrin. Scale bar: 10 µm. The number of centrioles per mitotic cell was determined based on centrin staining. N = 3 independent experiments with 100 mitotic cells per condition in each experiment. * $p < 0.05$ for > 4 centrin foci. Data are presented as mean +SD (Grossmann et al., 2024).

Next to centriole overduplication, cell division failures, such as cytokinesis defects, might be a second potential cause for the formation of supernumerary centrioles and PLK4 is known to have a function in cytokinesis (Rosario et al., 2010). To exclude the possibility that the multiple centrioles observed in response to DCAF1 knockdown result from a cytokinesis defect, I performed live cell imaging to show that doxycycline-induced DCAF1 knockdown in HeLa cells does not lead to cell division failures (Figure 24) (Grossmann et al., 2024).

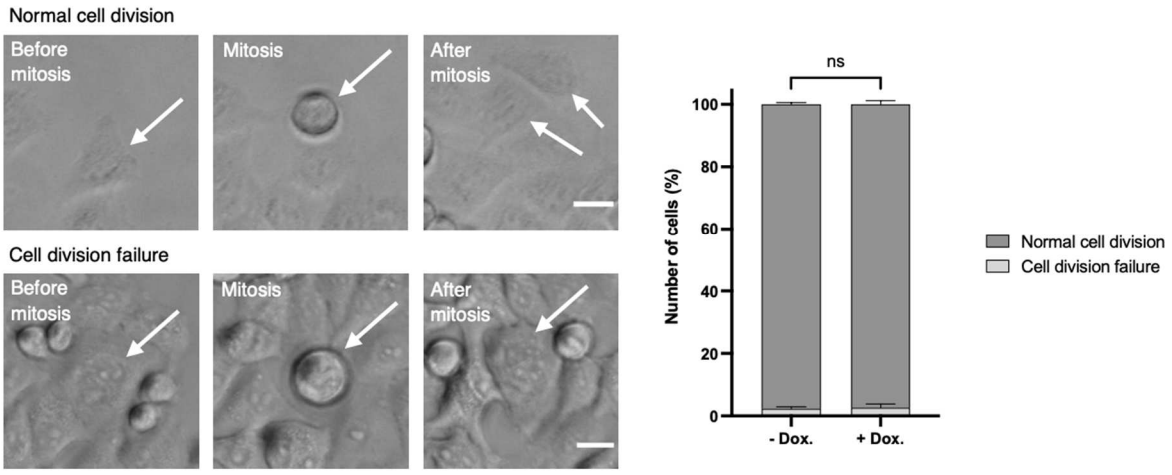

Figure 24: Absence of DCAF1 does not cause cell division failures.
Images from live cell imaging performed with HeLa tet-on shDCAF1 cells showing a normal cell division and a cell division failure. White arrows indicate representative cells. Scale bar: 20 µm. N = 3 independent experiments with n = 100 mitoses analyzed per condition for each experiment. ns p > 0.05. Data are presented as mean +SD (Grossmann et al., 2024).

3.3.3 CRL4^{DCAF1} regulates interaction between PLK4 and its substrates STIL and NEDD1

Next, I aimed at investigating the possible functions of PLK4 regulation by DCAF1 for the centriole duplication process further downstream of PLK4. After PLK4 is recruited to the centrosome, it binds to and phosphorylates its substrate STIL which then recruits SAS-6 for cartwheel formation and initiation of procentriole assembly. During mitosis however, STIL is bound by CDK1/ Cyclin B, preventing an early formation of the PLK4-STIL complex and phosphorylation of STIL by PLK4 to inhibit an untimely onset of centriole biogenesis (Zitouni et al., 2016). It is possible that also CRL4^{DCAF1} is involved in the regulation of PLK4-STIL complex formation by binding to PLK4 in G2 phase, similarly to CDK1/ Cyclin B binding to STIL in mitosis.

To decipher the role of DCAF1 in PLK4-STIL complex formation, I first analyzed the amount of STIL binding to PLK4 in presence and absence of DCAF1. I performed GFP-IP after simultaneous siRNA mediated knockdown of DCAF1 and doxycycline-induced overexpression of GFP-PLK4 in HeLa cells and found that upon depletion of DCAF1, a significantly higher amount of STIL co-precipitates with PLK4 (Figure 25 A). To confirm this result, I assessed how overexpression of DCAF1, instead of depletion of DCAF1, affects the PLK4-STIL interaction. I co-expressed Flag-PLK4 together with increasing amounts of Myc-DCAF1 in HEK293T cells and performed Flag-IP from cell

lysates to analyze the amount of STIL co-precipitating with PLK4 in presence of different amounts of DCAF1. In accordance with the finding that DCAF1 depletion increases the amount of STIL binding to PLK4, I found that overexpression of DCAF1 reduces the amount of STIL binding to PLK4 in a dose-dependent manner (Figure 25 B). Together, these results indicate an important regulatory function of DCAF1 not only for PLK4 itself, but also for its interaction with the substrate STIL further downstream in the centriole duplication process (Grossmann et al., 2024).

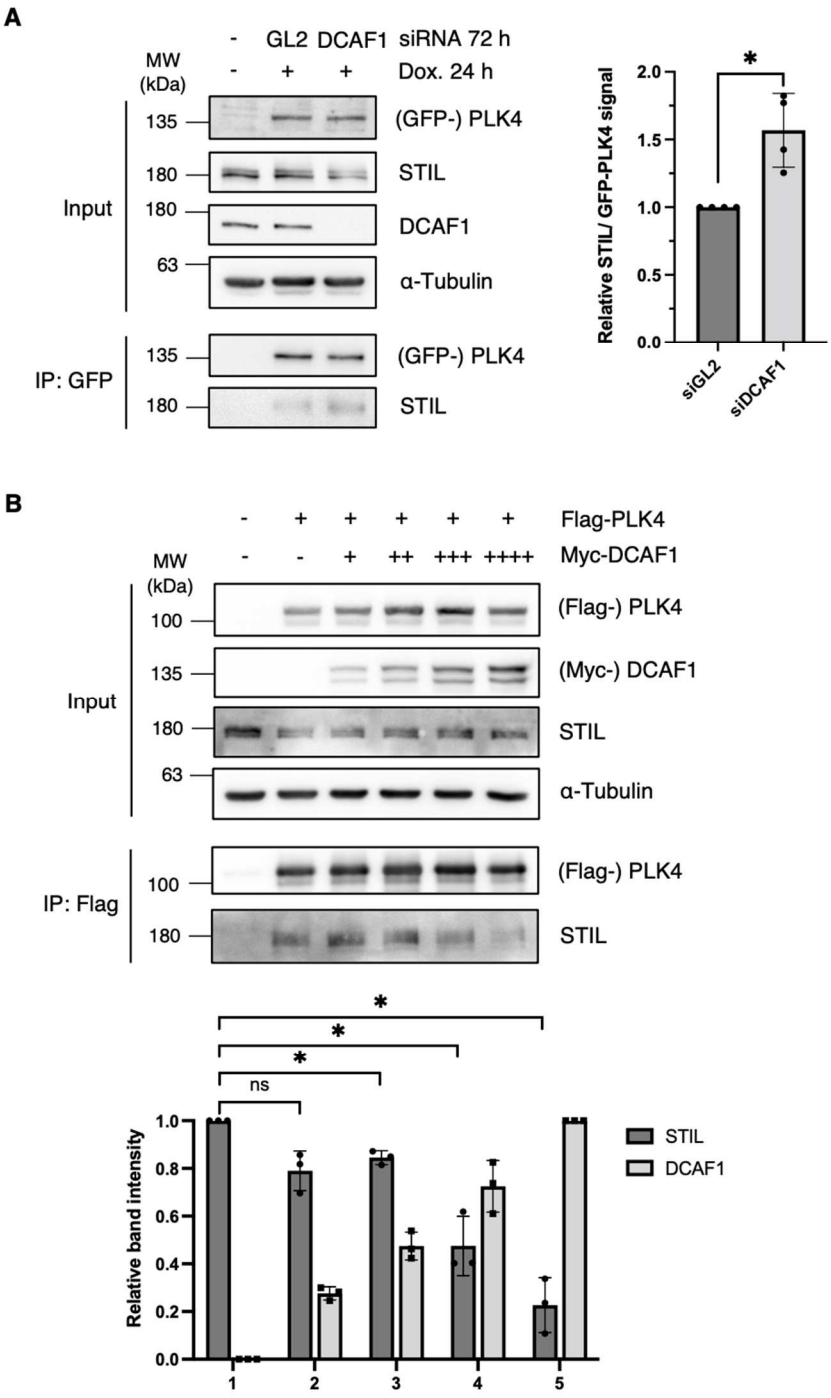

Figure 25: DCAF1 regulates the interaction between PLK4 and its substrate STIL.
(A) HeLa tet-on GFP-PLK4 cells were transfected twice every 24 h with 40 nM siRNA targeting GL2 (control) or DCAF1. Overexpression of GFP-PLK4 was induced by treatment with 2 µg/ml doxycycline 24 h prior to harvest. GFP-PLK4 was immunoprecipitated from cell lysates using GFP-trap beads. Quantification of relative STIL/ GFP-PLK4 signal normalized to GL2 (control), N = 4. * $p < 0.05$. Data are presented as mean ±SD. **(B)** Flag-PLK4 was overexpressed in HEK293T cells together with different amounts of Myc-DCAF1 in different samples (+, ++, +++, ++++) for 48 h. Co-precipitated STIL was detected by IP against the Flag tag and subsequent Western blot analysis. Quantification of relative STIL/ Flag-PLK4 and Myc-DCAF1 signal, N = 3. * $p < 0.05$, ns $p > 0.05$. Data are presented as mean ±SD (Grossmann et al., 2024).

Upon interaction with STIL, PLK4 kinase activity is activated, initiating the autophosphorylation and subsequent ubiquitylation and proteasomal degradation of PLK4 to keep its protein levels low. PLK4 kinase activity is detectable by S305 autophosphorylation on PLK4 (Sillibourne et al., 2010). Since depletion of DCAF1 increased the amount of STIL binding to PLK4, there is a possibility that it might also cause an increase in PLK4 S305 autophosphorylation. I depleted DCAF1 in HEK293T cells using siRNA and overexpressed Flag-PLK4 to perform Flag-IPs from cell lysates. Using a specific antibody against phosphorylated S305 on PLK4 (Park et al., 2014), I compared the amounts of autophosphorylated PLK4 in presence and absence of DCAF1. However, DCAF1 knockdown did not affect PLK4 p-S305 levels, one step further downstream of the interaction between PLK4 and STIL (Figure 26). Probably, detection of differences in this phosphorylation event is time-critical and potentially not possible in asynchronously cycling human cells.

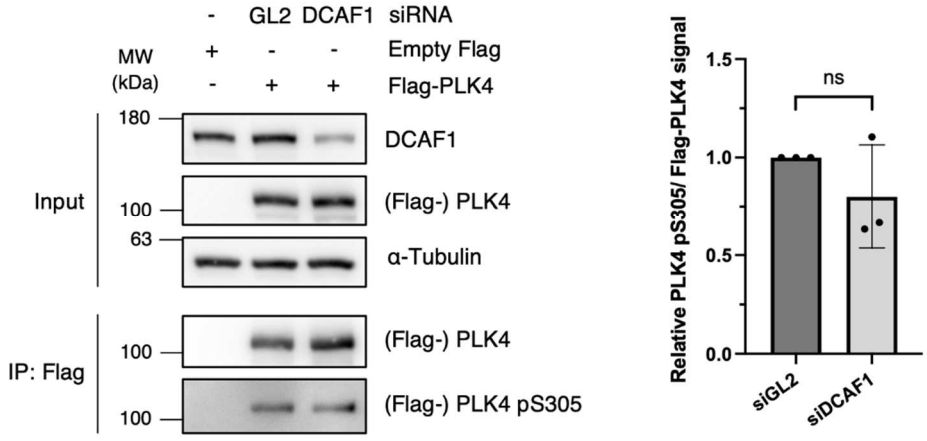

Figure 26: DCAF1 knockdown does not affect PLK4 S305 autophosphorylation.
HEK293T cells were transfected twice with siRNA against either GL2 (control) or DCAF1 and harvested 72 h after the first transfection. 24 h prior to harvest, empty Flag or Flag-PLK4 was overexpressed. Cells were harvested and cell lysates were subjected to Flag IP. Input and eluate samples were analyzed by

Western blot. Quantification of relative PLK4 pS305/ Flag-PLK4 signal normalized to GL2 (control), N = 3. ns p > 0.05. Data are presented as mean ±SD.

In addition to STIL, also NEDD1 is a substrate of PLK4, which is recruited to the centrosome, interacts with and is phosphorylated by PLK4 (Chi et al., 2021). I induced the knockdown of DCAF1 by doxycycline treatment of the inducible HeLa cell line and performed immunofluorescence microscopy to analyze NEDD1 levels at the centrosome in the presence and absence of DCAF1. I found significantly higher levels of NEDD1 at the centrosome upon knockdown of DCAF1, indicating that DCAF1 also affects the interaction between PLK4 and its substrate NEDD1 (Figure 27) (Grossmann et al., 2024).

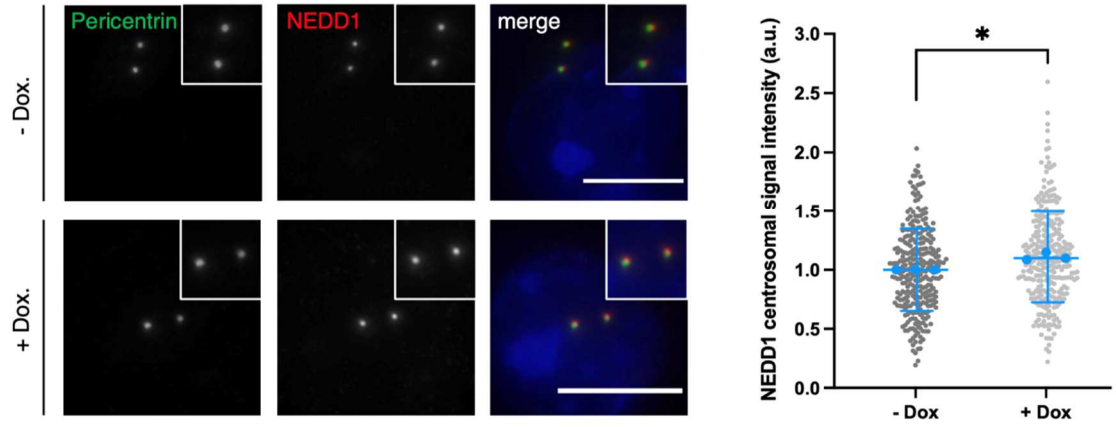

Figure 27: DCAF1 knockdown increases NEDD1 levels at the centrosome.
For knockdown of DCAF1, HeLa tet-on shDCAF1 cells were treated with 2 µg/ml doxycycline for 72 h prior to fixation. For immunofluorescence analysis, cells were stained with antibodies against Pericentrin and NEDD1. Scale bar: 10 µm. Centrosomal signal intensities were quantified and background fluorescence intensity was subtracted. Values were normalized to the untreated control. Individual values are presented with mean ±SD. In total, n = 300 centrosomes per condition were analyzed in N = 3 independent experiments. Statistical analysis of the mean values of three experiments. * p < 0.05 (Grossmann et al., 2024).

3.3.4 CRL4^{DCAF1} prevents premature centriole disengagement in G2 phase

The strong interaction between DCAF1 and PLK4 and the strong ubiquitylation of PLK4 by the CRL4^{DCAF1} ubiquitin ligase in G2 phase are indicators of an important regulatory function of DCAF1 in this phase of the cell cycle to prevent a premature onset of centriole duplication in mitosis. During a regular centriole duplication cycle, centrioles lose their tight orthogonal configuration upon mitotic exit and entry into G1 phase. The disengagement process licenses the centrioles for the subsequent round of

centrosome duplication (Tsou et al., 2009). A premature centriole disengagement in absence of DCAF1 could lead to a premature centriole re-duplication, as a cause for the supernumerary centrioles observed upon depletion of DCAF1 (Figure 23).

I induced DCAF1 knockdown in the doxycycline-inducible HeLa cell line, synchronized cells in G2 phase by treatment with the CDK1 inhibitor RO-3306 and performed U-ExM to identify and quantify cells with disengaged centrioles already in G2 phase. All centriole pairs with a distance of more than one centriole length between the two centrioles were considered as disengaged. I found that knockdown of DCAF1 significantly increased the percentage of cells with already disengaged centrioles (Figure 28 A). As the interference with CDK1 function by treatment of cells with the inhibitor RO-3306 might itself already have an effect on centriole disengagement, I additionally measured intercentriolar distances between two centrioles of a centriole pair in HeLa cells with four centrioles, which were not previously synchronized. Upon doxycycline induced knockdown of DCAF1, I found significantly increased intercentriolar distances (Figure 28 B), further indicating that the absence of DCAF1 triggers centriole disengagement leading to a premature centriole re-duplication and that its presence is required to ensure correct timing of the onset of the centriole duplication process (Grossmann et al., 2024).

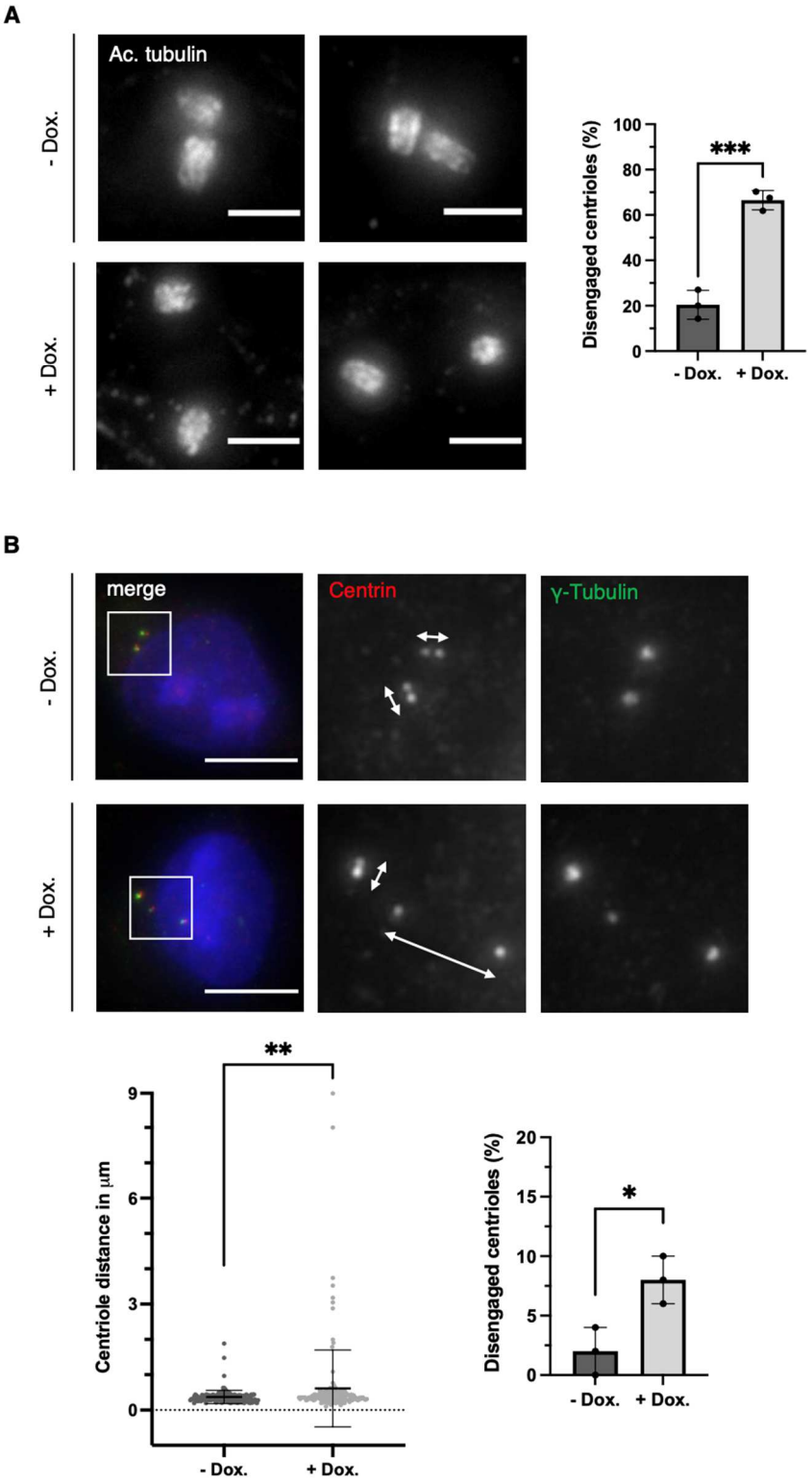

Figure 28: DCAF1 knockdown causes early centriole disengagement in G2 phase of the cell cycle.

(A) For knockdown of DCAF1, HeLa tet-on shDCAF1 cells were treated with 2 µg/ml doxycycline for 72 h prior to fixation. G2 arrest was induced by treatment with the CDK1 inhibitor RO-3306 for 18 h prior to fixation. Representative U-ExM images of centrioles stained against acetylated tubulin. Scale bar: 3 µm (physical scale), 0.68 µm (biological scale). Quantification of percentage of cells with disengaged centrioles in G2 phase. Centriolar distances of more than one centriole length were considered as

disengaged. N = 3 independent experiments with n = 37, 42 and 40 cells analyzed per condition. *** $p < 0.001$. Data are presented as mean ±SD. **(B)** For knockdown of DCAF1, HeLa tet-on shDCAF1 cells were treated with 2 µg/ml doxycycline for 72 h prior to fixation. For immunofluorescence analysis, cells were stained with antibodies against γ–Tubulin and centrin. White arrows indicate the distance between centrioles. Scale bar: 10 µm. Left panel: Centriole distance values from N = 3 independent experiments with n = 50 centriole pairs analyzed per condition for each experiment. ** $p < 0.01$. Data are presented as mean ±SD. Right panel: Quantification of percentage of cells with disengaged centrioles. Distances of more than 0.75 µm between the two centrioles of a centriole pair were considered as disengaged. * $p < 0.05$. Data are presented as mean ±SD (Grossmann et al., 2024).

4. Discussion

PLK4 is known as the master regulator of centrosome duplication, a process which has to be tightly controlled, as abnormal centrosome numbers have been linked to genomic instability, aneuploidy and cancer (Levine et al., 2017; Nigg and Holland, 2018). Strictly regulated PLK4 protein levels have been shown to be crucial, since PLK4 depletion prevents centriole duplication and causes mitotic defects, while PLK4 overexpression results in overamplification of centrioles. Consequently, it is likely that several distinct pathways or mechanisms controlling PLK4 levels exist, in order to ensure this tight regulation at all times. In the presented thesis, I identified the E3 ubiquitin ligase complex $CRL4^{DCAF1}$ as a novel regulator of PLK4 and unraveled its important functions in the centrosome duplication process.

4.1 PLK4 is a novel substrate of the $CRL4^{DCAF1}$ ubiquitin ligase

Recently, a mass spectrometry (MS) screen has been performed by A. Kratz (Hoffmann group, DKFZ Heidelberg) in collaboration with the DKFZ protein analysis facility in order to identify novel interaction partners of PLK4. Several known but also unknown candidate proteins were detected as potential upstream regulators or downstream substrates of PLK4. STIL, a positive hit from this screen, has been further characterized as an important substrate, which is phosphorylated by PLK4 and required for centriole duplication (Kratz et al., 2015).

Among other proteins related to the ubiquitin-proteasome system, the E3 ubiquitin ligase substrate receptor DCAF1 has been identified as a potential novel interaction partner of PLK4. In order to validate this finding from the MS screen, I performed co-immunoprecipitations of PLK4 and DCAF1. As expected, PLK4 and DCAF1 interacted with each other: Endogenous DCAF1 specifically co-precipitated with overexpressed Flag-PLK4 and reciprocally, endogenous PLK4 co-precipitated with overexpressed Flag-DCAF1. Also at the completely endogenous level, PLK4 specifically co-precipitated with DCAF1, confirming the MS results. In addition, *in vitro* binding assays proved that the interaction between PLK4 and DCAF1 is indeed direct and not mediated by another unidentified protein (Figure 9). Reciprocal interaction mapping, using truncated fragments of both proteins, revealed that PLK4 interacts via its C-terminal PB1-PB2 domain, while DCAF1 is dependent on its C-terminal acidic domain for the interaction with PLK4 (Figure 10 and Figure 12). The PLK4 PB domains have

been previously described to be involved in homodimerization and the mediation of protein-protein interactions (Slevin et al., 2012; Klebba et al., 2015), consistent with the finding that the smallest fragment containing only PB1 and PB2 is sufficient to mediate binding to DCAF1. However, this small fragment is not strictly limited to the PB1-PB2 domain but still contains parts of the L1 and L2 linker regions located right before and right behind the PB1-PB2 cassette. A potential contribution of these linker regions to the interaction with DCAF1 cannot be excluded. A shorter construct that lacks these regions and is precisely limited to the PB1-PB2 cassette could be generated and tested for its interaction with DCAF1.

Given that DCAF1 serves as a substrate receptor of the $CRL4^{DCAF1}$ E3 ubiquitin ligase, which can target proteins for ubiquitylation and proteasomal degradation, I investigated whether $CRL4^{DCAF1}$ regulates PLK4 protein levels. My results showed that PLK4 levels are elevated when DCAF1 is depleted in different cell lines, either by siRNA or by inducible shRNA in a stable cell line. Blocking protein synthesis by treating cells with cycloheximide, resulted in a slight stabilization of PLK4 levels in the absence of DCAF1 and a slight increase in PLK4 protein half-life (Figure 16 and Figure 17). In general, PLK4 has a short half-life, as it also has been observed in previous studies (Zhang et al., 2023), and is rapidly degraded by the $SCF^{\beta\text{-}TrCP}$ ubiquitin ligase, which makes differences attributable to the DCAF1 ubiquitin ligase difficult to detect.

Furthermore, I investigated whether PLK4 is a novel ubiquitylation target of the $CRL4^{DCAF1}$ ubiquitin ligase. $CRL4^{DCAF1}$ has been initially described to associate with the viral protein Vpr and induce the K48-linked polyubiquitylation of cellular proteins (Belzile et al., 2010). Performing *in vivo* and *in vitro* ubiquitylation assays, I found that DCAF1 promotes the ubiquitylation of PLK4 (Figure 20). In the *in vivo* experiments, the effect of DCAF1 overexpression on PLK4 ubiquitylation was strong and reversible by addition of the cullin-RING ligase inhibitor MLN4924. But since the inhibitor prevents neddylation, it inactivates cullin-RING ligases in general and not only the $CRL4^{DCAF1}$ ligase specifically. Thus, the strongly reduced ubiquitylation of PLK4 upon MLN4924 treatment is a more general indicator, that PLK4 is ubiquitylated by cullin-RING ligases and that DCAF1 most likely targets PLK4 for ubiquitylation as a substrate receptor of a cullin-RING E3 ligase complex. The effects in *in vitro* ubiquitylation assays were less pronounced. $CRL4^{DCAF1}$ has been described to cooperate with the E2 enzyme UBCH5C and the E1 enzyme UBA1 for the ubiquitylation of its substrates (Han et al.,

2020). Therefore, I performed my experiments in the presence of UBCH5C and UBA1. However, different combinations of E3 ligase and E2 enzyme might be possible and next to UBCH5C, also other E2 enzymes have been described to work together with $CRL4^{DCAF1}$ and could be tested in additional experiments. Further experiments would also be required to analyze the linkage type of the assembled polyubiquitin chains. K48-linked ubiquitylation has been previously described for $CRL4^{DCAF1}$ (Belzile et al., 2010) and would be consistent with the observed effect on PLK4 protein levels, as it is a signal for protein degradation by the proteasome.

Although DCAF1 has been mainly studied with respect to its function as a substrate receptor of an E3 ubiquitin ligase complex, it has also been recently shown to possess intrinsic kinase activity (Ghate et al., 2023). The first phosphorylation target identified is histone H2A, which is phosphorylated at threonine 120 resulting in the repression of chromatin transcription. H2A T120 phosphorylation by DCAF1 has been reported to downregulate 292 genes, a majority of these are associated with cell proliferation (Kim et al., 2013a). Although phosphorylation is not involved in the interaction between DCAF1 and PLK4, it would be interesting to further investigate a potential function of DCAF1 kinase activity for the regulation of PLK4.

Taken together, my results showed that $CRL4^{DCAF1}$ regulates PLK4 protein levels by ubiquitylation and proteasomal degradation and that the presence of DCAF1 is required to keep PLK4 levels low. Nevertheless, the possibility that also other proteins involved in the centriole duplication machinery are direct targets of $CRL4^{DCAF1}$ and thereby contribute to the effects observed in response to DCAF1 overexpression or depletion, cannot be excluded. My work presented in this thesis not only identified a novel mechanism for the regulation of PLK4 protein levels in centriole duplication, but also identified PLK4 as a novel substrate of the E3 ubiquitin ligase $CRL4^{DCAF1}$. As many substrates of CRL4 ubiquitin ligases still remain unknown today, future studies will undoubtedly identify new substrate candidates, potentially involved in centriole duplication or other tightly regulated cellular processes.

4.2 Potential correlation between the ubiquitin ligase EDD-DYRK2-$DDB1^{DCAF1}$ and PLK4

Strikingly, DCAF1 serves as a substrate receptor of both the cullin-RING E3 ubiquitin ligase $CRL4^{DCAF1}$ and the HECT-type E3 ligase EDD-DYRK2-$DDB1^{DCAF1}$. Next to DCAF1, the adaptor protein DDB1 is present in both complexes as well. Apart from

DDB1 and DCAF1, also the scaffold protein EDD has been detected as a potential interaction partner of PLK4 in the MS screen, raising the possibility that EDD-DYRK2-DDB1^{DCAF1} might be involved in the regulation of PLK4. However, my results revealed, that in contrast to CUL4, EDD does not interact with PLK4 and DCAF1 simultaneously in the same complex (Figure 15). Furthermore, overexpression of DCAF1 increased polyubiquitylation of PLK4 in the *in vivo* ubiquitylation assays, which was reversible by inhibition of cullin-RING ligases using MLN4924 (Figure 20), indicating that PLK4 is ubiquitylated by ubiquitin ligases belonging to the cullin-RING family rather than a HECT-family E3 ubiquitin ligase.

Recently, CEP78 has been identified as an upstream regulator of EDD-DYRK2-DDB1^{DCAF1} at the centrosome, which inhibits the E3 ligase and thereby the ubiquitylation of the novel substrate CP110 (Hossain et al., 2017). CEP78 colocalizes and interacts with PLK4 at the centrosome (Brunk et al., 2016), which might explain the observed interaction between PLK4 and EDD and the centrosomal localization of the EDD-DYRK2-DDB1^{DCAF1} complex components described previously (Hossain et al., 2017). Most likely, the interaction between PLK4 and EDD is mediated by CEP78, which could be addressed in future experiments. However, based on my results mentioned above, a function of EDD-DYRK2-DDB1^{DCAF1} in the regulation of PLK4 is highly unlikely.

4.3 Functional relationship between DCAF1 and CEP152/CEP192 in their interaction with PLK4

Performing interaction mapping, I identified the domains mediating the interaction between PLK4 and DCAF1. My results revealed that the C-terminal PB1-PB2 domain of PLK4, which has been previously shown to mediate protein-protein interactions, interacts with the C-terminal acidic tail of DCAF1. The DCAF1 acidic domain alone was sufficient to mediate the binding, however presence of the WD40 domain enhanced the interaction (Figure 10 and Figure 12). Almost all of the DCAF proteins identified today, contain a WD40 domain with a relatively conserved WDXR motif, which is critical for DDB1 binding and thereby for assembly of the E3 ligase complex (Lee and Zhou, 2007). Structural analysis of the DCAF1 domain architecture, performed by Gali Prag (Tel Aviv University, Israel) using AlphaFold2.0, revealed, that the DCAF1 N-terminus is comprised of two short acidic helices, which are connected by a flexible linker and bind to PB1-PB2 of PLK4 simultaneously (Grossmann et al., 2024). The centrosomal

proteins CEP152 and CEP192, implicated in centrosomal recruitment of PLK4, were previously shown to also interact with the PB1-PB2 domain of PLK4 (Kim et al., 2013b; Sonnen et al., 2013). Interestingly, both CEP152 and CEP192 contain acidic helical regions that bind to the PLK4 PB1-PB2 domain, very similar to the DCAF1 acidic helices. Because the binding interfaces are similar, these three proteins could potentially compete with each other for the binding site on PLK4. However, my results revealed that the PLK4 amino acids critical for DCAF1 binding are similar but not identical to those critical for the interaction with CEP152/CEP192. In particular, mutation of R691 within the PLK4 PB1-PB2 domain almost completely abolished the interaction with DCAF1 but did not affect the interaction between PLK4 and CEP152/CEP192. In line with that, increasing amounts of DCAF1 slightly decrease the amount of CEP152 binding to PLK4 but do not entirely prevent neither CEP152 nor CEP192 from interacting with PLK4 (Figure 13). A simultaneous or cell cycle regulated binding of these three proteins to the PB1-PB2 domain of PLK4 is possible and likely, as also another centrosomal protein, CEP135, has been previously reported to interact with this region on PLK4 (Galletta et al., 2016). Similarly, several proteins bind to the PB1-PB2 domain of PLK1 (Lowery et al., 2007; Park et al., 2010). Therefore, it is unlikely that DCAF1 is directly involved in regulating the centrosomal recruitment of PLK4 by CEP152/CEP192 or conversely, that CEP152/CEP192 influence the ubiquitylation of PLK4 by DCAF1, but the exact functional correlation between these proteins would remain to be investigated in additional experiments.

4.4 Complementary roles of the ubiquitin ligases $SCF^{\beta\text{-}TrCP}$ and $CRL4^{DCAF1}$ in the regulation of PLK4

The important function of the $SCF^{\beta\text{-}TrCP}$ ubiquitin ligase for the regulation of PLK4 protein levels in centriole duplication is well established and the mechanism of action has been unraveled. Recognition and binding of the substrate receptor β-TrCP requires autophosphorylation of PLK4 at S285 and T289 within the PEST destruction motif. However, several previous studies revealed that a PLK4 mutant, which is non-phosphorylatable within the β-TrCP recognition motif and therefore not bound by β-TrCP, was still ubiquitylated and only moderately stabilized, indicating that a second, yet unknown, phosphorylation-independent pathway for PLK4 ubiquitylation and proteasomal degradation might exist (Rogers et al., 2009; Holland et al., 2010; Klebba et al., 2013). My results clearly demonstrated that DCAF1 binds to a region within PLK4

that is distinct from the β-TrCP binding region. Additionally, I found that in contrast to the regulation of PLK4 by β-TrCP, PLK4 kinase activity is not required for the interaction with DCAF1 and that the interaction in general is not dependent on phosphorylation of any sites (Figure 14), indicating that $CRL4^{DCAF1}$ presents a new phosphorylation-independent pathway for ubiquitylation and proteasomal degradation of PLK4.

It is not surprising that the protein levels of PLK4 are not only regulated by one single ubiquitin ligase, as the tight regulation is crucial for centrosome duplication and deregulation would result in abnormal centrosome numbers which might be a cause for genomic instability, aneuploidy and cancer. The oncoprotein c-Myc and the tumor suppressor p53 are two examples of proteins that are highly regulated through ubiquitylation by several E3 ubiquitin ligases. Overabundance of p53 would result in apoptosis and be detrimental to normal cells, while high levels of c-Myc would drive uncontrolled cell growth and proliferation and subsequently promote tumorigenesis (Dai et al., 2006). In addition, cyclin E, an essential regulator of cell cycle progression, is regulated by more than one E3 ubiquitin ligase (Singer et al., 1999; Strohmaier et al., 2001). It is conceivable that similar to p53, c-Myc and cyclin E, also PLK4 is regulated by several distinct E3 ubiquitin ligases. In addition to $SCF^{β\text{-}TrCP}$, the E3 ligase MIB1 has been previously implicated in the regulation of PLK4 (Čajánek et al., 2015), while I identified $CRL4^{DCAF1}$ as a novel ubiquitin ligase regulating PLK4 protein levels. Potential additional regulators, next to $SCF^{β\text{-}TrCP}$, MIB1 and $CRL4^{DCAF1}$, remain to be identified in the future.

My results revealed an important function of DCAF1 especially in G2 phase of the cell cycle. The interaction between DCAF1 and PLK4, as well as the ubiquitylation of PLK4 by $CRL4^{DCAF1}$ were strongest in G2 phase and essential for the prevention of an early onset of centriole duplication in mitosis. Recently, Paul et al. developed a method to monitor β-TrCP activity in living cells and found that β-TrCP is constitutively active throughout the cell cycle but the activity is elevated in quiescent cells in G0 phase and slightly decreased in S and G2 phase (Paul et al., 2022). Together, this might indicate that β-TrCP and DCAF1 function complementary in terms of the timing of their activity, in order to ensure a tight regulation of PLK4 protein levels throughout the whole cell cycle.

4.5 CRL4^{DCAF1}-mediated regulation of PLK4 is required for correct timing of centriole duplication

Performing experiments in cell cycle synchronized cells, I showed that the regulation of PLK4 by the CRL4^{DCAF1} E3 ubiquitin ligase becomes most relevant in G2 phase of the cell cycle. Both the interaction with, as well as the ubiquitylation of PLK4 is strong (Figure 21 and Figure 22), preventing an early onset of centriole duplication in mitosis. In the absence of DCAF1, centriole disengagement starts to occur in G2 phase already (Figure 28), instead of in late mitosis, thereby licensing centrioles for a new round of centriole duplication, prematurely. Although PLK4 is not a direct regulator of the centriole disengagement process, elevated PLK4 levels due to the absence of DCAF1 seem to have a distinct effect. PLK1 and separase are described as the key enzymes responsible for this process, which are not directly regulated by PLK4 or DCAF1 (Tsou et al., 2009). However, wrong amounts of PLK4 at wrong times during the centriole duplication cycle due to the absence of DCAF1 might affect all subsequent steps and their tight temporal control. Therefore, the timing of centriole disengagement was analyzed not as a direct consequence of PLK4 regulation by DCAF1, but rather as a general read-out for the important regulatory function of DCAF1 in centriole duplication.

Additionally, I found that DCAF1 is involved in regulating the interaction between PLK4 and its substrate STIL. In the absence of DCAF1, the amount of STIL interacting with PLK4 was clearly increased, while conversely, overexpression of DCAF1 decreased the interaction between PLK4 and STIL in a dose-dependent manner (Figure 25). The centriole duplication cycle is highly temporally coordinated and regulatory mechanisms preventing an untimely onset of centriole biogenesis have been identified previously. Zitouni et al. showed that the mitotic kinase CDK1-CyclinB binds STIL during mitosis, in order to prevent precocious STIL-PLK4 complex formation and phosphorylation of STIL by PLK4. After mitotic exit, CDK1 is inactivated, allowing PLK4 to interact with and phosphorylate STIL, which recruits SAS-6 and initiates cartwheel formation (Zitouni et al., 2016). My results clearly demonstrated a function of CRL4^{DCAF1} in the regulation of PLK4 and the interaction with its substrate STIL, revealing a new layer of the regulation of STIL-PLK4 complex formation. I could show that similar to CDK1, which binds to STIL to prevent STIL-PLK4 complex formation, DCAF1 binds to PLK4 to prevent the STIL-PLK4 interaction. During G2 phase, the interaction between DCAF1 and PLK4 is strong, but upon entry in mitosis, the interaction becomes weak,

indicating that PLK4 is released. During mitosis, STIL remains bound to CDK1, however, slightly later upon mitotic exit also STIL is released from CDK1, allowing for the interaction between STIL and PLK4. Together, this indicates that two complementary mechanisms, one via CDK1 and one via DCAF1, exist to regulate the timing of the centriole duplication cycle at the step of STIL-PLK4 complex formation.

4.6 Working model

PLK4 is known as the master regulator of centrosome duplication, a process which is coupled to the cell cycle and tightly regulated at various levels, as centrosome abnormalities have been associated with cancer.

In the presented thesis, I identified the $CRL4^{DCAF1}$ E3 ubiquitin ligase as a novel regulator of PLK4 protein levels in centriole duplication. DCAF1 serves as a substrate receptor of the cullin-RING ligase complex, which further consists of DDB1 as an adaptor protein, CUL4A/B as a scaffold and RBX1, which associates with the ubiquitin-coupled E2 enzyme. The acidic domain of DCAF1 binds to the PB1-PB2 domain of the substrate PLK4 in a phosphorylation-independent manner. The interaction between PLK4 and DCAF1 and the ubiquitylation of PLK4 by the $CRL4^{DCAF1}$ ubiquitin ligase occurs predominantly in G2 phase. Thereby, DCAF1 not only regulates PLK4 protein levels, but also the interaction between PLK4 and its substrate STIL to prevent an early onset of centriole biogenesis. Similar to DCAF1 regulating PLK4, CDK1-CyclinB has been shown to bind to STIL in mitosis in order to prevent PLK4-STIL complex formation (Zitouni et al., 2016). Only upon mitotic exit, both PLK4 and STIL are released and allowed to interact, which results in the phosphorylation of STIL by PLK4, the recruitment of SAS-6 and the initiation of cartwheel formation for a new round of centriole duplication (Grossmann et al., 2024). The described working model is summarized in Figure 29.

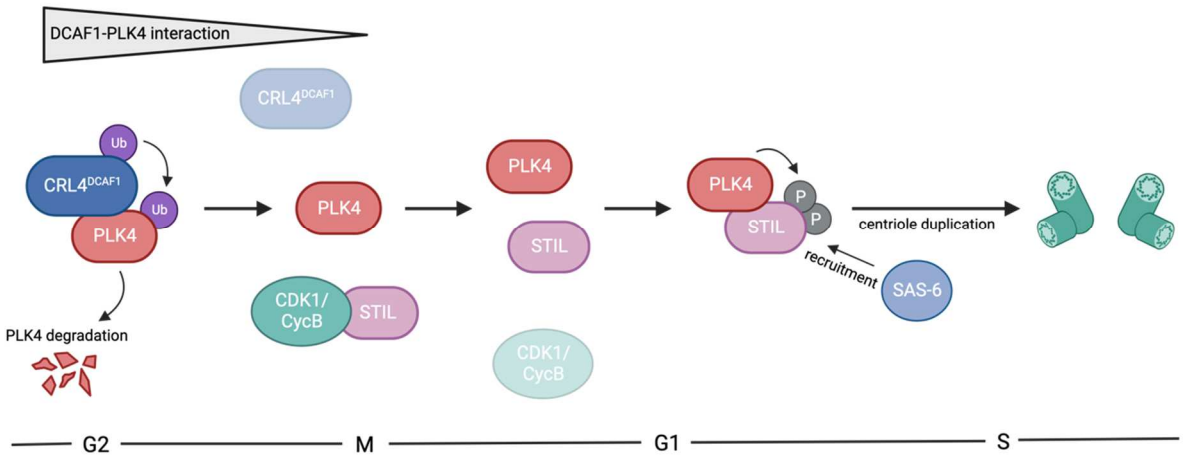

Figure 29: CRL4^{DCAF1} regulates PLK4 in centriole duplication

Graphical representation of the proposed involvement of the CRL4^{DCAF1} ubiquitin ligase in centriole duplication. PLK4 interacts with DCAF1 predominantly in G2 phase of the cell cycle, which leads to ubiquitylation and subsequent proteasomal degradation of PLK4. In mitosis, the strong interaction between PLK4 and DCAF1 is lost, releasing PLK4 to allow for the interaction with STIL. Simultaneously, STIL is bound to CDK1-CyclinB, still preventing the PLK4-STIL complex formation at this point of the cell cycle. Upon mitotic exit, STIL is released from binding to CDK1-Cyclin B, now also allowing for the interaction with PLK4. Once both PLK4 is released from DCAF1 and STIL is released from CDK1, the formation of the PLK4-STIL complex can occur in early G1 phase, which leads to phosphorylation of STIL by PLK4 and the recruitment of SAS-6 for the new round of centriole duplication in S phase. This figure was created with BioRender.com. Reproduced from Grossmann et al., 2024.

4.7 Future perspectives

In the presented thesis I identified the centrosomal protein PLK4 as a novel substrate of the $CRL4^{DCAF1}$ E3 ubiquitin ligase and conversely, $CRL4^{DCAF1}$ as a novel regulator of PLK4 in centriole duplication. However, several questions remain open and could be addressed in future experiments.

My results revealed that $CRL4^{DCAF1}$ recognizes and binds PLK4 in a phosphorylation-independent manner and identified the interacting domains of both proteins. The exact ubiquitylation site on PLK4 remains unknown. Most commonly, Lysine epsilon amino-groups serve as sites of ubiquitin attachment (Ciechanover and Ben-Saadon, 2004) and mutational analyses of Lys residues present in PLK4 could be performed to identify the ubiquitylation site. However, ubiquitin is not necessarily anchored to a specific Lys residue and in the case of cyclin B, any single Lys residue, even if it is artificially inserted into the protein sequence, can serve as a ubiquitin acceptor (King et al., 1996b). Furthermore, the linkage type of the ubiquitin chains attached to PLK4 remains to be identified. As I observed effects on PLK4 protein levels as a consequence of the ubiquitylation, K48-linkages, which are a signal for proteasomal degradation, are likely. Additionally, K11-linked ubiquitin chains are associated with proteasomal degradation and also other less studied or heterotypic and branched ubiquitin chains are possible.

Next to the $SCF^{\beta\text{-}TrCP}$ and MIB1 E3 ubiquitin ligases, I identified $CRL4^{DCAF1}$ as an additional, mechanistically distinct, regulator of PLK4 levels in centriole duplication. While my results suggest a complementary function for $SCF^{\beta\text{-}TrCP}$ and $CRL4^{DCAF1}$ regarding the timing and mechanism of action, it would be interesting to further unravel a potential correlation. As the individual knockdowns of both E3 ligases independently affect PLK4 protein levels and centriole numbers, it is however unlikely that in cases of mutation or absence of one E3 ligase, the remaining one could compensate the loss by an increased activity in order to keep PLK4 levels under control. Within the large family of cullin-RING ubiquitin ligases, many of the specific substrate proteins which are targeted remain unknown, although an involvement of an E3 ligase in a certain cellular process has been demonstrated already. Therefore, it is conceivable that additional, yet unknown ubiquitin ligases are involved in the regulation of PLK4. In particular for CUL4A/B E3 ligases, among the DCAF proteins which serve as their substrate receptors, many of their specific substrates remain unknown. Although DCAF5, which was also found to interact with PLK4, did not contribute to the regulation

of PLK4 protein abundance in centriole duplication, it might still target PLK4 as a novel substrate in another cellular context such as the regulation of protein-protein interactions or subcellular localization. A potential direct interaction or functional correlation between these proteins might be interesting to investigate in future experiments. Furthermore, ubiquitylation can be counteracted by DUBs, which remove ubiquitin molecules from target proteins. The DUB Spata2-CYLD has been recently shown to remove K63-linked polyubiquitin chains from PLK4 (Yang et al., 2020). It would be interesting to further investigate whether this deubiquitylation might counteract the ubiquitylation of PLK4 by $SCF^{\beta\text{-}TrCP}$ or $CRL4^{DCAF1}$ and to what extent it is involved in the regulation of PLK4 in centriole duplication.

As PLK4 is found to be overexpressed frequently in human tumors, several PLK4 inhibitors have been tested as potential cancer therapeutics. In contrast to small molecule inhibitors, PROTACs and GLUTACs can induce the degradation of their target in a highly specific and effective manner, instead of only inhibiting its catalytic activity. Therefore, they represent a promising novel approach for cancer therapy and receive increasing attention in recent years. With this thesis, I provide a more detailed understanding of the regulation of PLK4 by ubiquitylation and proteasomal degradation, which could pave the way for the development of PROTAC or GLUTAC technology for targeted degradation of overexpressed PLK4 in cancer. The first developed PROTAC was already designed to recruit the $SCF^{\beta\text{-}TrCP}$ ubiquitin ligase and could potentially be slightly modified to target PLK4 as a substrate (Sakamoto et al., 2001). Very recently, also efficient DCAF1-based PROTACs were developed and shown to provide an alternative strategy, especially in cases of acquired resistances (Schröder et al., 2024). Next to the $SCF^{\beta\text{-}TrCP}$ and $CRL4^{DCAF1}$ ubiquitin ligase complexes, also other ubiquitin ligases, which are not necessarily physiological interactors of PLK4, could be recruited by a specific PROTAC or GLUTAC molecule and target PLK4 as a neo-substrate, offering a wide range of possibilities to interfere with the ubiquitylation and degradation of overexpressed PLK4 as a novel approach for cancer therapy.

5. References

Ahn, J., Novince, Z., Concel, J., Byeon, C.-H., Makhov, A.M., Byeon, I.-J.L., Zhang, P., and Gronenborn, A.M. (2011). The Cullin-RING E3 ubiquitin ligase CRL4-DCAF1 complex dimerizes via a short helical region in DCAF1. Biochemistry *50*, 1359-1367. https://doi.org/10.1021/bi101749s.

Akutsu, M., Dikic, I., and Bremm, A. (2016). Ubiquitin chain diversity at a glance. Journal of cell science *129*, 875-880. https://doi.org/10.1242/jcs.183954.

Ammoun, S., and Hanemann, C.O. (2011). Emerging therapeutic targets in schwannomas and other merlin-deficient tumors. Nature reviews. Neurology *7*, 392-399. https://doi.org/10.1038/nrneurol.2011.82.

Andersen, J.S., Wilkinson, C.J., Mayor, T., Mortensen, P., Nigg, E.A., and Mann, M. (2003). Proteomic characterization of the human centrosome by protein correlation profiling. Nature *426*, 570-574. https://doi.org/10.1038/nature02166.

Angers, S., Li, T., Yi, X., MacCoss, M.J., Moon, R.T., and Zheng, N. (2006). Molecular architecture and assembly of the DDB1-CUL4A ubiquitin ligase machinery. Nature *443*, 590-593. https://doi.org/10.1038/nature05175.

Arquint, C., Gabryjonczyk, A.-M., and Nigg, E.A. (2014). Centrosomes as signalling centres. Philosophical transactions of the Royal Society of London. Series B, Biological sciences *369*. https://doi.org/10.1098/rstb.2013.0464.

Bahe, S., Stierhof, Y.-D., Wilkinson, C.J., Leiss, F., and Nigg, E.A. (2005). Rootletin forms centriole-associated filaments and functions in centrosome cohesion. The Journal of cell biology *171*, 27-33. https://doi.org/10.1083/jcb.200504107.

Bahtz, R., Seidler, J., Arnold, M., Haselmann-Weiss, U., Antony, C., Lehmann, W.D., and Hoffmann, I. (2012). GCP6 is a substrate of Plk4 and required for centriole duplication. Journal of cell science *125*, 486-496. https://doi.org/10.1242/jcs.093930.

Bai, C., Sen, P., Hofmann, K., Ma, L., Goebl, M., Harper, J.W., and Elledge, S.J. (1996). SKP1 connects cell cycle regulators to the ubiquitin proteolysis machinery through a novel motif, the F-box. Cell *86*, 263-274. https://doi.org/10.1016/s0092-8674(00)80098-7.

Bartz, S.R., Rogel, M.E., and Emerman, M. (1996). Human immunodeficiency virus type 1 cell cycle control: Vpr is cytostatic and mediates G2 accumulation by a mechanism which differs from DNA damage checkpoint control. Journal of virology *70*, 2324-2331. https://doi.org/10.1128/JVI.70.4.2324-2331.1996.

Basto, R., Brunk, K., Vinadogrova, T., Peel, N., Franz, A., Khodjakov, A., and Raff, J.W. (2008). Centrosome amplification can initiate tumorigenesis in flies. Cell *133*, 1032-1042. https://doi.org/10.1016/j.cell.2008.05.039.

Belzile, J.-P., Richard, J., Rougeau, N., Xiao, Y., and Cohen, E.A. (2010). HIV-1 Vpr induces the K48-linked polyubiquitination and proteasomal degradation of target cellular proteins to activate ATR and promote G2 arrest. Journal of virology *84*, 3320-3330. https://doi.org/10.1128/jvi.02590-09.

Bettencourt-Dias, M., and Glover, D.M. (2007). Centrosome biogenesis and function: centrosomics brings new understanding. Nature reviews. Molecular cell biology *8*, 451-463. https://doi.org/10.1038/nrm2180.

Bettencourt-Dias, M., Rodrigues-Martins, A., Carpenter, L., Riparbelli, M., Lehmann, L., Gatt, M.K., Carmo, N., Balloux, F., Callaini, G., and Glover, D.M. (2005). SAK/PLK4 is required for centriole duplication and flagella development. Current biology : CB *15*, 2199-2207. https://doi.org/10.1016/j.cub.2005.11.042.

Bhatia, N., Thiyagarajan, S., Elcheva, I., Saleem, M., Dlugosz, A., Mukhtar, H., and Spiegelman, V.S. (2006). Gli2 is targeted for ubiquitination and degradation by beta-TrCP ubiquitin ligase. The Journal of biological chemistry *281*, 19320-19326. https://doi.org/10.1074/jbc.M513203200.

Bhattacharyya, S., Yu, H., Mim, C., and Matouschek, A. (2014). Regulated protein turnover: snapshots of the proteasome in action. Nature reviews. Molecular cell biology *15*, 122-133. https://doi.org/10.1038/nrm3741.

Boveri, T. (2008). Concerning the origin of malignant tumours by Theodor Boveri. Translated and annotated by Henry Harris. Journal of cell science *121 Suppl 1*, 1-84. https://doi.org/10.1242/jcs.025742.

Brito, D.A., Gouveia, S.M., and Bettencourt-Dias, M. (2012). Deconstructing the centriole: structure and number control. Current opinion in cell biology *24*, 4-13. https://doi.org/10.1016/j.ceb.2012.01.003.

Brownlee, C.W., Klebba, J.E., Buster, D.W., and Rogers, G.C. (2011). The Protein Phosphatase 2A regulatory subunit Twins stabilizes Plk4 to induce centriole amplification. The Journal of cell biology *195*, 231-243. https://doi.org/10.1083/jcb.201107086.

Brunk, K., Zhu, M., Bärenz, F., Kratz, A.-S., Haselmann-Weiss, U., Antony, C., and Hoffmann, I. (2016). Cep78 is a new centriolar protein involved in Plk4-induced centriole overduplication. Journal of cell science *129*, 2713-2718. https://doi.org/10.1242/jcs.184093.

Čajánek, L., Glatter, T., and Nigg, E.A. (2015). The E3 ubiquitin ligase Mib1 regulates Plk4 and centriole biogenesis. Journal of cell science *128*, 1674-1682. https://doi.org/10.1242/jcs.166496.

Cang, Y., Zhang, J., Nicholas, S.A., Bastien, J., Li, B., Zhou, P., and Goff, S.P. (2006). Deletion of DDB1 in mouse brain and lens leads to p53-dependent elimination of proliferating cells. Cell *127*, 929-940. https://doi.org/10.1016/j.cell.2006.09.045.

Cassiday, P.A., DePaula-Silva, A.B., Chumley, J., Ward, J., Barker, E., and Planelles, V. (2015). Understanding the molecular manipulation of DCAF1 by the lentiviral accessory proteins Vpr and Vpx. Virology *476*, 19-25. https://doi.org/10.1016/j.virol.2014.11.024.

Chen, Z.J., and Sun, L.J. (2009). Nonproteolytic functions of ubiquitin in cell signaling. Molecular cell *33*, 275-286. https://doi.org/10.1016/j.molcel.2009.01.014.

Chi, W., Wang, G., Xin, G., Jiang, Q., and Zhang, C. (2021). PLK4-phosphorylated NEDD1 facilitates cartwheel assembly and centriole biogenesis initiations. The Journal of cell biology *220*. https://doi.org/10.1083/jcb.202002151.

Ciechanover, A., and Ben-Saadon, R. (2004). N-terminal ubiquitination: more protein substrates join in. Trends in cell biology *14*, 103-106. https://doi.org/10.1016/j.tcb.2004.01.004.

Ciechanover, A., Heller, H., Elias, S., Haas, A.L., and Hershko, A. (1980). ATP-dependent conjugation of reticulocyte proteins with the polypeptide required for protein degradation. Proceedings of the National Academy of Sciences of the United States of America *77*, 1365-1368. https://doi.org/10.1073/pnas.77.3.1365.

Cizmecioglu, O., Arnold, M., Bahtz, R., Settele, F., Ehret, L., Haselmann-Weiss, U., Antony, C., and Hoffmann, I. (2010). Cep152 acts as a scaffold for recruitment of Plk4 and CPAP to the centrosome. The Journal of cell biology *191*, 731-739. https://doi.org/10.1083/jcb.201007107.

Coelho, P.A., Bury, L., Shahbazi, M.N., Liakath-Ali, K., Tate, P.H., Wormald, S., Hindley, C.J., Huch, M., Archer, J., and Skarnes, W.C., et al. (2015). Over-expression of Plk4 induces centrosome amplification, loss of primary cilia and associated tissue hyperplasia in the mouse. Open biology *5*, 150209. https://doi.org/10.1098/rsob.150209.

Conduit, P.T., Wainman, A., and Raff, J.W. (2015). Centrosome function and assembly in animal cells. Nature reviews. Molecular cell biology *16*, 611-624. https://doi.org/10.1038/nrm4062.

Connor, R.I., Chen, B.K., Choe, S., and Landau, N.R. (1995). Vpr is required for efficient replication of human immunodeficiency virus type-1 in mononuclear phagocytes. Virology *206*, 935-944. https://doi.org/10.1006/viro.1995.1016.

Coux, O., Tanaka, K., and Goldberg, A.L. (1996). Structure and functions of the 20S and 26S proteasomes. Annual review of biochemistry *65*, 801-847. https://doi.org/10.1146/annurev.bi.65.070196.004101.

Cunha-Ferreira, I., Bento, I., Pimenta-Marques, A., Jana, S.C., Lince-Faria, M., Duarte, P., Borrego-Pinto, J., Gilberto, S., Amado, T., and Brito, D., et al. (2013). Regulation of autophosphorylation controls PLK4 self-destruction and centriole number. Current biology : CB *23*, 2245-2254. https://doi.org/10.1016/j.cub.2013.09.037.

Cunha-Ferreira, I., Rodrigues-Martins, A., Bento, I., Riparbelli, M., Zhang, W., Laue, E., Callaini, G., Glover, D.M., and Bettencourt-Dias, M. (2009). The SCF/Slimb ubiquitin ligase limits centrosome amplification through degradation of SAK/PLK4. Current biology : CB *19*, 43-49. https://doi.org/10.1016/j.cub.2008.11.037.

Dai, M.-S., Jin, Y., Gallegos, J.R., and Lu, H. (2006). Balance of Yin and Yang: ubiquitylation-mediated regulation of p53 and c-Myc. Neoplasia (New York, N.Y.) *8*, 630-644. https://doi.org/10.1593/neo.06334.

Denu, R.A., Shabbir, M., Nihal, M., Singh, C.K., Longley, B.J., Burkard, M.E., and Ahmad, N. (2018). Centriole Overduplication is the Predominant Mechanism Leading to Centrosome Amplification in Melanoma. Molecular cancer research : MCR *16*, 517-527. https://doi.org/10.1158/1541-7786.MCR-17-0197.

Denu, R.A., Zasadil, L.M., Kanugh, C., Laffin, J., Weaver, B.A., and Burkard, M.E. (2016). Centrosome amplification induces high grade features and is prognostic of worse outcomes in breast cancer. BMC cancer *16*, 47. https://doi.org/10.1186/s12885-016-2083-x.

Deshaies, R.J., and Joazeiro, C.A.P. (2009). RING domain E3 ubiquitin ligases. Annual review of biochemistry *78*, 399-434. https://doi.org/10.1146/annurev.biochem.78.101807.093809.

Duensing, A., Liu, Y., Perdreau, S.A., Kleylein-Sohn, J., Nigg, E.A., and Duensing, S. (2007). Centriole overduplication through the concurrent formation of multiple daughter centrioles at single maternal templates. Oncogene *26*, 6280-6288. https://doi.org/10.1038/sj.onc.1210456.

Dzhindzhev, N.S., Tzolovsky, G., Lipinszki, Z., Schneider, S., Lattao, R., Fu, J., Debski, J., Dadlez, M., and Glover, D.M. (2014). Plk4 phosphorylates Ana2 to trigger Sas6 recruitment and procentriole formation. Current biology : CB *24*, 2526-2532. https://doi.org/10.1016/j.cub.2014.08.061.

Eytan, E., Ganoth, D., Armon, T., and Hershko, A. (1989). ATP-dependent incorporation of 20S protease into the 26S complex that degrades proteins conjugated to ubiquitin. Proceedings of the National Academy of Sciences of the United States of America *86*, 7751-7755. https://doi.org/10.1073/pnas.86.20.7751.

Fan, G., Sun, L., Shan, P., Zhang, X., Huan, J., Zhang, X., Li, D., Wang, T., Wei, T., and Gu, X., et al. (2015). Loss of KLF14 triggers centrosome amplification and tumorigenesis. Nature communications *6*, 8450. https://doi.org/10.1038/ncomms9450.

Fei, C., Li, Z., Li, C., Chen, Y., Chen, Z., He, X., Mao, L., Wang, X., Zeng, R., and Li, L. (2013). Smurf1-mediated Lys29-linked nonproteolytic polyubiquitination of axin negatively regulates Wnt/β-catenin signaling. Molecular and cellular biology *33*, 4095-4105. https://doi.org/10.1128/MCB.00418-13.

Finley, D. (2009). Recognition and processing of ubiquitin-protein conjugates by the proteasome. Annual review of biochemistry *78*, 477-513. https://doi.org/10.1146/annurev.biochem.78.081507.101607.

Fischer, E.S., Böhm, K., Lydeard, J.R., Yang, H., Stadler, M.B., Cavadini, S., Nagel, J., Serluca, F., Acker, V., and Lingaraju, G.M., et al. (2014). Structure of the DDB1-CRBN E3 ubiquitin ligase in complex with thalidomide. Nature *512*, 49-53. https://doi.org/10.1038/nature13527.

Flotho, A., and Melchior, F. (2013). Sumoylation: a regulatory protein modification in health and disease. Annual review of biochemistry *82*, 357-385. https://doi.org/10.1146/annurev-biochem-061909-093311.

Fode, C., Binkert, C., and Dennis, J.W. (1996). Constitutive expression of murine Sak-a suppresses cell growth and induces multinucleation. Molecular and cellular biology *16*, 4665-4672. https://doi.org/10.1128/mcb.16.9.4665.

Fode, C., Motro, B., Yousefi, S., Heffernan, M., and Dennis, J.W. (1994). Sak, a murine protein-serine/threonine kinase that is related to the Drosophila polo kinase and involved in cell proliferation. Proceedings of the National Academy of Sciences of the United States of America *91*, 6388-6392. https://doi.org/10.1073/pnas.91.14.6388.

Freed, E., Lacey, K.R., Huie, P., Lyapina, S.A., Deshaies, R.J., Stearns, T., and Jackson, P.K. (1999). Components of an SCF ubiquitin ligase localize to the centrosome and regulate the centrosome duplication cycle. Genes & development *13*, 2242-2257. https://doi.org/10.1101/gad.13.17.2242.

Furukawa, M., He, Y.J., Borchers, C., and Xiong, Y. (2003). Targeting of protein ubiquitination by BTB-Cullin 3-Roc1 ubiquitin ligases. Nature cell biology *5*, 1001-1007. https://doi.org/10.1038/ncb1056.

Galisson, F., Mahrouche, L., Courcelles, M., Bonneil, E., Meloche, S., Chelbi-Alix, M.K., and Thibault, P. (2011). A novel proteomics approach to identify SUMOylated proteins and their modification sites in human cells. Molecular & cellular proteomics : MCP *10*, M110.004796. https://doi.org/10.1074/mcp.M110.004796.

Galletta, B.J., Fagerstrom, C.J., Schoborg, T.A., McLamarrah, T.A., Ryniawec, J.M., Buster, D.W., Slep, K.C., Rogers, G.C., and Rusan, N.M. (2016). A centrosome interactome provides insight into organelle assembly and reveals a non-duplication role for Plk4. Nature communications *7*, 12476. https://doi.org/10.1038/ncomms12476.

Ghate, N.B., Kim, S., Mehmood, R., Shin, Y., Kim, K., and An, W. (2023). VprBP/DCAF1 regulates p53 function and stability through site-specific phosphorylation. Oncogene *42*, 1405-1416. https://doi.org/10.1038/s41388-023-02685-8.

Godinho, S.A., Picone, R., Burute, M., Dagher, R., Su, Y., Leung, C.T., Polyak, K., Brugge, J.S., Théry, M., and Pellman, D. (2014). Oncogene-like induction of cellular invasion from centrosome amplification. Nature *510*, 167-171. https://doi.org/10.1038/nature13277.

Gönczy, P. (2012). Towards a molecular architecture of centriole assembly. Nature reviews. Molecular cell biology *13*, 425-435. https://doi.org/10.1038/nrm3373.

Gönczy, P. (2015). Centrosomes and cancer: revisiting a long-standing relationship. Nature reviews. Cancer *15*, 639-652. https://doi.org/10.1038/nrc3995.

Groll, M., Ditzel, L., Löwe, J., Stock, D., Bochtler, M., Bartunik, H.D., and Huber, R. (1997). Structure of 20S proteasome from yeast at 2.4 A resolution. Nature *386*, 463-471. https://doi.org/10.1038/386463a0.

Grossmann, J., Kratz, A.-S., Kordonsky, A., Prag, G., and Hoffmann, I. (2024). CRL4DCAF1 ubiquitin ligase regulates PLK4 protein levels to prevent premature centriole duplication. Life science alliance *7*. https://doi.org/10.26508/lsa.202402668.

Guardavaccaro, D., Kudo, Y., Boulaire, J., Barchi, M., Busino, L., Donzelli, M., Margottin-Goguet, F., Jackson, P.K., Yamasaki, L., and Pagano, M. (2003). Control of meiotic and mitotic progression by the F box protein beta-Trcp1 in vivo. Developmental cell *4*, 799-812. https://doi.org/10.1016/S1534-5807(03)00154-0.

Guderian, G., Westendorf, J., Uldschmid, A., and Nigg, E.A. (2010). Plk4 trans-autophosphorylation regulates centriole number by controlling betaTrCP-mediated degradation. Journal of cell science *123*, 2163-2169. https://doi.org/10.1242/jcs.068502.

Guo, Z., Kong, Q., Liu, C., Zhang, S., Zou, L., Yan, F., Whitmire, J.K., Xiong, Y., Chen, X., and Wan, Y.Y. (2016). DCAF1 controls T-cell function via p53-dependent and -independent mechanisms. Nature communications *7*, 10307. https://doi.org/10.1038/ncomms10307.

Habedanck, R., Stierhof, Y.-D., Wilkinson, C.J., and Nigg, E.A. (2005). The Polo kinase Plk4 functions in centriole duplication. Nature cell biology *7*, 1140-1146. https://doi.org/10.1038/ncb1320.

Han, X.-R., Sasaki, N., Jackson, S.C., Wang, P., Li, Z., Smith, M.D., Xie, L., Chen, X., Zhang, Y., and Marzluff, W.F., et al. (2020). CRL4DCAF1/VprBP E3 ubiquitin ligase controls ribosome biogenesis, cell proliferation, and development. Science advances *6*. https://doi.org/10.1126/sciadv.abd6078.

Hart, M., Concordet, J.P., Lassot, I., Albert, I., del los Santos, R., Durand, H., Perret, C., Rubinfeld, B., Margottin, F., and Benarous, R., et al. (1999). The F-box protein beta-TrCP associates with phosphorylated beta-catenin and regulates its activity in the cell. Current biology : CB *9*, 207-210. https://doi.org/10.1016/s0960-9822(99)80091-8.

Hatch, E.M., Kulukian, A., Holland, A.J., Cleveland, D.W., and Stearns, T. (2010). Cep152 interacts with Plk4 and is required for centriole duplication. The Journal of cell biology *191*, 721-729. https://doi.org/10.1083/jcb.201006049.

Hatzopoulos, G.N., Erat, M.C., Cutts, E., Rogala, K.B., Slater, L.M., Stansfeld, P.J., and Vakonakis, I. (2013). Structural analysis of the G-box domain of the microcephaly protein CPAP suggests a role in centriole architecture. Structure (London, England : 1993) *21*, 2069-2077. https://doi.org/10.1016/j.str.2013.08.019.

He, J., Choe, S., Walker, R., Di Marzio, P., Morgan, D.O., and Landau, N.R. (1995). Human immunodeficiency virus type 1 viral protein R (Vpr) arrests cells in the G2 phase of the cell cycle by inhibiting p34cdc2 activity. Journal of virology *69*, 6705-6711. https://doi.org/10.1128/JVI.69.11.6705-6711.1995.

He, Y.J., McCall, C.M., Hu, J., Zeng, Y., and Xiong, Y. (2006). DDB1 functions as a linker to recruit receptor WD40 proteins to CUL4-ROC1 ubiquitin ligases. Genes & development *20*, 2949-2954. https://doi.org/10.1101/gad.1483206.

Heckman, K.L., and Pease, L.R. (2007). Gene splicing and mutagenesis by PCR-driven overlap extension. Nature protocols *2*, 924-932. https://doi.org/10.1038/nprot.2007.132.

Hershko, A., and Ciechanover, A. (1998). The ubiquitin system. Annual review of biochemistry *67*, 425-479. https://doi.org/10.1146/annurev.biochem.67.1.425.

Hershko, A., Ciechanover, A., Heller, H., Haas, A.L., and Rose, I.A. (1980). Proposed role of ATP in protein breakdown: conjugation of protein with multiple chains of the polypeptide of ATP-dependent proteolysis. Proceedings of the National Academy of Sciences of the United States of America *77*, 1783-1786. https://doi.org/10.1073/pnas.77.4.1783.

Higa, L.A., Wu, M., Ye, T., Kobayashi, R., Sun, H., and Zhang, H. (2006). CUL4-DDB1 ubiquitin ligase interacts with multiple WD40-repeat proteins and regulates histone methylation. Nature cell biology *8*, 1277-1283. https://doi.org/10.1038/ncb1490.

Higa, L.A.A., Mihaylov, I.S., Banks, D.P., Zheng, J., and Zhang, H. (2003). Radiation-mediated proteolysis of CDT1 by CUL4-ROC1 and CSN complexes constitutes a new checkpoint. Nature cell biology *5*, 1008-1015. https://doi.org/10.1038/ncb1061.

Hinchcliffe, E.H., and Sluder, G. (2001). "It takes two to tango": understanding how centrosome duplication is regulated throughout the cell cycle. Genes & development *15*, 1167-1181. https://doi.org/10.1101/gad.894001.

Hoffmann, I., Clarke, P.R., Marcote, M.J., Karsenti, E., and Draetta, G. (1993). Phosphorylation and activation of human cdc25-C by cdc2--cyclin B and its involvement in the self-amplification of MPF at mitosis. The EMBO journal *12*, 53-63. https://doi.org/10.1002/j.1460-2075.1993.tb05631.x.

Holland, A.J., Lan, W., Niessen, S., Hoover, H., and Cleveland, D.W. (2010). Polo-like kinase 4 kinase activity limits centrosome overduplication by autoregulating its own stability. The Journal of cell biology *188*, 191-198. https://doi.org/10.1083/jcb.200911102.

Hopf, L.V.M., Baek, K., Klügel, M., Gronau, S. von, Xiong, Y., and Schulman, B.A. (2022). Structure of CRL7FBXW8 reveals coupling with CUL1-RBX1/ROC1 for multi-cullin-RING E3-catalyzed ubiquitin ligation. Nature structural & molecular biology *29*, 854-862. https://doi.org/10.1038/s41594-022-00815-6.

Hori, A., Barnouin, K., Snijders, A.P., and Toda, T. (2016). A non-canonical function of Plk4 in centriolar satellite integrity and ciliogenesis through PCM1 phosphorylation. EMBO reports *17*, 326-337. https://doi.org/10.15252/embr.201541432.

Hori, T., Osaka, F., Chiba, T., Miyamoto, C., Okabayashi, K., Shimbara, N., Kato, S., and Tanaka, K. (1999). Covalent modification of all members of human cullin family proteins by NEDD8. Oncogene *18*, 6829-6834. https://doi.org/10.1038/sj.onc.1203093.

Hossain, D., Javadi Esfehani, Y., Das, A., and Tsang, W.Y. (2017). Cep78 controls centrosome homeostasis by inhibiting EDD-DYRK2-DDB1VprBP. EMBO reports *18*, 632-644. https://doi.org/10.15252/embr.201642377.

Huang, L., Kinnucan, E., Wang, G., Beaudenon, S., Howley, P.M., Huibregtse, J.M., and Pavletich, N.P. (1999). Structure of an E6AP-UbcH7 complex: insights into ubiquitination by the E2-E3 enzyme cascade. Science (New York, N.Y.) *286*, 1321-1326. https://doi.org/10.1126/science.286.5443.1321.

Hudson, J.W., Kozarova, A., Cheung, P., Macmillan, J.C., Swallow, C.J., Cross, J.C., and Dennis, J.W. (2001). Late mitotic failure in mice lacking Sak, a polo-like kinase. Current biology : CB *11*, 441-446. https://doi.org/10.1016/s0960-9822(01)00117-8.

Huibregtse, J.M., Scheffner, M., and Howley, P.M. (1993). Localization of the E6-AP regions that direct human papillomavirus E6 binding, association with p53, and ubiquitination of associated proteins. Molecular and cellular biology *13*, 4918-4927. https://doi.org/10.1128/mcb.13.8.4918-4927.1993.

Jacotot, E., Ravagnan, L., Loeffler, M., Ferri, K.F., Vieira, H.L., Zamzami, N., Costantini, P., Druillennec, S., Hoebeke, J., and Briand, J.P., et al. (2000). The HIV-1 viral protein R induces apoptosis via a direct effect on the mitochondrial permeability transition pore. The Journal of experimental medicine *191*, 33-46. https://doi.org/10.1084/jem.191.1.33.

Jakobsen, L., Vanselow, K., Skogs, M., Toyoda, Y., Lundberg, E., Poser, I., Falkenby, L.G., Bennetzen, M., Westendorf, J., and Nigg, E.A., et al. (2011). Novel asymmetrically localizing components of human centrosomes identified by complementary proteomics methods. The EMBO journal *30*, 1520-1535. https://doi.org/10.1038/emboj.2011.63.

Jiang, J., and Struhl, G. (1998). Regulation of the Hedgehog and Wingless signalling pathways by the F-box/WD40-repeat protein Slimb. Nature *391*, 493-496. https://doi.org/10.1038/35154.

Jin, J., Arias, E.E., Chen, J., Harper, J.W., and Walter, J.C. (2006). A family of diverse Cul4-Ddb1-interacting proteins includes Cdt2, which is required for S phase destruction of the replication factor Cdt1. Molecular cell *23*, 709-721. https://doi.org/10.1016/j.molcel.2006.08.010.

Jin, J., Li, X., Gygi, S.P., and Harper, J.W. (2007). Dual E1 activation systems for ubiquitin differentially regulate E2 enzyme charging. Nature *447*, 1135-1138. https://doi.org/10.1038/nature05902.

Jin, J., Shirogane, T., Xu, L., Nalepa, G., Qin, J., Elledge, S.J., and Harper, J.W. (2003). SCFbeta-TRCP links Chk1 signaling to degradation of the Cdc25A protein phosphatase. Genes & development *17*, 3062-3074. https://doi.org/10.1101/gad.1157503.

Kamura, T., Maenaka, K., Kotoshiba, S., Matsumoto, M., Kohda, D., Conaway, R.C., Conaway, J.W., and Nakayama, K.I. (2004). VHL-box and SOCS-box domains determine binding specificity for Cul2-Rbx1 and Cul5-Rbx2 modules of ubiquitin ligases. Genes & development *18*, 3055-3065. https://doi.org/10.1101/gad.1252404.

Kang, B.S., French, O.G., Sando, J.J., and Hahn, C.S. (2000). Activation-dependent degradation of protein kinase C eta. Oncogene *19*, 4263-4272. https://doi.org/10.1038/sj.onc.1203779.

Kaur, M., Khan, M.M., Kar, A., Sharma, A., and Saxena, S. (2012). CRL4-DDB1-VPRBP ubiquitin ligase mediates the stress triggered proteolysis of Mcm10. Nucleic acids research *40*, 7332-7346. https://doi.org/10.1093/nar/gks366.

Kawakami, M., Mustachio, L.M., Zheng, L., Chen, Y., Rodriguez-Canales, J., Mino, B., Kurie, J.M., Roszik, J., Villalobos, P.A., and Thu, K.L., et al. (2018). Polo-like kinase 4 inhibition produces polyploidy and apoptotic death of lung cancers. Proceedings of the National Academy of Sciences of the United States of America *115*, 1913-1918. https://doi.org/10.1073/pnas.1719760115.

Kawakami, T., Chiba, T., Suzuki, T., Iwai, K., Yamanaka, K., Minato, N., Suzuki, H., Shimbara, N., Hidaka, Y., and Osaka, F., et al. (2001). NEDD8 recruits E2-ubiquitin to SCF E3 ligase. The EMBO journal *20*, 4003-4012. https://doi.org/10.1093/emboj/20.15.4003.

Khodjakov, A., Cole, R.W., Oakley, B.R., and Rieder, C.L. (2000). Centrosome-independent mitotic spindle formation in vertebrates. Current biology : CB *10*, 59-67. https://doi.org/10.1016/s0960-9822(99)00276-6.

Kim, K., Kim, J.-M., Kim, J.-S., Choi, J., Lee, Y.S., Neamati, N., Song, J.S., Heo, K., and An, W. (2013a). VprBP has intrinsic kinase activity targeting histone H2A and represses gene transcription. Molecular cell *52*, 459-467. https://doi.org/10.1016/j.molcel.2013.09.017.

Kim, T.-S., Park, J.-E., Shukla, A., Choi, S., Murugan, R.N., Lee, J.H., Ahn, M., Rhee, K., Bang, J.K., and Kim, B.Y., et al. (2013b). Hierarchical recruitment of Plk4 and regulation of centriole biogenesis by two centrosomal scaffolds, Cep192 and Cep152. Proceedings of the National Academy of Sciences of the United States of America *110*, E4849-57. https://doi.org/10.1073/pnas.1319656110.

King, R.W., Deshaies, R.J., Peters, J.M., and Kirschner, M.W. (1996a). How proteolysis drives the cell cycle. Science (New York, N.Y.) *274*, 1652-1659. https://doi.org/10.1126/science.274.5293.1652.

King, R.W., Glotzer, M., and Kirschner, M.W. (1996b). Mutagenic analysis of the destruction signal of mitotic cyclins and structural characterization of ubiquitinated intermediates. Molecular biology of the cell *7*, 1343-1357. https://doi.org/10.1091/mbc.7.9.1343.

Kitagawa, D., Busso, C., Flückiger, I., and Gönczy, P. (2009). Phosphorylation of SAS-6 by ZYG-1 is critical for centriole formation in C. elegans embryos. Developmental cell *17*, 900-907. https://doi.org/10.1016/j.devcel.2009.11.002.

Klebba, J.E., Buster, D.W., McLamarrah, T.A., Rusan, N.M., and Rogers, G.C. (2015). Autoinhibition and relief mechanism for Polo-like kinase 4. Proceedings of the National Academy of Sciences of the United States of America *112*, E657-66. https://doi.org/10.1073/pnas.1417967112.

Klebba, J.E., Buster, D.W., Nguyen, A.L., Swatkoski, S., Gucek, M., Rusan, N.M., and Rogers, G.C. (2013). Polo-like kinase 4 autodestructs by generating its Slimb-binding phosphodegron. Current biology : CB *23*, 2255-2261. https://doi.org/10.1016/j.cub.2013.09.019.

Ko, M.A., Rosario, C.O., Hudson, J.W., Kulkarni, S., Pollett, A., Dennis, J.W., and Swallow, C.J. (2005). Plk4 haploinsufficiency causes mitotic infidelity and carcinogenesis. Nature genetics *37*, 883-888. https://doi.org/10.1038/ng1605.

Komander, D., Clague, M.J., and Urbé, S. (2009). Breaking the chains: structure and function of the deubiquitinases. Nature reviews. Molecular cell biology *10*, 550-563. https://doi.org/10.1038/nrm2731.

Komander, D., and Rape, M. (2012). The ubiquitin code. Annual review of biochemistry *81*, 203-229. https://doi.org/10.1146/annurev-biochem-060310-170328.

Kratz, A.-S., Bärenz, F., Richter, K.T., and Hoffmann, I. (2015). Plk4-dependent phosphorylation of STIL is required for centriole duplication. Biology open *4*, 370-377. https://doi.org/10.1242/bio.201411023.

Krönke, J., Udeshi, N.D., Narla, A., Grauman, P., Hurst, S.N., McConkey, M., Svinkina, T., Heckl, D., Comer, E., and Li, X., et al. (2014). Lenalidomide causes selective degradation of IKZF1 and IKZF3 in multiple myeloma cells. Science (New York, N.Y.) *343*, 301-305. https://doi.org/10.1126/science.1244851.

Lau, A.W., Fukushima, H., and Wei, W. (2012). The Fbw7 and betaTRCP E3 ubiquitin ligases and their roles in tumorigenesis. Frontiers in bioscience (Landmark edition) *17*, 2197-2212. https://doi.org/10.2741/4045.

Ledoux, A.C., Sellier, H., Gillies, K., Iannetti, A., James, J., and Perkins, N.D. (2013). NFκB regulates expression of Polo-like kinase 4. Cell cycle (Georgetown, Tex.) *12*, 3052-3062. https://doi.org/10.4161/cc.26086.

Lee, J., and Zhou, P. (2007). DCAFs, the missing link of the CUL4-DDB1 ubiquitin ligase. Molecular cell *26*, 775-780. https://doi.org/10.1016/j.molcel.2007.06.001.

Lee, K., and Rhee, K. (2011). PLK1 phosphorylation of pericentrin initiates centrosome maturation at the onset of mitosis. The Journal of cell biology *195*, 1093-1101. https://doi.org/10.1083/jcb.201106093.

Lee, M., Seo, M.Y., Chang, J., Hwang, D.S., and Rhee, K. (2017). PLK4 phosphorylation of CP110 is required for efficient centriole assembly. Cell cycle (Georgetown, Tex.) *16*, 1225-1234. https://doi.org/10.1080/15384101.2017.1325555.

Lee, M.-Y., Moreno, C.S., and Saavedra, H.I. (2014). E2F activators signal and maintain centrosome amplification in breast cancer cells. Molecular and cellular biology *34*, 2581-2599. https://doi.org/10.1128/MCB.01688-13.

Lee, P.C.W., Sowa, M.E., Gygi, S.P., and Harper, J.W. (2011). Alternative ubiquitin activation/conjugation cascades interact with N-end rule ubiquitin ligases to control degradation of RGS proteins. Molecular cell *43*, 392-405. https://doi.org/10.1016/j.molcel.2011.05.034.

Lei, Q., Xiong, L., Xia, Y., Feng, Z., Gao, T., Wei, W., Song, X., Ye, T., Wang, N., and Peng, C., et al. (2018). YLT-11, a novel PLK4 inhibitor, inhibits human breast cancer growth via inducing maladjusted centriole duplication and mitotic defect. Cell death & disease *9*, 1066. https://doi.org/10.1038/s41419-018-1071-2.

Leng, F., Yu, J., Zhang, C., Alejo, S., Hoang, N., Sun, H., Lu, F., and Zhang, H. (2018). Methylated DNMT1 and E2F1 are targeted for proteolysis by L3MBTL3 and CRL4DCAF5 ubiquitin ligase. Nature communications *9*, 1641. https://doi.org/10.1038/s41467-018-04019-9.

Lettman, M.M., Wong, Y.L., Viscardi, V., Niessen, S., Chen, S.-H., Shiau, A.K., Zhou, H., Desai, A., and Oegema, K. (2013). Direct binding of SAS-6 to ZYG-1 recruits SAS-6 to the mother centriole for cartwheel assembly. Developmental cell *25*, 284-298. https://doi.org/10.1016/j.devcel.2013.03.011.

Leung, G.C., Hudson, J.W., Kozarova, A., Davidson, A., Dennis, J.W., and Sicheri, F. (2002). The Sak polo-box comprises a structural domain sufficient for mitotic subcellular localization. Nature structural biology *9*, 719-724. https://doi.org/10.1038/nsb848.

Levine, M.S., Bakker, B., Boeckx, B., Moyett, J., Lu, J., Vitre, B., Spierings, D.C., Lansdorp, P.M., Cleveland, D.W., and Lambrechts, D., et al. (2017). Centrosome Amplification Is Sufficient to Promote Spontaneous Tumorigenesis in Mammals. Developmental cell *40*, 313-322.e5. https://doi.org/10.1016/j.devcel.2016.12.022.

Li, J., Tan, M., Li, L., Pamarthy, D., Lawrence, T.S., and Sun, Y. (2005). SAK, a new polo-like kinase, is transcriptionally repressed by p53 and induces apoptosis upon RNAi silencing. Neoplasia (New York, N.Y.) *7*, 312-323. https://doi.org/10.1593/neo.04325.

Li, W., You, L., Cooper, J., Schiavon, G., Pepe-Caprio, A., Zhou, L., Ishii, R., Giovannini, M., Hanemann, C.O., and Long, S.B., et al. (2010). Merlin/NF2 suppresses tumorigenesis by inhibiting the E3 ubiquitin ligase CRL4(DCAF1) in the nucleus. Cell *140*, 477-490. https://doi.org/10.1016/j.cell.2010.01.029.

Li, Z., Dai, K., Wang, C., Song, Y., Gu, F., Liu, F., and Fu, L. (2016). Expression of Polo-Like Kinase 4(PLK4) in Breast Cancer and Its Response to Taxane-Based Neoadjuvant Chemotherapy. Journal of Cancer *7*, 1125-1132. https://doi.org/10.7150/jca.14307.

Li, Z., Fan, S., Wang, J., Chen, X., Liao, Q., Liu, X., Ouyang, G., Cao, H., and Xiao, W. (2020). Zebrafish F-box Protein fbxo3 Negatively Regulates Antiviral Response through Promoting K27-Linked Polyubiquitination of the Transcription Factors irf3 and irf7. Journal of immunology (Baltimore, Md. : 1950) *205*, 1897-1908. https://doi.org/10.4049/jimmunol.2000305.

Lohse, I., Mason, J., Cao, P.M., Pintilie, M., Bray, M., and Hedley, D.W. (2017). Activity of the novel polo-like kinase 4 inhibitor CFI-400945 in pancreatic cancer patient-derived xenografts. Oncotarget *8*, 3064-3071. https://doi.org/10.18632/oncotarget.13619.

Lopez, J., and Tait, S.W.G. (2014). Killing the Killer: PARC/CUL9 promotes cell survival by destroying cytochrome C. Science signaling *7*, pe17. https://doi.org/10.1126/scisignal.2005619.

Lowery, D.M., Clauser, K.R., Hjerrild, M., Lim, D., Alexander, J., Kishi, K., Ong, S.-E., Gammeltoft, S., Carr, S.A., and Yaffe, M.B. (2007). Proteomic screen defines the Polo-box domain interactome and identifies Rock2 as a Plk1 substrate. The EMBO journal *26*, 2262-2273. https://doi.org/10.1038/sj.emboj.7601683.

Lu, G., Middleton, R.E., Sun, H., Naniong, M., Ott, C.J., Mitsiades, C.S., Wong, K.-K., Bradner, J.E., and Kaelin, W.G. (2014). The myeloma drug lenalidomide promotes the cereblon-dependent destruction of Ikaros proteins. Science (New York, N.Y.) *343*, 305-309. https://doi.org/10.1126/science.1244917.

Lu, Z., and Hunter, T. (2009). Degradation of activated protein kinases by ubiquitination. Annual review of biochemistry *78*, 435-475. https://doi.org/10.1146/annurev.biochem.013008.092711.

Lyapina, S., Cope, G., Shevchenko, A., Serino, G., Tsuge, T., Zhou, C., Wolf, D.A., Wei, N., and Deshaies, R.J. (2001). Promotion of NEDD-CUL1 conjugate cleavage by COP9 signalosome. Science (New York, N.Y.) *292*, 1382-1385. https://doi.org/10.1126/science.1059780.

Maddika, S., and Chen, J. (2009). Protein kinase DYRK2 is a scaffold that facilitates assembly of an E3 ligase. Nature cell biology *11*, 409-419. https://doi.org/10.1038/ncb1848.

Marshall, R.S., and Vierstra, R.D. (2019). Dynamic Regulation of the 26S Proteasome: From Synthesis to Degradation. Frontiers in molecular biosciences *6*, 40. https://doi.org/10.3389/fmolb.2019.00040.

Marshall, W.F. (2009). Centriole evolution. Current opinion in cell biology *21*, 14-19. https://doi.org/10.1016/j.ceb.2009.01.008.

Matsumoto, M.L., Wickliffe, K.E., Dong, K.C., Yu, C., Bosanac, I., Bustos, D., Phu, L., Kirkpatrick, D.S., Hymowitz, S.G., and Rape, M., et al. (2010). K11-linked polyubiquitination in cell cycle control revealed by a K11 linkage-specific antibody. Molecular cell *39*, 477-484. https://doi.org/10.1016/j.molcel.2010.07.001.

McCall, C.M., Miliani de Marval, P.L., Chastain, P.D., Jackson, S.C., He, Y.J., Kotake, Y., Cook, J.G., and Xiong, Y. (2008). Human immunodeficiency virus type 1 Vpr-binding protein VprBP, a WD40 protein associated with the DDB1-CUL4 E3 ubiquitin ligase, is essential for DNA replication and embryonic development. Molecular and cellular biology *28*, 5621-5633. https://doi.org/10.1128/MCB.00232-08.

Metzger, M.B., Hristova, V.A., and Weissman, A.M. (2012). HECT and RING finger families of E3 ubiquitin ligases at a glance. Journal of cell science *125*, 531-537. https://doi.org/10.1242/jcs.091777.

Mohamed, W.I., Schenk, A.D., Kempf, G., Cavadini, S., Basters, A., Potenza, A., Abdul Rahman, W., Rabl, J., Reichermeier, K., and Thomä, N.H. (2021). The CRL4DCAF1 cullin-RING ubiquitin ligase is activated following a switch in oligomerization state. The EMBO journal *40*, e108008. https://doi.org/10.15252/embj.2021108008.

Morimoto, M., Nishida, T., Honda, R., and Yasuda, H. (2000). Modification of cullin-1 by ubiquitin-like protein Nedd8 enhances the activity of SCF(skp2) toward p27(kip1). Biochemical and biophysical research communications *270*, 1093-1096. https://doi.org/10.1006/bbrc.2000.2576.

Morris, J.R., and Solomon, E. (2004). BRCA1 : BARD1 induces the formation of conjugated ubiquitin structures, dependent on K6 of ubiquitin, in cells during DNA replication and repair. Human molecular genetics *13*, 807-817. https://doi.org/10.1093/hmg/ddh095.

Moyer, T.C., and Holland, A.J. (2019). PLK4 promotes centriole duplication by phosphorylating STIL to link the procentriole cartwheel to the microtubule wall. eLife *8*. https://doi.org/10.7554/eLife.46054.

Nakagawa, T., Mondal, K., and Swanson, P.C. (2013). VprBP (DCAF1): a promiscuous substrate recognition subunit that incorporates into both RING-family CRL4 and HECT-family EDD/UBR5 E3 ubiquitin ligases. BMC molecular biology *14*, 22. https://doi.org/10.1186/1471-2199-14-22.

Nichols, A.F., Itoh, T., Graham, J.A., Liu, W., Yamaizumi, M., and Linn, S. (2000). Human damage-specific DNA-binding protein p48. Characterization of XPE mutations and regulation following UV irradiation. The Journal of biological chemistry *275*, 21422-21428. https://doi.org/10.1074/jbc.M000960200.

Nigg, E.A., and Holland, A.J. (2018). Once and only once: mechanisms of centriole duplication and their deregulation in disease. Nature reviews. Molecular cell biology *19*, 297-312. https://doi.org/10.1038/nrm.2017.127.

Nigg, E.A., and Raff, J.W. (2009). Centrioles, centrosomes, and cilia in health and disease. Cell *139*, 663-678. https://doi.org/10.1016/j.cell.2009.10.036.

Ohta, M., Ashikawa, T., Nozaki, Y., Kozuka-Hata, H., Goto, H., Inagaki, M., Oyama, M., and Kitagawa, D. (2014). Direct interaction of Plk4 with STIL ensures formation of a single procentriole per parental centriole. Nature communications *5*, 5267. https://doi.org/10.1038/ncomms6267.

Ohta, T., Michel, J.J., Schottelius, A.J., and Xiong, Y. (1999). ROC1, a homolog of APC11, represents a family of cullin partners with an associated ubiquitin ligase activity. Molecular cell *3*, 535-541. https://doi.org/10.1016/s1097-2765(00)80482-7.

Ordureau, A., Heo, J.-M., Duda, D.M., Paulo, J.A., Olszewski, J.L., Yanishevski, D., Rinehart, J., Schulman, B.A., and Harper, J.W. (2015). Defining roles of PARKIN and ubiquitin phosphorylation by PINK1 in mitochondrial quality control using a ubiquitin replacement strategy. Proceedings of the National Academy of Sciences of the United States of America *112*, 6637-6642. https://doi.org/10.1073/pnas.1506593112.

Osaka, F., Kawasaki, H., Aida, N., Saeki, M., Chiba, T., Kawashima, S., Tanaka, K., and Kato, S. (1998). A new NEDD8-ligating system for cullin-4A. Genes & development *12*, 2263-2268. https://doi.org/10.1101/gad.12.15.2263.

Park, J.-E., Soung, N.-K., Johmura, Y., Kang, Y.H., Liao, C., Lee, K.H., Park, C.H., Nicklaus, M.C., and Lee, K.S. (2010). Polo-box domain: a versatile mediator of polo-like kinase function. Cellular and molecular life sciences : CMLS *67*, 1957-1970. https://doi.org/10.1007/s00018-010-0279-9.

Park, S.-Y., Park, J.-E., Kim, T.-S., Kim, J.H., Kwak, M.-J., Ku, B., Tian, L., Murugan, R.N., Ahn, M., and Komiya, S., et al. (2014). Molecular basis for unidirectional scaffold switching of human Plk4 in centriole biogenesis. Nature structural & molecular biology *21*, 696-703. https://doi.org/10.1038/nsmb.2846.

Paul, D., Kales, S.C., Cornwell, J.A., Afifi, M.M., Rai, G., Zakharov, A., Simeonov, A., and Cappell, S.D. (2022). Revealing β-TrCP activity dynamics in live cells with a genetically encoded biosensor. Nature communications *13*, 6364. https://doi.org/10.1038/s41467-022-33762-3.

Peth, A., Uchiki, T., and Goldberg, A.L. (2010). ATP-dependent steps in the binding of ubiquitin conjugates to the 26S proteasome that commit to degradation. Molecular cell *40*, 671-681. https://doi.org/10.1016/j.molcel.2010.11.002.

Piel, M., Meyer, P., Khodjakov, A., Rieder, C.L., and Bornens, M. (2000). The respective contributions of the mother and daughter centrioles to centrosome activity and behavior in vertebrate cells. The Journal of cell biology *149*, 317-330. https://doi.org/10.1083/jcb.149.2.317.

Piva, R., Liu, J., Chiarle, R., Podda, A., Pagano, M., and Inghirami, G. (2002). In vivo interference with Skp1 function leads to genetic instability and neoplastic transformation. Molecular and cellular biology *22*, 8375-8387. https://doi.org/10.1128/MCB.22.23.8375-8387.2002.

Pla-Prats, C., Cavadini, S., Kempf, G., and Thomä, N.H. (2023). Recognition of the CCT5 di-Glu degron by CRL4DCAF12 is dependent on TRiC assembly. The EMBO journal *42*, e112253. https://doi.org/10.15252/embj.2022112253.

Prakash, S., Tian, L., Ratliff, K.S., Lehotzky, R.E., and Matouschek, A. (2004). An unstructured initiation site is required for efficient proteasome-mediated degradation. Nature structural & molecular biology *11*, 830-837. https://doi.org/10.1038/nsmb814.

Re, F., Braaten, D., Franke, E.K., and Luban, J. (1995). Human immunodeficiency virus type 1 Vpr arrests the cell cycle in G2 by inhibiting the activation of p34cdc2-cyclin B. Journal of virology *69*, 6859-6864. https://doi.org/10.1128/JVI.69.11.6859-6864.1995.

Read, M.A., Brownell, J.E., Gladysheva, T.B., Hottelet, M., Parent, L.A., Coggins, M.B., Pierce, J.W., Podust, V.N., Luo, R.S., and Chau, V., et al. (2000). Nedd8 modification of cul-1 activates SCF(beta(TrCP))-dependent ubiquitination of IkappaBalpha. Molecular and cellular biology *20*, 2326-2333. https://doi.org/10.1128/MCB.20.7.2326-2333.2000.

Rechsteiner, M., and Rogers, S.W. (1996). PEST sequences and regulation by proteolysis. Trends in biochemical sciences *21*, 267-271.

Reichermeier, K.M., Straube, R., Reitsma, J.M., Sweredoski, M.J., Rose, C.M., Moradian, A., den Besten, W., Hinkle, T., Verschueren, E., and Petzold, G., et al. (2020). PIKES Analysis Reveals Response to Degraders and Key Regulatory Mechanisms of the CRL4 Network. Molecular cell *77*, 1092-1106.e9. https://doi.org/10.1016/j.molcel.2019.12.013.

Rodrigues-Martins, A., Riparbelli, M., Callaini, G., Glover, D.M., and Bettencourt-Dias, M. (2007). Revisiting the role of the mother centriole in centriole biogenesis. Science (New York, N.Y.) *316*, 1046-1050. https://doi.org/10.1126/science.1142950.

Rogers, G.C., Rusan, N.M., Roberts, D.M., Peifer, M., and Rogers, S.L. (2009). The SCF Slimb ubiquitin ligase regulates Plk4/Sak levels to block centriole reduplication. The Journal of cell biology *184*, 225-239. https://doi.org/10.1083/jcb.200808049.

Rosario, C.O., Ko, M.A., Haffani, Y.Z., Gladdy, R.A., Paderova, J., Pollett, A., Squire, J.A., Dennis, J.W., and Swallow, C.J. (2010). Plk4 is required for cytokinesis and maintenance of chromosomal stability. Proceedings of the National Academy of Sciences of the United States of America *107*, 6888-6893. https://doi.org/10.1073/pnas.0910941107.

Sakamoto, K.M., Kim, K.B., Kumagai, A., Mercurio, F., Crews, C.M., and Deshaies, R.J. (2001). Protacs: chimeric molecules that target proteins to the Skp1-Cullin-F box complex for ubiquitination and degradation. Proceedings of the National Academy of Sciences of the United States of America *98*, 8554-8559. https://doi.org/10.1073/pnas.141230798.

Sander, B., Xu, W., Eilers, M., Popov, N., and Lorenz, S. (2017). A conformational switch regulates the ubiquitin ligase HUWE1. eLife *6*. https://doi.org/10.7554/eLife.21036.

Schabla, N.M., Mondal, K., and Swanson, P.C. (2019). DCAF1 (VprBP): emerging physiological roles for a unique dual-service E3 ubiquitin ligase substrate receptor. Journal of molecular cell biology *11*, 725-735. https://doi.org/10.1093/jmcb/mjy085.

Scheffner, M., Huibregtse, J.M., Vierstra, R.D., and Howley, P.M. (1993). The HPV-16 E6 and E6-AP complex functions as a ubiquitin-protein ligase in the ubiquitination of p53. Cell *75*, 495-505. https://doi.org/10.1016/0092-8674(93)90384-3.

Scheffner, M., and Kumar, S. (2014). Mammalian HECT ubiquitin-protein ligases: biological and pathophysiological aspects. Biochimica et biophysica acta *1843*, 61-74. https://doi.org/10.1016/j.bbamcr.2013.03.024.

Schmidt, T.I., Kleylein-Sohn, J., Westendorf, J., Le Clech, M., Lavoie, S.B., Stierhof, Y.-D., and Nigg, E.A. (2009). Control of centriole length by CPAP and CP110. Current biology : CB *19*, 1005-1011. https://doi.org/10.1016/j.cub.2009.05.016.

Schröder, M., Renatus, M., Liang, X., Meili, F., Zoller, T., Ferrand, S., Gauter, F., Li, X., Sigoillot, F., and Gleim, S., et al. (2024). DCAF1-based PROTACs with activity against clinically validated targets overcoming intrinsic- and acquired-degrader resistance. Nature communications *15*, 275. https://doi.org/10.1038/s41467-023-44237-4.

Schuh, M., and Ellenberg, J. (2007). Self-organization of MTOCs replaces centrosome function during acentrosomal spindle assembly in live mouse oocytes. Cell *130*, 484-498. https://doi.org/10.1016/j.cell.2007.06.025.

Seol, J.H., Feldman, R.M., Zachariae, W., Shevchenko, A., Correll, C.C., Lyapina, S., Chi, Y., Galova, M., Claypool, J., and Sandmeyer, S., et al. (1999). Cdc53/cullin and the essential Hrt1 RING-H2 subunit of SCF define a ubiquitin ligase module that activates the E2 enzyme Cdc34. Genes & development *13*, 1614-1626. https://doi.org/10.1101/gad.13.12.1614.

Serçin, Ö., Larsimont, J.-C., Karambelas, A.E., Marthiens, V., Moers, V., Boeckx, B., Le Mercier, M., Lambrechts, D., Basto, R., and Blanpain, C. (2016). Transient PLK4 overexpression accelerates tumorigenesis in p53-deficient epidermis. Nature cell biology *18*, 100-110. https://doi.org/10.1038/ncb3270.

Shiyanov, P., Nag, A., and Raychaudhuri, P. (1999). Cullin 4A associates with the UV-damaged DNA-binding protein DDB. The Journal of biological chemistry *274*, 35309-35312. https://doi.org/10.1074/jbc.274.50.35309.

Sillibourne, J.E., and Bornens, M. (2010). Polo-like kinase 4: the odd one out of the family. Cell division *5*, 25. https://doi.org/10.1186/1747-1028-5-25.

Sillibourne, J.E., Tack, F., Vloemans, N., an Boeckx, Thambirajah, S., Bonnet, P., Ramaekers, F.C.S., Bornens, M., and Grand-Perret, T. (2010). Autophosphorylation of polo-like kinase 4 and its role in centriole duplication. Molecular biology of the cell *21*, 547-561. https://doi.org/10.1091/mbc.e09-06-0505.

Singer, J.D., Gurian-West, M., Clurman, B., and Roberts, J.M. (1999). Cullin-3 targets cyclin E for ubiquitination and controls S phase in mammalian cells. Genes & development *13*, 2375-2387. https://doi.org/10.1101/gad.13.18.2375.

Sir, J.-H., Pütz, M., Daly, O., Morrison, C.G., Dunning, M., Kilmartin, J.V., and Gergely, F. (2013). Loss of centrioles causes chromosomal instability in vertebrate somatic cells. The Journal of cell biology *203*, 747-756. https://doi.org/10.1083/jcb.201309038.

Skaar, J.R., Pagan, J.K., and Pagano, M. (2013). Mechanisms and function of substrate recruitment by F-box proteins. Nature reviews. Molecular cell biology *14*, 369-381. https://doi.org/10.1038/nrm3582.

Skowyra, D., Craig, K.L., Tyers, M., Elledge, S.J., and Harper, J.W. (1997). F-box proteins are receptors that recruit phosphorylated substrates to the SCF ubiquitin-ligase complex. Cell *91*, 209-219. https://doi.org/10.1016/s0092-8674(00)80403-1.

Slevin, L.K., Nye, J., Pinkerton, D.C., Buster, D.W., Rogers, G.C., and Slep, K.C. (2012). The structure of the plk4 cryptic polo box reveals two tandem polo boxes required for centriole duplication. Structure (London, England : 1993) *20*, 1905-1917. https://doi.org/10.1016/j.str.2012.08.025.

Sonnen, K.F., Gabryjonczyk, A.-M., Anselm, E., Stierhof, Y.-D., and Nigg, E.A. (2013). Human Cep192 and Cep152 cooperate in Plk4 recruitment and centriole duplication. Journal of cell science *126*, 3223-3233. https://doi.org/10.1242/jcs.129502.

Stevens, N.R., Dobbelaere, J., Brunk, K., Franz, A., and Raff, J.W. (2010). Drosophila Ana2 is a conserved centriole duplication factor. The Journal of cell biology *188*, 313-323. https://doi.org/10.1083/jcb.200910016.

Stewart, S.A., Poon, B., Jowett, J.B., and Chen, I.S. (1997). Human immunodeficiency virus type 1 Vpr induces apoptosis following cell cycle arrest. Journal of virology *71*, 5579-5592. https://doi.org/10.1128/JVI.71.7.5579-5592.1997.

Strohmaier, H., Spruck, C.H., Kaiser, P., Won, K.A., Sangfelt, O., and Reed, S.I. (2001). Human F-box protein hCdc4 targets cyclin E for proteolysis and is mutated in a breast cancer cell line. Nature *413*, 316-322. https://doi.org/10.1038/35095076.

Tan, L., Ehrlich, E., and Yu, X.-F. (2007). DDB1 and Cul4A are required for human immunodeficiency virus type 1 Vpr-induced G2 arrest. Journal of virology *81*, 10822-10830. https://doi.org/10.1128/jvi.01380-07.

Tan, P., Fuchs, S.Y., Chen, A., Wu, K., Gomez, C., Ronai, Z., and Pan, Z.Q. (1999). Recruitment of a ROC1-CUL1 ubiquitin ligase by Skp1 and HOS to catalyze the ubiquitination of I kappa B alpha. Molecular cell *3*, 527-533. https://doi.org/10.1016/s1097-2765(00)80481-5.

Tsou, M.-F.B., Wang, W.-J., George, K.A., Uryu, K., Stearns, T., and Jallepalli, P.V. (2009). Polo kinase and separase regulate the mitotic licensing of centriole duplication in human cells. Developmental cell *17*, 344-354. https://doi.org/10.1016/j.devcel.2009.07.015.

Uchiumi, T., Longo, D.L., and Ferris, D.K. (1997). Cell cycle regulation of the human polo-like kinase (PLK) promoter. The Journal of biological chemistry *272*, 9166-9174. https://doi.org/10.1074/jbc.272.14.9166.

Vasquez-Limeta, A., and Loncarek, J. (2021). Human centrosome organization and function in interphase and mitosis. Seminars in cell & developmental biology *117*, 30-41. https://doi.org/10.1016/j.semcdb.2021.03.020.

Verdecia, M.A., Joazeiro, C.A.P., Wells, N.J., Ferrer, J.-L., Bowman, M.E., Hunter, T., and Noel, J.P. (2003). Conformational flexibility underlies ubiquitin ligation mediated by the WWP1 HECT domain E3 ligase. Molecular cell *11*, 249-259. https://doi.org/10.1016/s1097-2765(02)00774-8.

Vitre, B., Holland, A.J., Kulukian, A., Shoshani, O., Hirai, M., Wang, Y., Maldonado, M., Cho, T., Boubaker, J., and Swing, D.A., et al. (2015). Chronic centrosome amplification without tumorigenesis. Proceedings of the National Academy of Sciences of the United States of America *112*, E6321-30. https://doi.org/10.1073/pnas.1519388112.

Wang, D., Kon, N., Lasso, G., Le Jiang, Leng, W., Zhu, W.-G., Qin, J., Honig, B., and Gu, W. (2016). Acetylation-regulated interaction between p53 and SET reveals a widespread regulatory mode. Nature *538*, 118-122. https://doi.org/10.1038/nature19759.

Wang, J., Ren, D., Sun, Y., Xu, C., Wang, C., Cheng, R., Wang, L., Jia, G., Ren, J., and Ma, J., et al. (2020). Inhibition of PLK4 might enhance the anti-tumour effect of bortezomib on glioblastoma via PTEN/PI3K/AKT/mTOR signalling pathway. Journal of cellular and molecular medicine *24*, 3931-3947. https://doi.org/10.1111/jcmm.14996.

Wang, X., Arceci, A., Bird, K., Mills, C.A., Choudhury, R., Kernan, J.L., Zhou, C., Bae-Jump, V., Bowers, A., and Emanuele, M.J. (2017). VprBP/DCAF1 Regulates the Degradation and Nonproteolytic Activation of the Cell Cycle Transcription Factor FoxM1. Molecular and cellular biology *37*. https://doi.org/10.1128/MCB.00609-16.

Wang, X., Singh, S., Jung, H.-Y., Yang, G., Jun, S., Sastry, K.J., and Park, J.-I. (2013). HIV-1 Vpr protein inhibits telomerase activity via the EDD-DDB1-VPRBP E3 ligase complex. The Journal of biological chemistry *288*, 15474-15480. https://doi.org/10.1074/jbc.M112.416735.

Wang, X.S., Cotton, T.R., Trevelyan, S.J., Richardson, L.W., Lee, W.T., Silke, J., and Lechtenberg, B.C. (2023). The unifying catalytic mechanism of the RING-between-RING E3 ubiquitin ligase family. Nature communications *14*, 168. https://doi.org/10.1038/s41467-023-35871-z.

Ward, A., and Hudson, J.W. (2014). p53-Dependent and cell specific epigenetic regulation of the polo-like kinases under oxidative stress. PloS one *9*, e87918. https://doi.org/10.1371/journal.pone.0087918.

Watanabe, N., Arai, H., Nishihara, Y., Taniguchi, M., Watanabe, N., Hunter, T., and Osada, H. (2004). M-phase kinases induce phospho-dependent ubiquitination of somatic Wee1 by SCFbeta-TrCP. Proceedings of the National Academy of Sciences of the United States of America *101*, 4419-4424. https://doi.org/10.1073/pnas.0307700101.

Weber, J., Polo, S., and Maspero, E. (2019). HECT E3 Ligases: A Tale With Multiple Facets. Frontiers in physiology *10*, 370. https://doi.org/10.3389/fphys.2019.00370.

Wiesner, S., Ogunjimi, A.A., Wang, H.-R., Rotin, D., Sicheri, F., Wrana, J.L., and Forman-Kay, J.D. (2007). Autoinhibition of the HECT-type ubiquitin ligase Smurf2 through its C2 domain. Cell *130*, 651-662. https://doi.org/10.1016/j.cell.2007.06.050.

Winston, J.T., Strack, P., Beer-Romero, P., Chu, C.Y., Elledge, S.J., and Harper, J.W. (1999). The SCFbeta-TRCP-ubiquitin ligase complex associates specifically with phosphorylated destruction motifs in IkappaBalpha and beta-catenin and stimulates IkappaBalpha ubiquitination in vitro. Genes & development *13*, 270-283. https://doi.org/10.1101/gad.13.3.270.

Wu-Baer, F., Lagrazon, K., Yuan, W., and Baer, R. (2003). The BRCA1/BARD1 heterodimer assembles polyubiquitin chains through an unconventional linkage involving lysine residue K6 of ubiquitin. The Journal of biological chemistry *278*, 34743-34746. https://doi.org/10.1074/jbc.C300249200.

Yang, L., WenTao, T., ZhiYuan, Z., Qi, L., YuXiang, L., Peng, Z., Ke, L., XiaoNa, J., YuZhi, P., and MeiLing, J., et al. (2022). Cullin-9/p53 mediates HNRNPC degradation to inhibit erastin-induced ferroptosis and is blocked by MDM2 inhibition in colorectal cancer. Oncogene *41*, 3210-3221. https://doi.org/10.1038/s41388-022-02284-z.

Yang, X., Menon, S., Lykke-Andersen, K., Tsuge, T., Di Xiao, Wang, X., Rodriguez-Suarez, R.J., Zhang, H., and Wei, N. (2002). The COP9 signalosome inhibits p27(kip1) degradation and impedes G1-S phase progression via deneddylation of SCF Cul1. Current biology : CB *12*, 667-672. https://doi.org/10.1016/s0960-9822(02)00791-1.

Yang, X.-D., Li, W., Zhang, S., Wu, D., Jiang, X., Tan, R., Niu, X., Wang, Q., Wu, X., and Liu, Z., et al. (2020). PLK4 deubiquitination by Spata2-CYLD suppresses NEK7-mediated NLRP3 inflammasome activation at the centrosome. The EMBO journal *39*, e102201. https://doi.org/10.15252/embj.2019102201.

Ye, Y., and Rape, M. (2009). Building ubiquitin chains: E2 enzymes at work. Nature reviews. Molecular cell biology *10*, 755-764. https://doi.org/10.1038/nrm2780.

Zhang, C., Leng, F., Saxena, L., Hoang, N., Yu, J., Alejo, S., Lee, L., Qi, D., Lu, F., and Sun, H., et al. (2019a). Proteolysis of methylated SOX2 protein is regulated by L3MBTL3 and CRL4DCAF5 ubiquitin ligase. The Journal of biological chemistry *294*, 476-489. https://doi.org/10.1074/jbc.RA118.005336.

Zhang, C., Ma, X., Wei, G., Zhu, X., Hu, P., Chen, X., Wang, D., Li, Y., Ruan, T., and Zhang, W., et al. (2023). Centrosomal protein 120 promotes centrosome amplification and gastric cancer progression via USP54-mediated deubiquitination of PLK4. iScience *26*, 105745. https://doi.org/10.1016/j.isci.2022.105745.

Zhang, S., Feng, Y., Narayan, O., and Zhao, L.J. (2001). Cytoplasmic retention of HIV-1 regulatory protein Vpr by protein-protein interaction with a novel human cytoplasmic protein VprBP. Gene *263*, 131-140. https://doi.org/10.1016/S0378-1119(00)00583-7.

Zhang, X., Wei, C., Liang, H., and Han, L. (2021). Polo-Like Kinase 4's Critical Role in Cancer Development and Strategies for Plk4-Targeted Therapy. Frontiers in Oncology *11*. https://doi.org/10.3389/fonc.2021.587554.

Zhang, Z., Wang, Z., Huang, K., Liu, Y., Wei, C., Zhou, J., Zhang, W., Wang, Q., Liang, H., and Zhang, A., et al. (2019b). PLK4 is a determinant of temozolomide sensitivity through phosphorylation of IKBKE in glioblastoma. Cancer letters *443*, 91-107. https://doi.org/10.1016/j.canlet.2018.11.034.

Zhao, L.J., Mukherjee, S., and Narayan, O. (1994). Biochemical mechanism of HIV-I Vpr function. Specific interaction with a cellular protein. The Journal of biological chemistry *269*, 15577-15582.

Zheng, J., Yang, X., Harrell, J.M., Ryzhikov, S., Shim, E.H., Lykke-Andersen, K., Wei, N., Sun, H., Kobayashi, R., and Zhang, H. (2002a). CAND1 binds to unneddylated CUL1 and regulates the formation of SCF ubiquitin E3 ligase complex. Molecular cell *10*, 1519-1526. https://doi.org/10.1016/S1097-2765(02)00784-0.

Zheng, N., Schulman, B.A., Song, L., Miller, J.J., Jeffrey, P.D., Wang, P., Chu, C., Koepp, D.M., Elledge, S.J., and Pagano, M., et al. (2002b). Structure of the Cul1-Rbx1-Skp1-F boxSkp2 SCF ubiquitin ligase complex. Nature *416*, 703-709. https://doi.org/10.1038/416703a.

Zheng, Y., Wong, M.L., Alberts, B., and Mitchison, T. (1995). Nucleation of microtubule assembly by a gamma-tubulin-containing ring complex. Nature *378*, 578-583. https://doi.org/10.1038/378578a0.

Zhou, Q., Fan, G., and Dong, Y. (2020a). Polo-like kinase 4 correlates with greater tumor size, lymph node metastasis and confers poor survival in non-small cell lung cancer. Journal of clinical laboratory analysis *34*, e23152. https://doi.org/10.1002/jcla.23152.

Zhou, Z., Song, X., Wavelet, C.M., and Wan, Y. (2020b). Cullin 4-DCAF Proteins in Tumorigenesis. Advances in experimental medicine and biology *1217*, 241-259. https://doi.org/10.1007/978-981-15-1025-0_15.

Zitouni, S., Francia, M.E., Leal, F., Montenegro Gouveia, S., Nabais, C., Duarte, P., Gilberto, S., Brito, D., Moyer, T., and Kandels-Lewis, S., et al. (2016). CDK1 Prevents Unscheduled PLK4-STIL Complex Assembly in Centriole Biogenesis. Current biology : CB *26*, 1127-1137. https://doi.org/10.1016/j.cub.2016.03.055.

Zitouni, S., Nabais, C., Jana, S.C., Guerrero, A., and Bettencourt-Dias, M. (2014). Polo-like kinases: structural variations lead to multiple functions. Nature reviews. Molecular cell biology *15*, 433-452. https://doi.org/10.1038/nrm3819.

6. Appendix

6.1 Abbreviations

γ-TuRC	γ-Tubulin ring complex
A	Alanine
AL	Activation loop
APS	Ammonium peroxodisulfate
ATP	Adenosine triphosphate
bp	Base pair
BSA	Bovine serum albumin
BTB	Bric-a-brac/Tramtrack/Broad
CDK	Cyclin-dependent kinase
CEP152/192	Centrosomal protein 152/192
CHX	Cycloheximide
CP	Core protease
CP110	Centriolar coiled-coil protein 110
CPAP	Centrosomal P4.1-associated protein
CPB	Cryptic polo-box
CRL	Cullin-RING E3 ubiquitin ligase
CUL	Cullin
DCAF	DDB1- and CUL4-associated factor
DDB1	DNA damage binding protein 1
DMEM	Dulbecco's Modified Eagle's Medium
DMSO	Dimethyl sulfoxide
DNA	Deoxyribonucleic acid
Dox	Doxycycline
DTT	Dithiothreitol
DUB	Deubiquitylating enzyme
E	Glutamic acid
EDTA	Ethylenediaminetetraacetic acid
FBS	Fetal bovine serum
GFP	Green fluorescent protein
GST	Glutathione S-transferase
HECT	Homologous to the E6-associated protein carboxyl terminus
HLH	Helix-loop-helix
HRP	Horseradish peroxidase
I	Isoleucine
IF	Immunofluorescence
IP	Immunoprecipitation
IPTG	Isopropyl β-D-thiogalactopyranoside
K	Lysine
kb	Kilobase
kDa	Kilodalton
L1	Linker 1
LB	Lysogeny broth
LDS	Lithium dodecyl sulfate
LisH	Lissencephaly type-1-like homology motif
Lys	Lysine

MBP	Maltose-binding protein
MIB1	Mind bomb 1
MS	Mass spectrometry
MTOC	Microtubule-organizing center
MW	Molecular weight
NEM	N-ethylmaleimide
NFκB	Nuclear factor kappa B
ns	not significant
OD	Optical density
PAGE	Polyacrylamide gel electrophoresis
PB	Polo-box
PBS	Phosphate buffered saline
PCM	Pericentriolar material
PCR	Polymerase chain reaction
PD	Pulldown
PEI	Polyethylenimine
PLK	Polo-like kinase
PROTAC	Proteolysis-targeting chimera
R	Arginine
RBR	RING-between-RING
RING	Really interesting new gene
RP	Regulatory particle
RT	Room temperature
S	Serine
SAC	Spindle assembly checkpoint
SAS-6	Spindle assembly abnormal protein 6
SCF	SKP1-CUL1-F-box protein complex
SD	Standard deviation
SDS	Sodium dodecyl sulfate
shRNA	Short hairpin RNA
siRNA	Small interfering RNA
SKP1	S-phase kinase-associated protein 1
SOCS	Suppressor of cytokine signaling
STIL	SCL-interrupting locus protein
SUMO	Small ubiquitin-like modifier
T	Threonine
TERT	Telomerase reverse transcriptase
U	Unit
U-ExM	Ultrastructure expansion microscopy
VHL	Von Hippel-Lindau
VprBP	Vpr binding protein
WB	Western blot
WT	Wild-type

6.2 List of figures

6.3 List of tables

7. Acknowledgements

As my time as a PhD student at the DKFZ in Heidelberg is coming to an end, I would like to express my gratitude towards those, who supported me in the past years. First of all, I would like to thank Prof. Dr. Ingrid Hoffmann for giving me the opportunity to work on this interesting research topic and to become a member of her research group. I am thankful for the scientific discussions, the support and the great opportunity to participate in the DKFZ-MOST Israel program, which allowed for our collaboration with Prof. Gali Prag from Tel Aviv University.

I would also like to thank Prof. Dr. Martin Müller and Dr. Julien Guizetti for being part of my thesis advisory committee and their helpful advice and the critical discussions in my thesis advisory committee meetings. Moreover, I thank Prof. Dr. Matthias Mayer for immediately agreeing to join my thesis examination committee.

I am grateful to all current and past members of the Hoffmann lab: Vesna Živanović and Simon Hänle-Kreidler, with your advice and support you helped me a lot, especially in the beginning of my PhD. You soon became more than just colleagues and I am very happy to have met you. Alexandra Turi da Fonte Dias and Kübra Gürkaslar, as the last three PhD students we were sitting in the same boat from the beginning until the end and I am thankful for the nice and supportive working atmosphere you created in the lab. In addition, I thank all other lab members, I had a chance to work with: Bettina Dörr, Yagmur Keser, Miriam Erles, Claudia Dang, Alina Maier, Sophia Grossi-Mayer and Lucia Pigazzini.

Finally, I would like to express my gratitude towards my family for the continuous support, encouragement and trust throughout the last years. Especially, I would like to thank Henrik for your love and understanding. You are always there for me and I could not have finished this journey without your support.